

**A NEW PUNCHING SHEAR STRENGTHENING
TECHNIQUE
FOR REINFORCED CONCRETE SLABS AT INTERIOR
SLAB-COLUMN CONNECTIONS**

by

Bamidele Adetifa

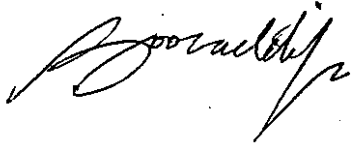
A thesis
presented to the University of Waterloo
in fulfilment of the
thesis requirement for the degree of
Master of Applied Science
in
Civil Engineering

Waterloo, Ontario, Canada, 2003

© Bamidele Adetifa 2003

I hereby declare that I am the sole author of this thesis.

I authorize the University of Waterloo to lend this thesis to other institutions or individuals for the purpose of scholarly research.

A handwritten signature in cursive script, appearing to read "Bozadeti".

I further authorize the University of Waterloo to reproduce this thesis by photocopying or by other means, in total or in part, at the request of other institutions or individuals for the purpose of scholarly research.

A second handwritten signature in cursive script, identical to the one above, appearing to read "Bozadeti".

The University of Waterloo requires the signatures of all persons using or photocopying this thesis.
Please sign below, and give address and date.

Abstract

In certain situations the punching strength of a connection may become inadequate after construction due to changes of connection geometry from drilling or coring, or from changes of building use, or construction and design errors. The use of shear reinforcement in the form of Shear Bolts is a new approach to strengthening slab-column connections.

Reported in this thesis are the results of research on the use of shear bolts for reinforced concrete interior slab-column connections without unbalanced moments. Six slab specimens were tested with different configurations of shear bolts and without shear reinforcement to verify the effectiveness of this method of reinforcement.

The central idea is an externally applied shear reinforcing technique that provides strength in shear at par with other conventional reinforcement types on the one hand and offering the distinct advantage and flexibility of external application after construction. A shear bolt consists of an unhardened steel shaft threaded at one end and flared out to form a bearing/anchor surface on the other end.

All six specimens were designed to fail in shear before reaching their flexural capacity, two of which were more critical than the others because of the presence of openings simulating utility ducts around the column perimeter.

From the tests, comparisons of predicted loads with the failure loads indicated a higher ultimate load for slab reinforced with the bolt system. Similarly, strain measurements from strain gauges attached to the longitudinal steel and deflection profiles of the slab showed that the new method was efficient in increasing the shear capacity of the slabs. In summary, the test program showed that shear bolts are effective in transforming the behaviour of the slab-column connections from a brittle punching shear failure mode to a more ductile flexural one. Deflection profiles at different load stages, and particularly at failure, show increased deflections for specimens reinforced with bolt reinforcements. This indicates an increased ductility at the connection. Similarly, load and flexural reinforcement strain magnitudes show substantial improvements in the strength of the connections.

Acknowledgements

The author is grateful to everyone who helped in the course of this research program: the laboratory staff, colleagues and friends.

Special thanks to Professor M.A Polak for her kind sponsorship and supervision of this research.

Table of Contents

Abstract.....	iv
Acknowledgements.....	v
Table of Contents.....	vi
List of Figures.....	x
List of Tables.....	xiii
Chapter 1 Introduction.....	1
1.1 Background.....	1
1.2 Punching Shear.....	2
1.3 Openings Around Columns.....	2
1.4 Conventional Slab-Column Tests.....	3
1.5 Objectives.....	3
1.6 Scope of Research.....	4
1.7 Contents of Thesis.....	4
Chapter 2 Review of Literature.....	6
2.1 Punching Shear Models.....	6
2.1.1 Rotational Models.....	6
2.1.1.1 Kinnunen and Nylander.....	6
2.1.1.2 Shehata.....	7
2.1.1.3 Broms.....	9
2.1.2 Models based on Classical Plasticity Theory.....	10
2.1.2.1 Braestrup et al.....	10
2.1.2.2 Plasticity Model by Bortolotti.....	11
2.1.3 Other Models.....	12
2.1.3.1 Fracture Mechanics Model by Bazant and Cao.....	12
2.1.3.2 Truss Model by Alexander and Simmonds.....	13
2.1.3.3 Bond Model by Alexander and Simmonds.....	14
2.1.3.4 Empirical Model by Moe.....	15
2.2 Code Shear Design Procedures for Reinforced Concrete Slabs.....	16
2.2.1 American Code ACI 318-99.....	16
2.2.2 Canadian Code CSA A23.3-94.....	17

2.2.3	Eurocode 2 ENV 1992-1-1.....	18
2.2.4	CEB-FIP MC 1990.....	20
2.3	Selected Experimental Studies on Punching Shear.....	21
2.3.1	Dilger and Ghali: Shear Reinforcement for Concrete Slabs.....	21
2.3.2	Ghali, Sargious and Huizer: Vertical Prestressing of Flat Plates Around Columns.....	23
2.3.3	Marzouk and Hussein: Experimental Investigation on the Behaviour of High Strength Concrete Slabs.....	24
2.3.4	Elgabry and Ghali: Design of Stud-Shear Reinforcement for Slabs.....	25
2.3.5	El-Salakawy, Polak and Soudki: New Shear Strengthening Technique for Concrete Slab-Column Connections.....	26
2.3.6	Rankin and Long: Predicting the Punching Shear Strength of Conventional Slab-Column Specimens.....	27
Chapter 3	Test Program	28
3.1	General Description.....	28
3.1.1	Material Properties.....	28
3.2	Experimental Program.....	33
3.2.1	Equivalent Continuous Slab System.....	33
3.2.2	Test Specimens.....	33
3.2.3	Slab Flexural Reinforcement.....	35
3.2.4	Slab Shear Reinforcement.....	37
3.2.5	Column Reinforcement.....	38
3.3	Preparation of the Test Specimens.....	38
3.3.1	Form-work building.....	38
3.3.2	Caging.....	38
3.3.3	Casting.....	39
3.3.4	Curing.....	39
3.4	Test Set-Up and Experimental Apparatus.....	40
3.4.1	Pedestal Support.....	40
3.4.2	Boundary Conditions.....	42
3.4.3	Corner Restraint.....	42
3.5	Instrumentation.....	43
3.5.1	Strain Gauges.....	43

3.5.2	Displacement transducers.....	44
3.5.3	Video Camera.....	45
Chapter 4	Design of Test Specimens	46
4.1	Dimension and Specimen Selection.....	46
4.2	Yield-Line Analysis.....	47
4.3	Structural Analysis of Continuous Slab System.....	48
4.3.1	Direct Design Method.....	48
4.3.2	Elastic Frame Analysis.....	49
4.4	Two Step Approach to Conventional Slab Design by Rankin and Long....	51
4.4.1	Full Yielding (consideration of yield line) Flexural Failure.....	51
4.4.2	Localized Compression Failure.....	51
4.4.3	Partial Yielding Flexural Failure.....	51
4.4.4	Shear Punching Resistance.....	52
4.5	Shear Design by Code of Practice Requirements.....	53
4.5.1	Shear Resistance without Openings/No Shear Reinforcement.....	54
4.5.2	Shear Resistance with Two Openings/No Shear Reinforcement.....	55
4.5.3	Shear Resistance with Four Openings/No Shear Reinforcement.....	55
4.5.4	Shear Resistance with Transverse Reinforcement by CSA A23.3-94....	56
Chapter 5	Experimental Procedures and Observations	57
5.1	Testing Procedures.....	57
5.2	Test Observations.....	58
5.2.1	Slab SB1.....	58
5.2.2	Slab SB2.....	61
5.2.3	Slab SB3.....	63
5.2.4	Slab SB4.....	65
5.2.5	Slab SB5.....	67
5.2.6	Slab SB6.....	70
Chapter 6	Analysis of Experimental Results.....	73
6.1	Comparison of Various Code Predictions and Theoretical Analysis.....	73
6.2	Stiffness and Ductility.....	74
6.3	Deflection.....	74
6.4	Strains in Longitudinal Reinforcement.....	77
6.5	Strains in Shear Bolts.....	78

6.6 Effectiveness of Shear Bolts in Reducing Crack Width.....	81
Chapter 7 Conclusions and Recommendations.....	83
7.1 Conclusions.....	83
7.2 Recommendations.....	84
Appendix A: Elastic Frame Analysis	85
Appendix B: Experimental Results.....	96
References	132

List of Figures

Figure 1-1:	Flat Plate.....	1
Figure 1-2:	Punching Shear Failure Surface.....	2
Figure 2-1:	Shehata's Model.....	8
Figure 2-2:	Bortolotti's Failure Mechanism and Failure Profile.....	11
Figure 2-3:	Assembly of Load Resisting Struts.....	13
Figure 2-4:	Layout of Radial Strips.....	14
Figure 2-5:	Types of Shear Reinforcement Investigated by Dilger and Ghali.....	22
Figure 2-6:	Load-Deflection Graphs from Dilger and Ghali.....	23
Figure 2-7:	Comparison of Deflection for Prestressed and non-Prestressed Slabs...	24
Figure 2-8:	Shear Stud Reinforcement Specifications.....	26
Figure 2-9:	Typical Arrangement of Shear Bolts in El-Salakawy's Tests.....	27
Figure 3-1:	Typical Specimen.....	29
Figure 3-2:	Specimens Tested.....	30
Figure 3-3:	Typical Stress-Strain Curve for Longitudinal Reinforcement.....	32
Figure 3-4:	Typical Stress-Strain Curve for Shear Bolts.....	32
Figure 3-5:	Test Specimen Shown in Equivalent Structure being Modelled.....	34
Figure 3-6:	Top Mat (Compression Reinforcement).....	35
Figure 3-7:	Bottom Mat (Tension Reinforcement).....	36
Figure 3-8:	Bar Hooks	36
Figure 3-9:	Typical Shear Bolt.....	38
Figure 3-10:	Typical Cage.....	39
Figure 3-11:	Casting by Bucket and Crane Method.....	40
Figure 3-12:	Test Set-up with Pedestals and Slab in Place (Front).....	41
Figure 3-13:	Testing Set-up Frame Only (Side View).....	41
Figure 3-14:	Testing Frame, Data Acquisition and Specimen in Place.....	42
Figure 3-15:	Dimensions of Corner Restraints and Connecting Rods.....	43
Figure 3-16:	Strain Gauge and Terminals.....	43
Figure 3-17:	Position of Strain Gauges.....	44
Figure 3-18:	Positions of LVDTs on a Typical Specimen.....	45
Figure 4-1:	The conventional Slab-Column Specimen.....	46
Figure 4-2:	Yield-Line Pattern for Conventional Slab-Column Specimen.....	47

Figure 4-4:	Moment Coefficients for the Direct Design Method.....	49
Figure 4-5:	Distribution of Statical Moment by the Direct Design method.....	49
Figure 4-6:	Elastic Frame Model Showing Moment of Inertia of Members.....	50
Figure 4-7:	Moments from Elastic Frame Analysis.....	50
Figure 4-8:	Modes of Flexural Failure.....	51
Figure 5-1:	Crack Pattern after Failure.....	60
Figure 5-2:	Crack Pattern after Failure of Specimen SB2.....	62
Figure 5-3:	Crack Pattern after Failure of Specimen SB3.....	64
Figure 5-4:	Crack Pattern after Failure of Specimen SB4.....	66
Figure 5-5:	Crack Pattern after Failure of Specimen SB5.....	69
Figure 5-6:	Crack Pattern after Failure of Specimen SB6.....	71
Figure 6-1:	Load vs Bottom Central LVDT Displacement.....	75
Figure 6-2:	Load vs Internal LVDT Displacement.....	75
Figure 6-3:	Load vs Displacement at LVDT 8.....	76
Figure 6-4:	Load vs Displacement at LVDT 9.....	76
Figure 6-5:	Load vs Longitudinal Reinforcement Strain at L6.....	78
Figure 6-6:	Position of Shear Bolts in Figure 6-7 to 6-11.....	78
Figure 6-7:	Bolt Strain Relative to Distance from the Column of Specimen SB2...	79
Figure 6-8:	Bolt Strain Relative to Distance from the Column of Specimen SB3...	79
Figure 6-9:	Bolt Strain Relative to Distance from the Column of Specimen SB4...	80
Figure 6-10:	Bolt Strain Relative to Distance from the Column of Specimen SB5...	80
Figure 6-11:	Bolt Strain Relative to Distance from the Column of Specimen SB6...	81
Figure 6-12:	Load vs Vertical Crack Width of Specimen SB1.....	82
Figure A-1:	Node Labels.....	94
Figure A-2:	Member Labels.....	95
Figure B-1:	Load-Displacement Graphs of Specimen SB1.....	97
Figure B-2:	Load-Vertical Crack Width of Specimen SB1.....	99
Figure B-3:	Load-Longitudinal Reinforcement Strain Graphs of Specimen SB1.....	100
Figure B-4:	Load-Displacement Graphs of Specimen SB2.....	102
Figure B-5:	Load vs Vertical Crack Width of Specimen SB2.....	104
Figure B-6:	Load-Longitudinal Reinforcement Strain Graphs of Specimen SB2.....	105
Figure B-7:	Load-Bolt Strains Graphs of Specimen SB2.....	107
Figure B-8:	Load-Displacement Graphs of Specimen SB3.....	108

Figure B-9:	Load vs Vertical Crack Width of Specimen SB3.....	110
Figure B-10:	Load-Longitudinal Reinforcement Strain Graphs of Specimen SB3.....	111
Figure B-11:	Load-Bolt Strains Graphs of Specimen SB3.....	113
Figure B-12:	Load-Displacement Graphs of Specimen SB4.....	114
Figure B-13:	Load vs Vertical Crack Width of Specimen SB4.....	116
Figure B-14:	Load-Longitudinal Reinforcement Strain Graphs of Specimen SB4.....	117
Figure B-15:	Load-Bolt Strain Graphs of Specimen SB4.....	119
Figure B-16:	Load-Displacement Graphs of Specimen SB5.....	120
Figure B-17:	Load vs Vertical Crack Width of Specimens SB5.....	122
Figure B-18:	Load-Longitudinal Reinforcement Strain Graphs of Specimen SB5.....	123
Figure B-19:	Load-Bolt Strains Graphs of Specimen SB5.....	125
Figure B-20:	Load-Displacement Graphs of Specimen SB6.....	126
Figure B-21:	Load vs Vertical Crack Width of Specimens SB6.....	128
Figure B-22:	Load-Longitudinal Reinforcement Strain Graphs of Specimen SB6.....	129
Figure B-23:	Load-Bolt Strains Graphs of Specimen SB6.....	131

List of Tables

Table 3-1:	Compressive Strength of Test Cylinders.....	31
Table 3-2:	Summary of Experimental Program.....	34
Table 4-1:	Slab Capacity from Rankin and Long's Method.....	52
Table 4-2:	Shear Resistance of Specimens by Code Provisions.....	54
Table 4-3:	Shear Resistance of Specimens with Two Openings by Code Provisions..	55
Table 4-4:	Shear Resistance of Specimens with Four Openings by Code Provisions..	55
Table 4-5:	Shear Resistance of Specimens Reinforced with Shear Bolts.....	56
Table 5-1:	Longitudinal Reinforcement Strains at Ultimate Load of Slab SB1.....	59
Table 5-2:	Longitudinal Reinforcement Strains at Ultimate Load of Slab SB2.....	63
Table 5-3:	Longitudinal Reinforcement Strains at Ultimate Load of Slab SB3.....	65
Table 5-4:	Longitudinal Reinforcement Strains at Ultimate Load of Slab SB4.....	67
Table 5-5:	Longitudinal Reinforcement Strains at Ultimate Load of Slab SB5.....	68
Table 5-6:	Longitudinal Reinforcement Strains at Ultimate Load of Slab SB6.....	72
Table 6-1:	Test Specimens, Code Provisions and Experimental Results.....	73
Table 6-2:	Stiffness, Displacements and Ductility.....	74
Table 6-3:	Test Results: Yielding of Longitudinal Reinforcement.....	77
Table 6-4:	Maximum Crack Widths.....	81

Chapter 1

Introduction

1.1 Background

Reinforced concrete slabs are relatively thin and flat structural members that function to transfer loads applied perpendicular to their plane. Slabs have a variety of applications in building construction. Primarily they serve as floors and roofs in buildings but are also used as walls, foundation mats, and bridge decks, where they transmit uniformly distributed load components parallel to their plane or relatively heavy concentrated loading.

Reinforced concrete floor slabs are constructed in a variety of ways: in-situ, precast or composite. These may also take a number of different structural forms including: solid, ribbed or waffle and may be reinforced or prestressed. In building construction, slabs are typically supported on beams or girders, which in turn frame into columns or walls. In Canada, slabs supported directly on columns without beams are called flat slabs. The first true North American flat slab was constructed in 1906 by C.A.P. Turner in Minneapolis (McGregor, 2000). Flat plates are flat slabs without drop panels and column capitals. Flat slabs are usually used rather than flat plates for loads in excess of 4.8 kPa and for spans of 6 m to 9 m (McGregor, 2000). A flat plate floor is shown in Figure 1.1.

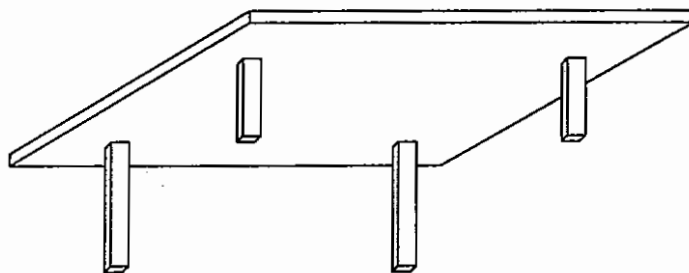


Figure 1-1: Flat Plate

Flat plate construction is very popular mainly because of economy reasons. They are used for multistory building construction because of such advantages as: flat ceilings, simplified formwork, reduced story height and unobstructed lightening. However, with flat plate construction there's

always the problem of high stresses at the column supports that can result in a so-called punching shear failure.

1.2 Punching Shear

Punching shear is a significant failure mode that must be accounted for in the design of slabs. It is critical because it happens without warning. Punching shear (or two-way shear) involves movement of a truncated cone or pyramid-shaped surface around a column as shown in Figure 1.2.

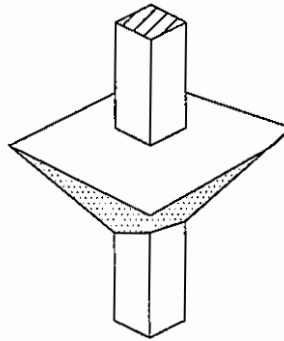


Figure 1-2: Punching Shear Failure Surface

1.3 Openings Around Columns

Holes and ducts around columns in slabs are undesirable structurally because they cause an effective reduction in the critical perimeter for punching shear. In some situations however, these cannot be avoided for functionality reasons. Therefore, codes of practice have recommended ways to take into account the strength reduction at slab-column connections due to such openings.

Typically the codes recommend projecting the dimensions of the openings on the critical perimeter. Reagan (1974) has pointed out that the design standards have not accounted for unsymmetrical arrangement of openings. When openings are unsymmetrical in an interior connection eccentricity of loading is introduced at the critical perimeter.

1.4 Conventional Slab-Column Tests

Two different types of set-ups have been adopted in tests studying the behavior of slab-column connections. These are isolated slab-column connections and slab-column subsystems.

Isolated slab-column connections consist of a column stub integrally cast with an area of surrounding slab. The dimensions of the surrounding slab are chosen to represent the span of the lines of contraflexure or zero moment in a continuous slab system. In isolated tests, the slab is either supported along its boundary and load applied through the column or the column is supported and the load applied transversely at some distance from the column (FIB, 2001).

Slab-column subsystem tests are not very popular due to their cost. They would usually consist of more than one column stub or columns integrally cast with an area of surrounding slab whose boundaries represent lines of contraflexure.

1.5 Objectives

Bent-up bars, stirrups (closed and U-shaped), shearheads and shear studs are some of the acceptable methods for reinforcing new slabs against punching shear failure. Dilger et al (1981) identified the requirements for ideal punching shear reinforcement as follows: good anchorage at top and bottom of shear reinforcement, minimal interference with placing flexural reinforcement, ease of installation in thin slabs, no significant anchor plate projection above slab surface and economy of use. When additional strength is needed after construction due to design errors or drilling of openings for local services a need arises for a method of retrofit reinforcing that will provide the additional punching shear resistance.

The main objective of this program was to determine the effectiveness of a new type of reinforcement, called shear bolt, in strengthening interior slab-column connections against punching shear failure.

In addition, the effectiveness of shear bolt reinforcement in strengthening slabs with openings around the column was also studied.

1.6 Scope of Research

The present study was an experimental investigation of interior slab-column connections. A study on the use of shear bolts in strengthening edge slab column connection was previously carried out by El-Salakawy et al (2003).

Six isolated slab-column specimens representing interior slab-column connections were constructed. The specimens had varying amounts of punching shear reinforcement and were with or without openings. Loading, displacement and strain data were collected during testing. The data was compared to predictions from codes of practice and other analytical methods.

1.7 Contents of Thesis

This thesis is divided into six chapters and three appendices.

Chapter 1 is the introduction and contains a background, objectives and scope of the research program.

Chapter 2 provides further background information and a review of past research in literature on punching shear.

Chapter 3 is a detailed description of the test program designed to study the effects of shear bolts.

Chapter 4 summarizes the design process. The stipulations of design specifications are investigated. The yield line method is presented as well as other methods used.

Chapter 5 contains details of the experimental procedures and observations. Crack patterns, strain history and maximum deflections are discussed.

Chapter 6 reviews the results and data from the test in light of codes of practice and other analytical methods.

Chapter 7 contains the conclusions drawn from this study and recommendations are provided for further research.

Presented in the **appendices** is a print out of the elastic frame analysis and graphs showing the data collected during testing for all slabs.

Review of Literature

2.1 Punching Shear Models

2.1.1 Rotational Models

2.1.1.1 Kinnunen and Nylander

Kinnunen and Nylander (1960) published the first mathematical model for punching shear. Their model essentially considered a circular polar-symmetric slab supported by a centralized column and loaded externally with a uniformly distributed load on the slab area. The derivation was based on experimental testing on 61 slabs not reinforced transversely. The model consists of rigid sectors outside the punching cone of a typical punching shear failure. The boundaries of the sectors consist of two radial crack planes and an inclined crack surface. Further, the sectors are supported by a triaxially compressed truncated conical shell extending from the column to the root of the inclined shear crack surface.

Failure criteria were defined as a limitation on either the inclined radial compressive stress or the tangential compressive strain at the shear crack. Kinnunen and Nylander derived Equation 2.1 and 2.2 to predict the ultimate load of a non-shear-reinforced slab by iteration of the ratio of the concrete compression zone k_x such that $V_{u,c}$ and $V_{u,s}$ are equal..

$$V_{u,c} = \kappa\pi\eta d^2 k_x \frac{1 + \frac{2k_x}{\eta}}{1 + \frac{k_x}{\eta}} \sigma_{cu} f(\alpha) \quad (2.1)$$

$$V_{u,s} = \kappa 4\pi\rho f_y d r_f \left[1 + \ln\left(\frac{\delta d}{2r_u}\right) \right] \frac{1 - \frac{k_x}{3}}{\delta - \eta} \quad (2.2)$$

where,

$$f(\alpha) = \frac{\tan \alpha (1 - \tan \alpha)}{1 + \tan^2 \alpha}$$

k_x = concrete compression zone

η = column size to depth ratio

d = effective depth

α = inclination of conical shell

σ_{cu} = ultimate concrete stress

$$\delta = \frac{l_{slab}}{d}$$

r_u = radius of conical shell

r_f = radius of yielded circular area inside conical shell

2.1.1.2 Shehata

Shehata and Regan (1989) modified the Kinnunen/Nylander model. He described the punching region of a slab as made up of rigid radial segments with a fulcrum at the level of the neutral axis on the column face. Shehata identified external and internal forces acting on a radial segment of the slab as follows: the external applied load P ($\Delta\Phi/2\pi$) at radius $r = r_p$; the radial component of the resultant ring tension forces $F_{st}\Delta\Phi$ due to slab deformation; the radial component of the resultant ring compression forces $F_{st}\Delta\Phi$ due to slab deformation; the inclined bearing force dF_{cr} at the column face acting on the axis of symmetry of the prismatic frontal part of the segment; the radial net force dF_{st} ; and the dowel force dD on the steel cutting across the inclined crack (Figure 2-1).

Failure criteria were defined by a limitation on the ability of the frontal part of the radial segment to support the force at the column face. There were three possible cases as follows: if the angle α of the compressive force reaches 20° , there are principal tensile stresses in the compressed front part and failure occurs by concrete splitting; if the average radial strain on the compressed face reaches a value of 0.0035 in the plastic length starting from the column face, there is a radial crushing of the concrete; or if the tangential strain of the compressed face reaches 0.0035 at a distance x from the column face, there is a tangential crushing of the concrete.

The ultimate punching resistance can be obtained by satisfying Equation 2.3 and two other equations given in their publication, when a rotation ψ_u at which one of the critical states is reached is found.

$$P \frac{\Delta\phi}{2\pi} (r_p - r_o) = (dF_{sr} + dF_{sr,p} + F_{st}\Delta\phi + F_{st,p}\Delta\phi) \cdot z + dD(r_w - r_o) \quad (2.3)$$

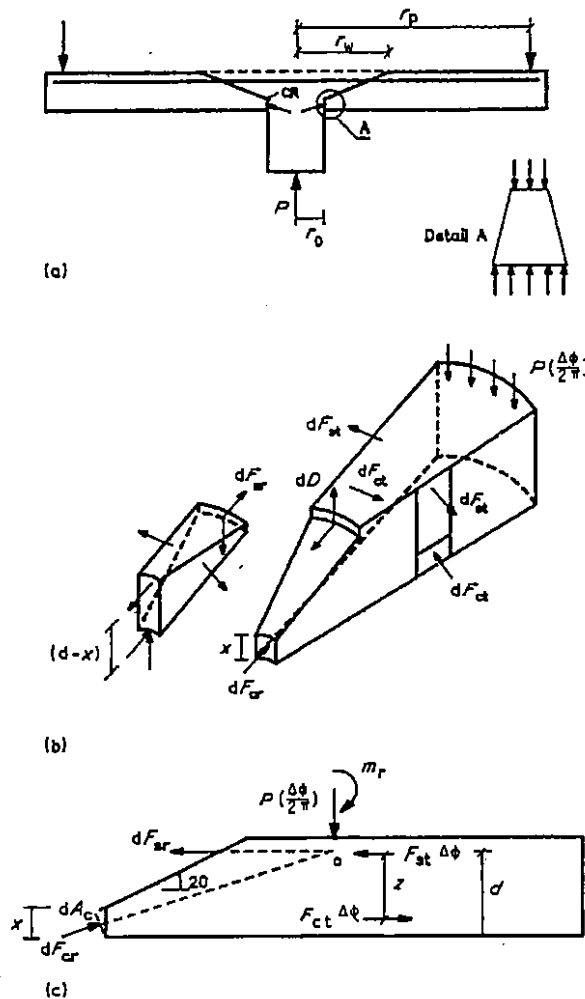


Figure 2-1: Shehata's Model (a) Stress Concentration (b) Forces acting on a Segment (c) Forces acting on a Segment in a Radial Plane (Shehata and Regan, 1989)

where,

D = dowel force

d = effective depth of a slab

r_p = radius of a peripheral load or reaction

r_o = radius of the column or loaded area

r_w = wedge radius (punching radius)

$\Delta\phi$ = small sectoral angle

2.1.1.3 Broms

Broms (1990) introduced two principal modifications to the Kinnunen/Nylander rotational model. First, he adopted standard values of concrete properties rather than calibrated values from test results. Secondly, he calculated different heights of the compression zone in the radial and tangential directions opposed to the Kinnunen and Nylander's iterative approach. He further accounts for unsymmetrical punching and size effect in his modified model. Just like the Kinnunen and Nylander's model, two broad failure mechanisms were identified as possible causes of failure in punching. For the high tangential compressive strain failure mechanism, a limiting value of ε_{cpu} as in Equation 2.4 was proposed from which a value of punching load V_e could be calculated (see Broms, 1990 for the equations for V_e).

$$\varepsilon_{cpu} = 0.0008 \left(\frac{150}{\alpha x_{pu}} \cdot \frac{25}{f'_c} \right)^{0.333} \quad (2.4)$$

The radial concrete compressive stress failure mechanism comes into play when the compressive stress in the imaginary conical shell reaches a critical value of $1.1f'_c$ at the bottom of the shear crack. The punching load is described by Equation 2.5.

$$V_\sigma \approx 0.46(b + 3.5y)yf'_c \left(\frac{300}{y} \right)^{0.333} \quad (2.5)$$

The critical punching load is determined as the lesser of V_e and V_σ .

where,

x_{pu} = height of the compression zone at flexure in the tangential direction when punching occurs

αx_{pu} = height of the equivalent rectangular stress block with the stress f'_c

y = approximate thickness of conical shell

b = diameter of column

2.1.2 Models based on Classical Plasticity Theory

2.1.2.1 Braestrup et al

Braestrup et al (1976) observed that there are distinct surfaces of discontinuity when a shear failure occurs. They considered these discontinuities to be narrow, rigid-plastic regions of concrete that move relative to each other. By applying classical plasticity theory, they assumed that work dissipated in the discontinuity could be calculated. This work, added to any work dissipated in the reinforcement, is then equated to the work done by the applied load causing the relative movement, to arrive at an upper bound method.

The failure criterion adopted for the concrete in the narrow plastic zone is the modified Coulomb Yield criterion defined by three parameters: cohesion c , the angle of friction Φ , and the effective tensile strength f_{te} . Further, the yield criterion was described as a combination of two parts: the sliding criterion in Equation 2.6 and the separation criterion in Equation 2.7.

$$\tau = c - \sigma \tan \phi \quad (2.6)$$

$$\sigma = f_{te} \quad (2.7)$$

For the case of punching shear, an upper bound solution for the axisymmetric punching strength of a slab was derived. In general implicit form, the total work dissipated in a failure surface is obtained from Equation 2.8.

$$W_i = \delta \int_0^h F(r, r') dx \quad (2.8)$$

And the external work done by load is $P\delta$

The work equation derived is shown in Equation 2.9. The explicit form is solved by variational calculus from which the lowest upper bound and hence the solution can be found.

$$P = \int_0^h F(r, r') dx \quad (2.9)$$

where,

δ = virtual displacement

$F(r,r')$ = function of r and r'

2.1.2.2 Plasticity Model by Bortolotti

Bortolotti’s model (1990), takes into account strain softening in concrete. A rigid-plastic failure mechanism subjected to a uniform vertical displacement rate field v was assumed.

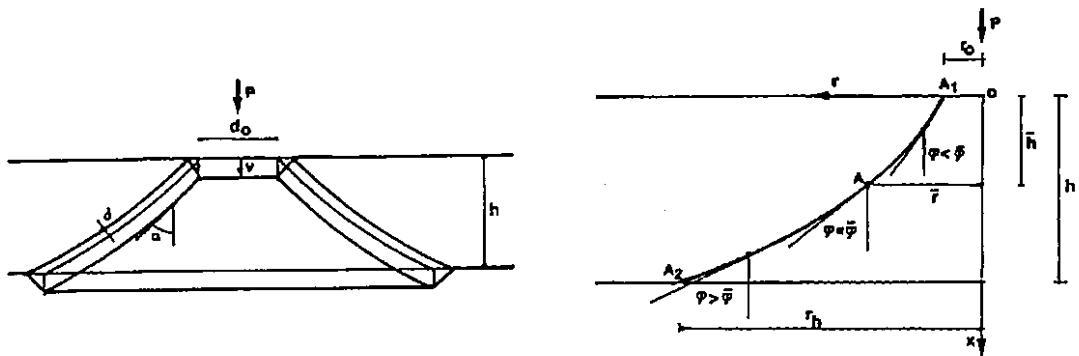


Figure 2-2: Bortolotti’s Failure Mechanism and Failure Profile (Bortolotti, 1990)

Bortolotti considered the failure profile shown in Figure 2-2 and assumed that every point in the tract AA_1 of the failure profile, where $\Psi < \Phi$, undergoes a compression like softening. In tract AA_2 , where $\Psi > \Phi$, it is assumed points undergo tension like softening.

The failure conditions in Equations 2.10 and 2.11 were proposed:

$$\varphi < \Phi \quad \sigma_1.(1 + \sin \Phi) - \sigma_3(1 - \sin \Phi) - 2f_t = 0 \tag{2.10}$$

$$\varphi > \Phi \quad \sigma_1.(1 + \sin \Phi) - \sigma_3(1 - \sin \Phi) - f_c(1 - \sin \Phi) = 0 \tag{2.11}$$

where,

φ = internal friction angle

Φ = instantaneous value of the internal friction angle

2.1.3 Other Models

2.1.3.1 Fracture Mechanics Model by Bazant/Cao

Bazant and Cao (1987) in their proposed model attempted to account for the variability of nominal shear stress at failure of geometrically similar reinforced concrete slabs on different scales. They based the failure load on energy and stability ultimate criteria rather than strength criteria as in the plasticity theory. A new nonlinear form of fracture mechanics was formulated that models the size effect more accurately from a blunt crack band model.

For analysis based on plastic theory, the normal shear stress at failure $v_u = P_u/bd$ of geometrically similar structures is independent of size. However, a decrease in normal shear stress v_u was observed as structure size increases for both the classical linear elastic fracture mechanics and non-linear fracture mechanics. Bazant/Cao proposed Equation 2.12 based on non-linear fracture mechanics theory.

$$v_u = C \left(1 + \frac{d}{\lambda_o d_a} \right)^{-\frac{1}{2}} \quad (2.12)$$

where,

$$C = k_1 f_t' \left(1 + k_2 \frac{d}{b} \right)$$

k_1, k_2 = empirical constants

b = punch diameter

d = slab thickness

λ = empirical parameter characterizing the fracture energy of the material and the shape of the structure

d_a = maximum aggregate size

2.1.3.2 Truss Model for Two-way Shear by Alexander and Simmonds

Alexander and Simmonds (1987) developed a quantitative model for punching based on the plasticity theory. They suggest that an appropriate model for both ultimate capacity and slab-column connection behavior must account for the following variation in parameters: the overall connection geometry, the concrete strength, and the yield strength of flexural reinforcement.

Alexander and Simmonds proposed a 3-D space-truss model composed of concrete compression struts and steel tension ties. The compression struts were either parallel to the plane of the slab (anchoring struts) or were at some angle α to the plane of the slab (shear struts). The shear struts were further differentiated into:

- Gravity Struts: these oppose the downward movement of the slab relative to the column and are tied by top mat steel.
- Uplift Struts: Shear struts that oppose the upward movement of the slab relative to the column and are tied by bottom mat steel.

Figure 2-3 shows a qualitative description of the truss model for punching shear. A failure criterion was defined in terms of three possible modes: first, failure of the tension tie, second, failure of the compression struts and lastly, a shear strut failure, which may occur if the out of plane component of the compression strut exceeds the confining strength of the slab.

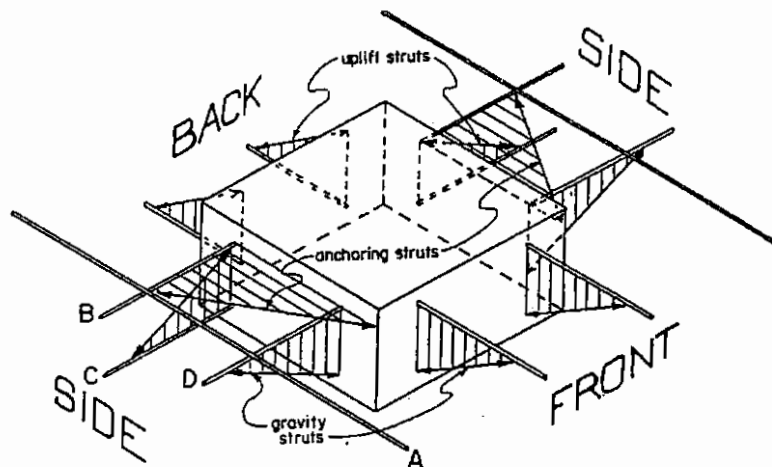


Figure 2-3: Assembly of Load Resisting Struts (Alexander and Simmonds, 1987)

2.1.3.1 Bond Model by Alexander and Simmonds

Alexander and Simmonds (1992) developed a model describing the behavior of concentrically loaded flat-plate-column connections at failure. Their bond model, which is a modification of Alexander-Simmonds (1987), gave a description of the mechanism of shear transfer for orthogonally reinforced slab-column connections that is consistent with test observations.

As in the truss model, the bond model describes the slab-column connection as an assembly of steel tension ties and concrete compression struts. Alexander and Simmonds noted from tests that the compression strut was actually a curved arch as shown in the Figure 2-4.

The revised model suggests a link for shear transfer in a slab-column connection to force gradients in the reinforcement close to the column. However, since force gradient in reinforcement is closely linked to bond, the new model is called the Bond Model. Like the truss model, the bond model requires a rectangular layout of reinforcement. Four radial strips, which carry all loads reaching the column, extend from the column parallel to the reinforcement as shown in Figure 2-4.

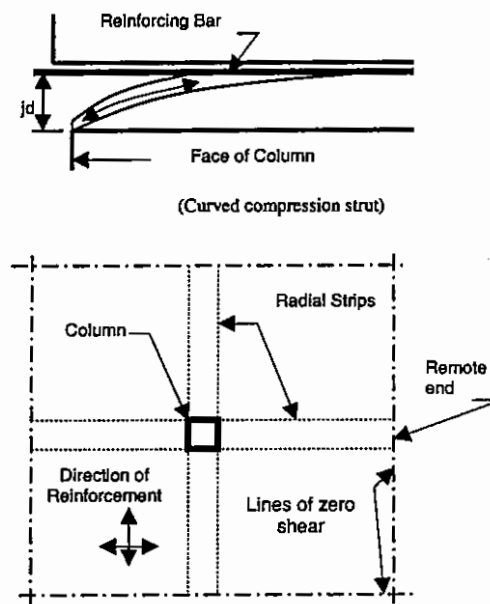


Figure 2-4: Layout of Radial Strips (Alexander and Simmons, 1992)

The punching capacity of the slab-column connection P is obtained by summing the contribution of each radial strip. The final equation predicting the shear capacity of the connections is given in Equation 2.13.

$$P = \sum P_s = 8\sqrt{M_s \times w} \quad (2.13)$$

$$M_s = \frac{2 \times w l^2}{2}$$

2.1.3.3 Empirical Based Model by Moe

This empirical model proposed by Moe in 1961 is the basis of ACI 318 1963. Two limit states are used to describe punching failure, namely V_{flex} and V_{shear} . Moe suggested the following relationship between flexural and shear capacity.

$$\frac{V_u}{V_{shear}} + A \frac{V_u}{V_{flex}} = 1 \quad (2.14)$$

in Equation 2.14, A is an empirical factor from test results. The final equation for ultimate shear capacity he proposed is:

$$V_u = \frac{Cw(1 - 0.058\eta)u_{col}d\sqrt{f_c}}{1 + \frac{0.436}{V_{flex}}u_{col}d\sqrt{f_c}} \quad (2.15)$$

where,

$$V_{flex} = Cw(1 - 0.59w)d^2 f_c$$

$$w = \rho \frac{f_y}{f_c}$$

$$\eta = \frac{c_2}{d}$$

$$C = \text{Constant}$$

$$u_{col} = \text{perimeter of column or loaded area}$$

2.2 Shear Design Procedures for Reinforced Concrete Slabs

The various reinforced concrete design standards (ACI, CSA, BS8110, Euro code, Model Code) examined are based on a limit state design. The requirements for shear design in all the codes is such that the capacity must be greater than the nominal load, stated as follows:

$$V_u \leq V_n \quad (2.16)$$

$$V_u = \frac{V}{u \cdot d} \quad (2.17)$$

$$V_n = V_c + V_s \quad (2.18)$$

where,

V_n = nominal shear capacity of the critical section

V_u = ultimate shear stress

V_c = punching shear resistance of concrete

V_s = punching resistance of the steel

All the standards specify that in shear reinforced slabs, the nominal shear stress must be limited to the resistance of the slab at a critical perimeter. And then checks are made at outer perimeters such that the shear stress does not exceed the resistance anywhere at the connection.

2.2.1 American Specification ACI 318-99

Critical Perimeter

The critical section is defined as 0.5d from column perimeter.

Shear resistance of a section without shear reinforcement

$$v_c = \min \left\{ \begin{array}{l} \frac{1}{3} \sqrt{f'_c} \\ \frac{\sqrt{f'_c}}{12} \left(2 + \frac{4}{\beta_c} \right) \\ \frac{\sqrt{f'_c}}{12} \left(2 + \frac{\alpha_s d}{b_o} \right) \end{array} \right\} \quad (\text{MPa}) \quad (2.19)$$

$\alpha_s = 40$ for interior column, $\beta_c =$ column aspect ratio

Shear resistance with shear reinforcement

$$V_u \leq \phi V_r \quad (2.20)$$

$\phi = 0.85$ for shear

$$v_r = v_c + v_s \quad (2.21)$$

where,

$$v_s = \frac{\phi_s A_{vs} f_{yv}}{b_o s} \quad (2.22)$$

$$f_{yv} \leq 414 \text{ MPa}$$

For headed shear reinforcement, maximum resistance of concrete with shear reinforcement,

$$v_c = 0.167 \lambda \phi_c \sqrt{f'_c} \quad (2.23)$$

Maximum shear resistance of section with shear reinforcement

$$V_{f \max} \leq 0.67 \lambda \phi_c \sqrt{f'_c} \quad (2.24)$$

where,

A_{vs} = the area of shear reinforcement

f_{yv} = yield strength of shear reinforcement

b_o = length of the critical perimeter

s = spacing of concentric rows of shear reinforcement around a column

γ = strength factor of concrete

ϕ_c = resistance factor for concrete

2.2.2 Canadian Standard CSA A23.3-94

Critical Perimeter

The critical section is defined as 0.5d from column perimeter

Shear resistance of a section without shear reinforcement

$$v_c = \min \begin{cases} 0.4\sqrt{f'_c} \\ 0.2\sqrt{f'_c} \left(1 + \frac{2}{\beta_c} \right) \\ \sqrt{f'_c} \left(0.2 + \frac{\alpha_s d}{b_o} \right) \end{cases} \quad (\text{MPa}) \quad (2.25)$$

Shear resistance with shear reinforcement

$$\phi V_f \leq V_r \quad (2.26)$$

$$v_r = v_c + v_s \quad (2.27)$$

where,

$$v_s = \frac{\phi_s A_{vs} f_{yv}}{b_o s} \quad (2.28)$$

For headed shear reinforcement maximum resistance of concrete with shear reinforcement,

$$v_c = 0.3\lambda\phi_c\sqrt{f'_c} \quad (2.29)$$

Maximum shear resistance of section with shear reinforcement

$$V_{f \max} \leq 0.8\lambda\phi_c\sqrt{f'_c} \quad (2.30)$$

2.2.3 Eurocode 2 ENV 1992-1-1

The Eurocode 2 ENV 1992-1-1 document defines the following parameters for shear design:

- V_{Rd1} is the design shear resistance per unit length of the critical perimeter, for a slab without shear reinforcement
- V_{Rd2} is the maximum design shear resistance per unit length of the critical perimeter, for a slab with shear reinforcement
- V_{Rd3} is the design shear resistance per unit length of the critical perimeter, for a slab with shear reinforcement

V_{sd} the shear force per unit length along the critical section

Critical Perimeter

The critical perimeter is defined as the perimeter surrounding the loaded area and at a distance $1.5d$ from it.

Shear resistance of a section without shear reinforcement

When,

$$v_{sd} \leq v_{Rd1} \text{ , no shear reinforcement is required} \quad (2.31)$$

$$V_{Rd1} = \tau_{Rd} k(1.2 + 40\rho_l)d \quad (2.32)$$

$$\tau_{Rd} = 0.25f_{ct}k0.05/\gamma_c$$

$$k = (1.6 - d) \geq 1.0$$

Shear resistance of a section with shear reinforcement

When Equation 2.35 is not satisfied, shear reinforcement is required such that

$$V_{sd} \leq V_{Rd3} \quad (2.33)$$

where,

$$V_{Rd3} = V_{Rd1} + \sum A_{sw} f_{yd} \frac{\sin \alpha}{u} \quad (2.34)$$

Maximum shear resistance of section with shear reinforcement

$$V_{Rd2} = 1.6 \cdot V_{Rd1} \quad (2.35)$$

where,

v_{sd} = shear force per unit length along critical section

f_{yd} = design yield stress of the reinforcement

ρ_l = equivalent longitudinal reinforcement ratio

τ_{Rd} = basic Shear strength of members without shear reinforcement

u = perimeter of critical section for punching shear

α = angle between reinforcement and the plane of the slab

2.2.4 CEB-FIP Model Code 90

Critical Perimeter

The critical section is defined as $2.0d$ from the column perimeter.

Shear resistance of a section without shear reinforcement

It should be verified that

$$v_{Sdc} \leq v_{Rd1} \quad (2.36)$$

where,

$$v_{Rd1} = 0.12\xi(100\rho \cdot f_{ck})^{\frac{1}{3}} \quad (2.37)$$

and,

$$\xi = 1 + \sqrt{200/d}$$

Shear resistance of a section with shear reinforcement

The model requires that punching shear resistance be verified in three zones

- The zone immediately adjacent to the loaded area

$$P_{sd} \leq u_o d (0.5 f_{cd2}) \quad (2.38)$$

- The zone in which the shear reinforcement is placed

$$P_{sd} \leq 0.75V_{Rd1} + 1.5 \frac{d}{S_r} A_{sw} f_{ywd} \sin \alpha \quad (2.39)$$

$$f_{ywd} \leq 300 \text{ MPa}$$

- The zone outside the shear reinforcement

$$P_{sd} \leq 0.12\xi(100\rho f_{ck})^{\frac{1}{3}} u_{n,ef} d \quad (2.40)$$

Maximum shear resistance of section with shear reinforcement

$$\frac{P_{sd,ef}}{u_o d} \leq 0.5 f_{cd2} \quad (2.41)$$

$$f_{cd2} = 0.6(1 - f_u/250) \cdot u_o \cdot d$$

where,

- v_{sdc} = shear stress on concrete section
- f_{ck} = characteristic strength of concrete
- f_{ywd} = characteristic strength of steel
- ρ_l = ratio of flexural tensile reinforcement
- u_o = length of periphery of column or loaded area
- s_r = radial spacing of layers of shear reinforcement
- $u_{n,ef}$ = the critical perimeter 2.0 d from the out layer of shear reinforcement
- A_{sw} = area of shear reinforcement in a layer around the column

2.3 Selected Experimental Studies on Punching Shear

2.3.1 Dilger and Ghali: Shear Reinforcement for Concrete Slabs

Dilger and Ghali (1981) investigated four different types of shear reinforcement at the University of Calgary. Figure 2-5 shows three of the types studied.

They tested 40 slab-column connections with various types of shear reinforcement they developed. Most of the specimens were subjected to pure concentric axial load. The flexural reinforcement provided had a ratio of approximately 1.1% and concrete design strength was 28 MPa. From their tests, they reported that full yield strength of the types of shear reinforcement was reached and that only shear in excess of $0.33\sqrt{f'_c}$ (MPa) needed to be resisted by the shear reinforcement. CSA A23.3-M77 and ACI 318-1977 both require that shear stresses higher than $0.17\sqrt{f'_c}$ (MPa) be carried by shear steel (CSA now requires $0.2\sqrt{f'_c}$ due to lower load safety factors).

They compared their findings to ACI Specification 318-1977 and Canadian Standard CAN A23.3-

M77 (which both required $0.17\sqrt{f_c'}$ (MPa)) and an ultimate nominal shear resisted by steel and concrete as $0.5\sqrt{f_c'}$ (MPa). A typical load-deflection curve from their test is shown in Figure 2-6. They suggested from their experiment that the upper limit of shear resistance could be as high as $0.67\sqrt{f_c'}$ (MPa). They also found that v_c' decreases as the distance of the critical section from the column face increases.

They suggested design rules for punching shear at the critical section at $d/2$ from the column face.

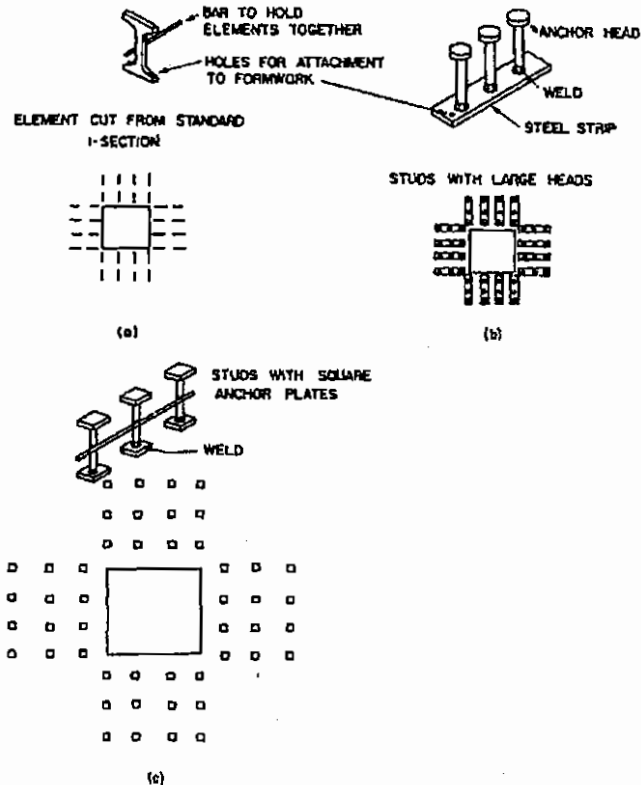


Figure 2-5: Types of Shear Reinforcement Investigated by Dilger and Ghali
(Dilger and Ghali, 1981)

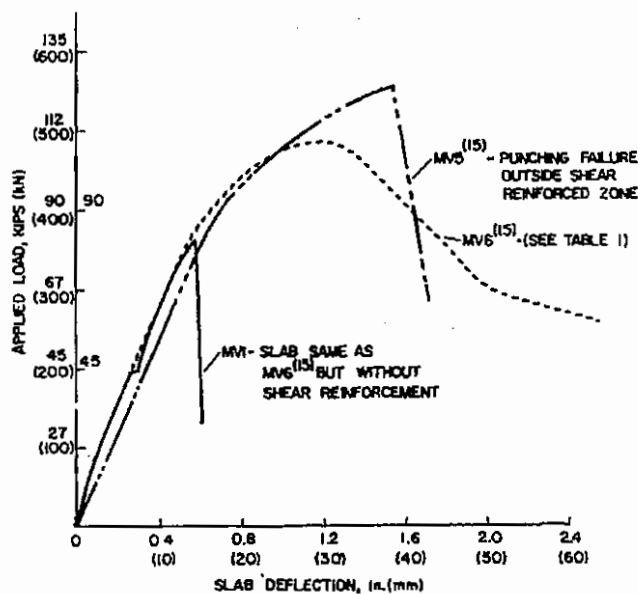


Figure 2-6: Load-Deflection Graphs from Dilger and Ghali
(Dilger and Ghali, 1981)

2.3.2 Ghali, Sargious and Huizer: Vertical Prestressing of Flat Plates Around Columns

Ghali et al (1974) tested 10 specimens to study the effect of vertical prestressing near the column perimeter on the punching shear capacity of reinforced concrete slabs. Vertical prestressing was provided by unbonded high tensile steel bolts.

Figure 2-7 is a graph from their research showing a comparison of the non-prestressed and prestressed specimens. The figure and other results they presented showed that the prestressed slabs could withstand a much higher deflection before failure occurs. This is an indication of the merits of the prestressing in substantially increasing the ductility of the connection.

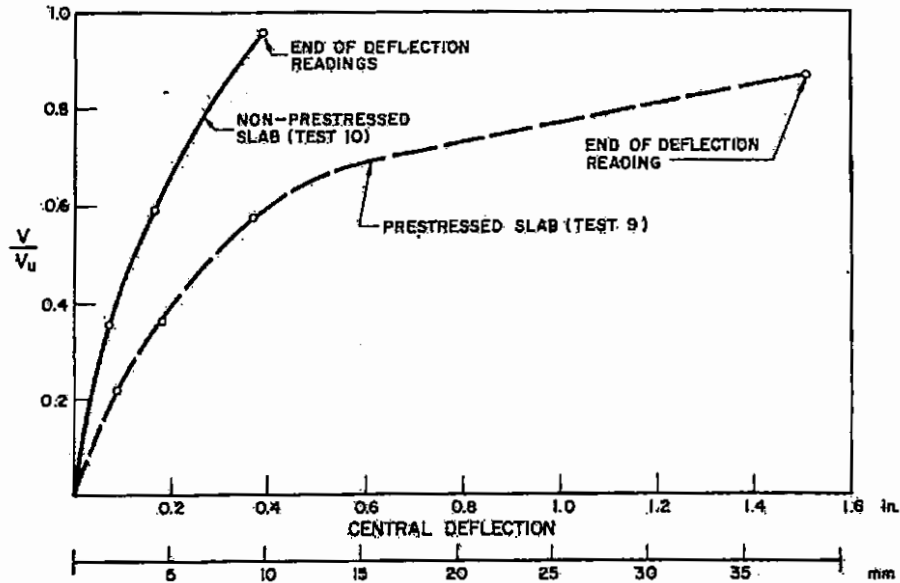


Figure 2-7: Comparison of Deflection for Prestressed and Non-Prestressed Slabs
(Ghali et al, 1974.)

2.3.3 Marzouk and Hussein: Experimental Investigation on the Behavior of High-Strength Concrete Slabs

Marzouk and Hussein (1991) tested 17 reinforced concrete slabs to investigate the deformation and strength characteristics of punching shear failure of high-strength concrete slabs. These characteristics were studied with respect to the following parameters: deformation, slab-rotation, strains, ultimate capacity, ductility, energy absorption, and failure mode.

Marzouk and Hussein described the slab stiffness in terms of the load deflection curve. "For most slabs failing in punching shear, the load deflection curves can be represented by two straight lines with different slopes". The first is the stiffness of the uncracked slab and the other is the stiffness of the cracked slab. The stiffness of the uncracked slab is described as the slope of the load deflection curves reaching loads of up to 0.2 times ultimate load. The stiffness of the cracked slab μ is the slope of the load- deflection curve extending up to the load that causes first yielding of

reinforcement. Ductility was also defined as the ratio of the ultimate deflection to the deflection at first yield.

The variables of their test were slab depth, reinforcement ratio and concrete compressive strength. They defined three failure types as: pure flexural failure, pure punching failure and ductile shear failure. Pure flexural failure took place in slabs when most of the reinforcement yielded before punching occurred and the slab consequently experienced large deflections prior to failure. In pure shear failure, the slab showed small deflections, with the yielding of the tension steel being much localized at the column head. The third type of failure was a transition between the two cases.

They reported a punching shear surface for most slabs forming at a distance of 1.2 to 1.6 times the slab depth from the column face. One significant conclusion from their paper was that the influence of concrete strength in the North American codes of practice is conservative and that adopting a cubic root of the compressive strength will result in more accurate and consistent analysis.

2.3.4 Elgabry and Ghali: Design of Stud-Shear Reinforcement for Slabs

Elgabry and Ghali (1990) presented design and detailing rules for use of shear stud reinforcement based on previous experimental data. Based on extensive testing, they recommended the following as illustrated in Figure 2-8:

- Bottom anchors should be in the form of steel strips and its width should be greater than $2.5D$,
- Top anchors could be in the form of circular or square plates with the limitations that the areas be at least 10 times the area of the stem,
- In the direction parallel to a column face, the distance between anchor strips should not exceed $2d$, d is the effective depth of the slab.
- Bottom anchor strips should be aligned parallel to column faces
- Minimum distance of the first peripheral line from the column s_o should be $d/4$. They suggested upper limits for both s_o and the spacing s based on the value of the factored shear stress.

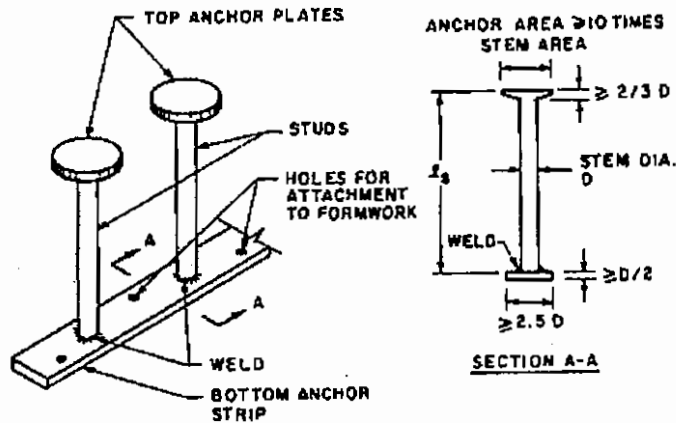


Figure 2-8: Shear Stud Reinforcement Specifications (Elgabry and Ghali, 1990)

2.3.5 El-Salakawy et al: New Shear Strengthening Technique for Concrete Slab-Column Connections

El-Salakawy et al (2003) carried out a study on the same method of transverse reinforcing. They tested a total of six specimens. The objective of their study was to determine the effectiveness of shear bolt transverse reinforcement at edge slab-column connections with a combination of concentric and eccentric loading. Test slabs were 1540 x 1020 x 120 mm in dimension monolithically cast with a column 250 mm square section. The average reinforcement ratio in the tension mat of the specimens was 0.75 %, while they provided an average of 0.45 % in the compression mat. The arrangement of shear bolts from their paper is shown in Figure 2-9.

El-Salakawy reported maximum deflections measured at ultimate load of between 54 – 162 % larger for the specimens reinforced with shear bolts than for those not reinforced. Secondly, they reported that maximum flexural steel strain was observed directly underneath the front face (parallel to the free edge) of the column. The maximum strains for the specimens reinforced with shear bolts were between 8 and 39 % than for corresponding specimens without shear bolt reinforcement. Finally, there was a reported enhancement of ultimate strength of 12 to 13 % for the reinforced specimens.

The conclusion was that the bolts were effective transverse reinforcement that can be used for strengthening and retrofit of existing slabs.

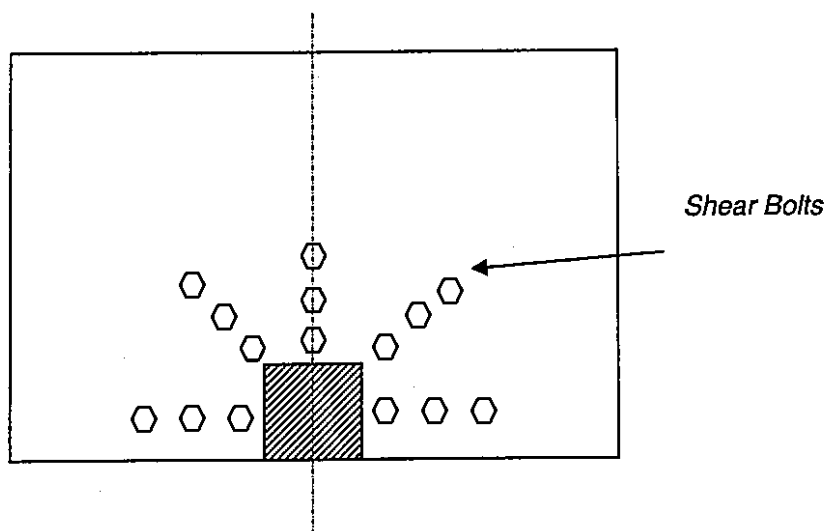


Figure 2-9: Typical Arrangement of Shear Bolts in El-Salakawy's Tests

(El-Salakawy et al, 2003)

2.3.6 Rankin and Long: Predicting the Punching Strength of Conventional Slab-Column Specimens

Rankin and Long (1987) proposed a method for predicting the strength of conventional slab-column specimens from rational concepts of various failure modes. The failure modes were classified broadly as flexural or shear. For either failure mode, in conventional specimens, experiments have shown that the ultimate load capacity is reached when a truncated cone or pyramid of concrete is punched through the slab by the loaded column (Rankin and Long).

Long (1975) suggested that punching strength is the lesser of either a flexural or shear criterion of failure. Rankin and Long's approach is a modification of Long (1975) in which the ultimate moment capacity is derived as a (analytically based linear interpolative moment) factor of the yield moment. The punching shear capacity was based on a semi-empirical relationship of the vertical shear stress on the critical section for failure. Three possible modes of flexural failure are described as full-yielding (yield-line), localized compression failure, and partial yielding. The shear mode of failure is precipitated by internal diagonal tension cracking prior to the development of yielding of the reinforcement or crushing of the concrete (Long, 1975).

The predicted punching strength of the conventional slab-column specimen was defined as a lesser of the flexural failure mode or the shear failure mode.

Chapter 3

Test Program

3.1 General Description

A total of six slabs of dimensions 1800 mm by 1800 mm by 120 mm were built and tested. A typical specimen is shown in Figure 3-1. All specimens had the same amount and placement of orthogonal longitudinal reinforcement. The specimens had column stubs through which the loading was applied to the slab during testing. Each column had a square cross-section: 150 mm by 150 mm and a height of 150 mm extending beyond the top and bottom face of the slab. All columns were reinforced with four 20 mm bars enclosed in four 8 mm ties.

Two of the specimens were built with openings placed next to the column stub; the remaining four had no openings. Openings were to simulate reinforced concrete construction in which openings are made in floors to allow wells or ducts for ventilation, electrical and other services. The six specimens constructed are shown in Figure 3-2.

The variables of the test program were the number of peripheral rows of shear bolts reinforcement applied, and number of symmetrically placed openings around the column.

3.1.1 Material Properties

Concrete

The specimens were cast with concrete made from normal Portland cement. Ready-mix concrete with a specified compressive strength of 25 MPa was used. A super-plasticizer was added to the second batch to improve workability. *Normal $f'_c = 25 \text{ MPa}$*

A combination of at least six 150 mm by 300 mm and six 101.6 mm by 101.6 mm (4 inch by 8 inch) control cylinders was made for each casting batch. Standard material properties of concrete were determined from these control cylinders. The cylinders were made, compacted and tested according

to Canadian Standard A23.3.2-9C and A23.3.2-13C, for the compressive strength and splitting tensile strength of the specimens respectively.

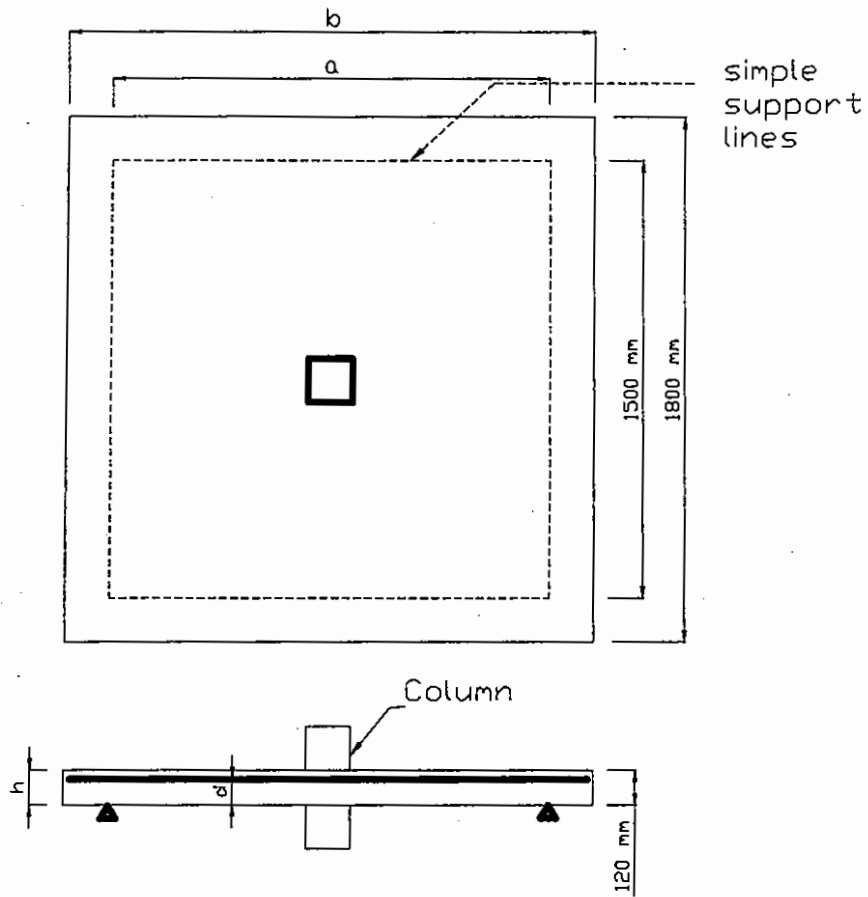


Figure 3-1: Typical Specimen in Plan and Elevation

The control cylinders were cured under the same conditions as the test specimens and compression tests were carried out at the end of the first test. Splitting tensile tests were carried out later. Table 3-1 lists the results from the material properties tests.

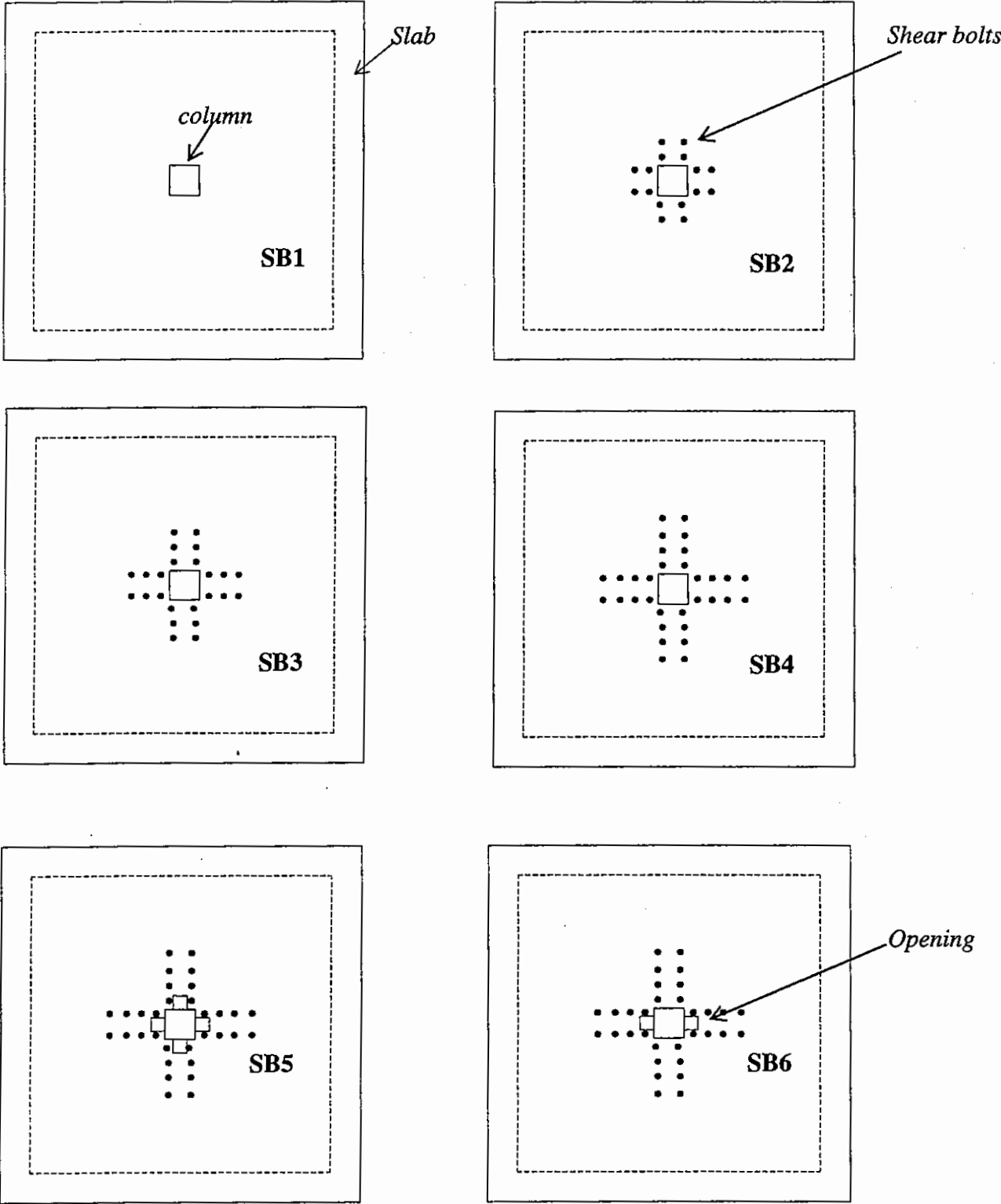


Figure 3-2: Specimens Tested

Table 3-1: Compressive Strength of Test Cylinders

Description	Slab Specimens in group	Compressive Strength (MPa)	Tensile Strength (MPa)	Age at testing
4" x 8"	SB2, SB3, SB4	42.0	2.34	25 weeks
150 mm x 300 mm		40.9	2.07	
	SB1, SB5, SB6	44.1		23 weeks
150 mm x 300 mm			2.19	

Reinforcing Steel

Steel used for longitudinal reinforcement was supplied on site pre-bent by Albrecht Steel Ltd. The top and bottom longitudinal reinforcement mats consist of 10 mm bars. In the column, four 20 mm bars were used enclosed by 8 mm plain bars as ties. Shear bolts were manufactured and donated by Continental Steels (Decon). These were designated DECON STUD 3/8 x 5-7/8 in.

Tension tests from standard coupons were carried out to determine the strengths of the steel. The longitudinal steel comprising of 10 mm ridged bars were tested using reduced cross-section coupons prepared according to ASTM E 8M-00b. The Shear Bolts were tested without any alterations by using a bracket in the jaws of the pulling device.

From testing, the yield strength of 10 mm bars was determined to be 455 MPa on the average, the average tensile strength was found to be 610 MPa. A stress-strain curve for one of the coupons from which the average values were determined is shown in Figure 3-3.

Also, the yield strength of the shear bolts was determined to be 381 MPa. A stress-strain is shown in Figure 3-4.

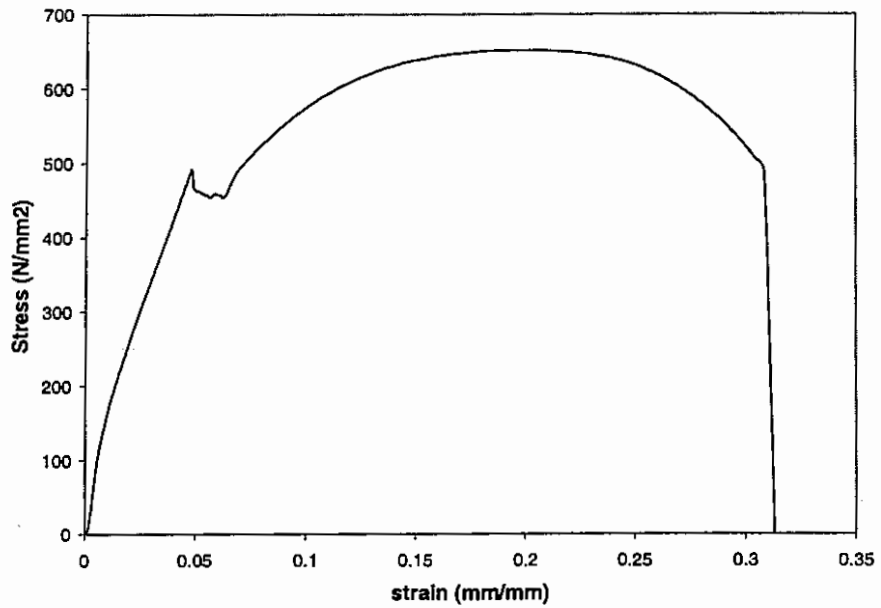


Figure 3-3: Typical Stress-Strain Curve for Longitudinal Reinforcement

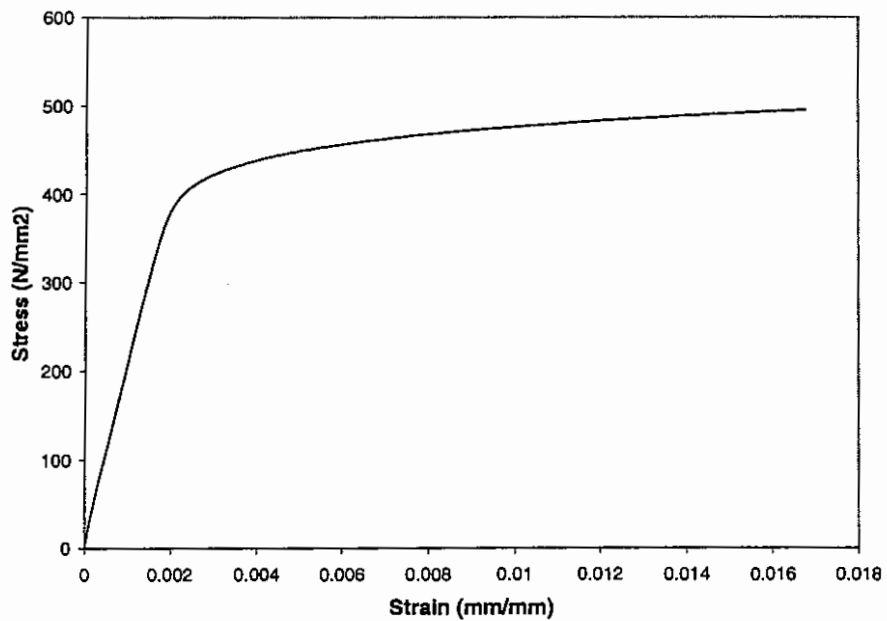


Figure 3-4: Typical Stress-Strain Curve for Shear Bolt

3.2 Experimental Program

3.2.1 Equivalent Continuous Slab System

The test specimens are full-scale models assumed to be equivalent to a slab-column connection in the continuous slab system shown in Figure 3-5. The continuous system shown is a flat plate construction consisting of five 3.75 m span bays in one direction and an infinite number of spans in the other direction. A summary of the experimental program is presented in Table 3-2.

3.2.2 Test Specimens

Test specimens represent a portion of the continuous slab system. The dimensions of the specimens are boundaries representing the lines of contraflexure (approximately 0.4 times the span). The typical specimen in Figure 3-1 shows outer boundaries of the slabs and the support lines at 1500 mm. The simple support system at the support lines is assumed to have the same effect as the lines of contraflexure (no moment) in the parent system. The overhang portion over the supports, 150 mm length at each side, was to ensure adequate development length and to prevent anchorage or bond failure.

A simple support system was achieved by the use of 1500 mm long flat solid bars. The solid bars had cross-section dimensions of 1500 mm by 40 mm by 25 mm thick. Neoprene strips of the same surface dimensions as the solid bars were bonded to the bars to ensure uniformity of contact during testing. The simple support system was placed on a symmetric square perimeter 1500 mm by 1500 mm.

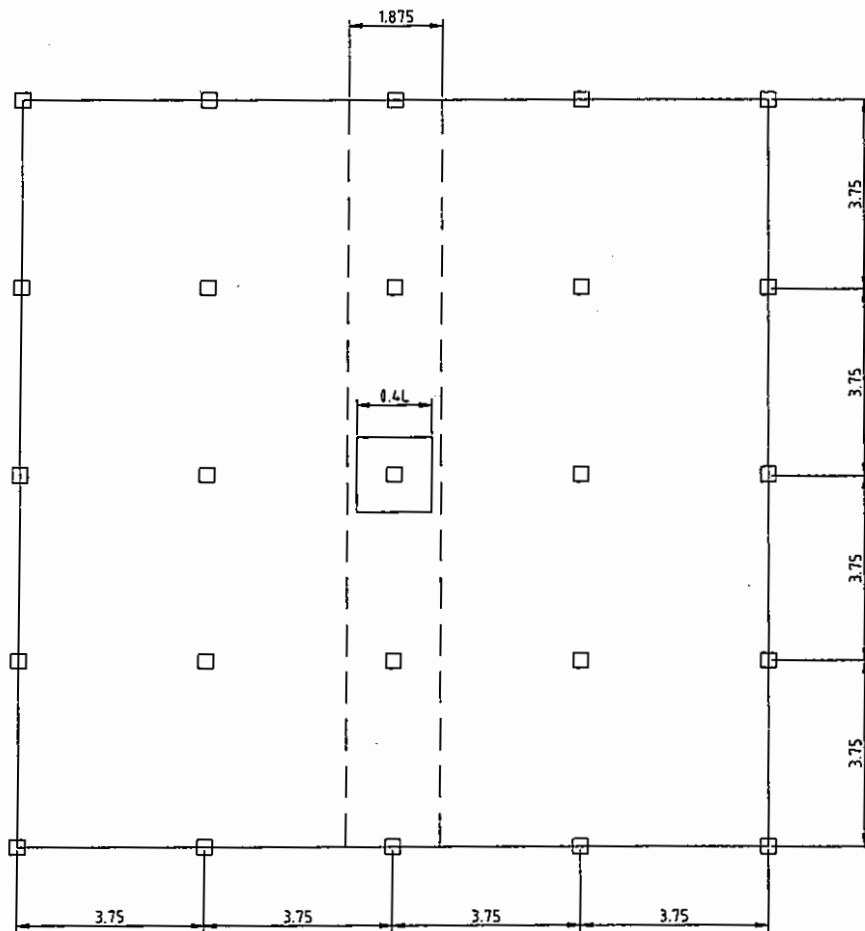


Figure 3-5: Test Specimen Shown in Equivalent Structure being Modelled (Units: mm)

Table 3-2: Summary of Experimental Program

Specimen	b* (mm)	a* (mm)	h* (mm)	ρ (%) average of 2 layers	d* (mm)	Number of Openings	Shear bolts
SB1	1800	1500	120	1.2	88.7	0	none
SB2	1800	1500	120	1.2	88.7	0	8*2 rows
SB3	1800	1500	120	1.2	88.7	0	8*3 rows
SB4	1800	1500	120	1.2	88.7	0	8*4 rows
SB5	1800	1500	120	1.2	88.7	4	8*4 rows
SB6	1800	1500	120	1.2	88.7	2	8*4 rows

* See Figure 3-1

3.2.3 Slab Flexural Reinforcement

The design consideration for the slabs was according to CSA A23.3-94. The specimens were designed by varying the percentage of tensile reinforcement such that failure occurs in punching before the flexural capacity is reached for the specimen without shear bolts.

All six specimens were reinforced with top and bottom layers running in orthogonal directions. The tension layer was designed such that the slab was as close as possible to being orthotropic. This was achieved by using slightly different spacing of reinforcement for the top and bottom layers of the tension (bottom) mat. The average main reinforcement ratio ρ is 1.2 % ($\rho = A_s/bd$).

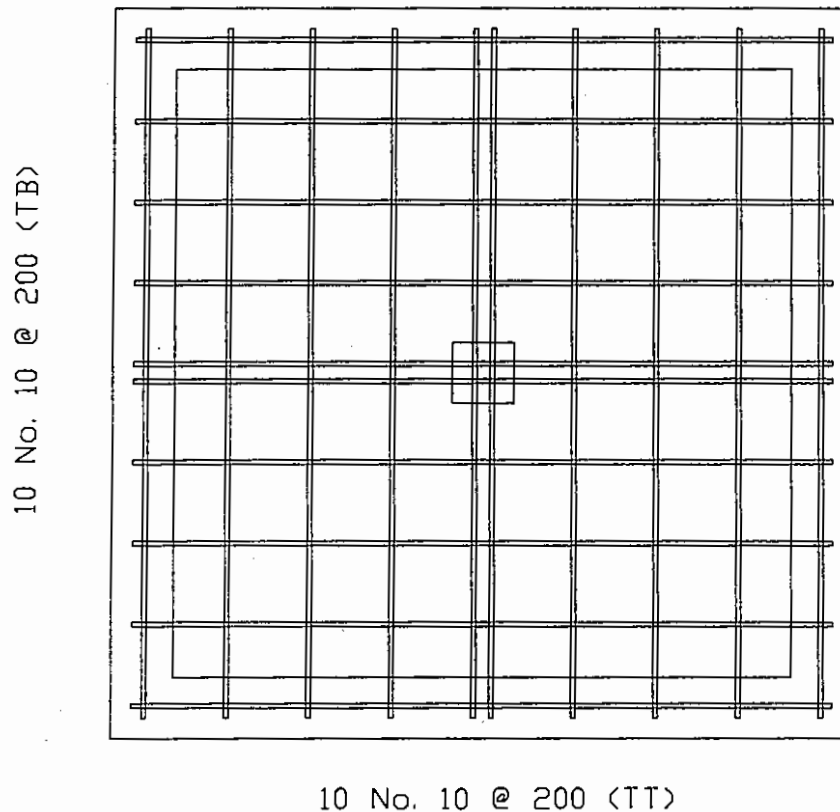


Figure 3-6: Top Mat (Compression Reinforcement)

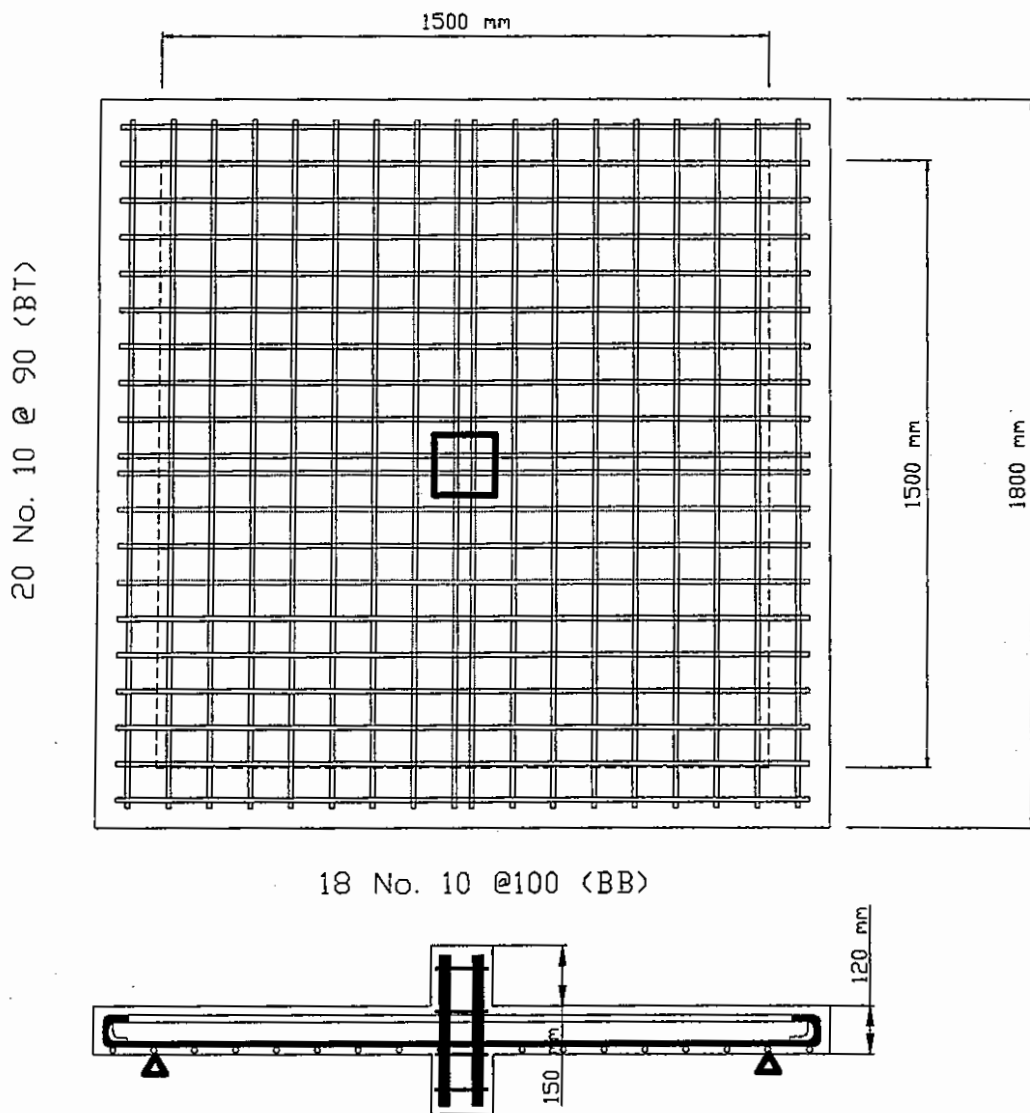


Figure 3-7: Bottom Mat (Tension Reinforcement)

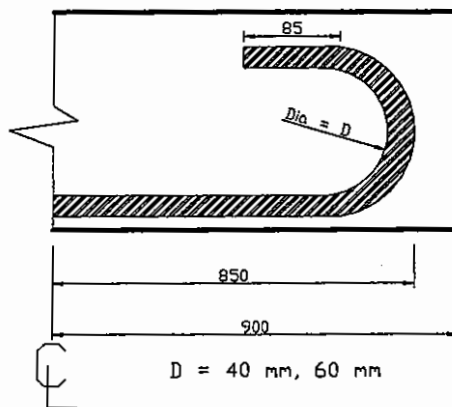


Figure 3-8: Bar Hooks

The tensile reinforcement used is as follows:

- The bottom mat lower layer was 10M bars at 100 mm centres. The upper layer was 10M bars at 90 mm centres.
- For the top mat 10M bars were used. The spacing for both layers was 200 mm.

The yield strength, as previously mentioned, was determined to be 455 MPa. The clear cover at the top and bottom of the slabs was taken to be 20 mm. It should be noted, that due to the experimental set-up design, the slabs were tested in the “upside down” position when compared to the real slab-column system. The tension reinforcement was therefore placed on the bottom of the specimens. Figures 3-6 and 3-7 below show the typical reinforcement layout for the slab specimens tested. For each layer in both mats two 10 M bars in both directions pass through the column between the column dowels, for purposes of structural integrity.

All the bars used were hooked at their ends to provide adequate anchorage. A sketch of the anchorage hooks is shown in Figure 3-7 and blown up in Figure 3-8 for the two dimensions of hooks used.

3.2.4 Slab Shear Reinforcement

Shear reinforcement for the slab specimens consist of a new type of device referred to as shear bolts. They consist of a shaft with a forged circular head (30 mm diameter) and a threaded end for the nuts that hold them in place. Fabricated, non-standard circular washers (44 mm diameter, 10 mm thick recommended) were used at the threaded end as anchor plates for the shear bolts. Shear bolts are installed in holes drilled in the slab shortly before testing.

The holes were drilled perpendicular to the slab plane using 16 mm (5/8 inch) diamond coring bits. The bolts were torqued to a strain between 5 – 10% (200-250 $\mu\epsilon$) of their yield strength just before testing. The shear bolts were arranged in concentric rows parallel to the perimeter of the column, following CSA A23.3 Clause 13.4.8.4. Each concentric row consist of eight bolts- two each parallel to the faces of the square column. The first row was place at between 45 mm to 60 mm from the

face of the column and subsequent rows were between 75 – 90 mm. A typical bolt is shown in the Figure 3-9.



Figure 3-9: Typical Shear Bolt

3.2.5 Column Reinforcement

The reinforcement in the stub column consist of four 20 mm bars running from top to bottom through the slab and enclosed by 8 mm ties placed at 100 mm spacing and tied to the column at the corners.

3.3 Preparation of the Test Specimens

3.3.1 Form-work Building

Forms were designed and built using plywood and sectional lumber. Rigidity of the formwork was achieved using bracing systems and double ply in some cases. Connections were done using screws, nails and adhesives.

3.3.2 Caging

Caging was done in the laboratory. The reinforcement was ordered pre-bent from the supplier. Uniformity was achieved by building rigs for arranging the reinforcement in place prior to tying, which was done manually. The cages were then hoisted into place in the forms. A typical cage is shown in Figure 3-10.

3.3.3 Casting

Casting took place in two batches of three slabs each. The concrete was ready-mix and was supplied by HOGG Ready-mix Concrete. The concrete was ordered in batches of about 2.0 cubic metres, providing enough concrete for three specimens and 10 test cylinders.

The concrete was transferred from the delivery truck to the formwork using a bucket and crane available in the laboratory as shown in Figure 3-11. A 25 mm rod vibrator was used to vibrate and compact the concrete so that no segregation occurred. A superplasticizer was added to the second batch to improve workability. For lifting purposes, hooks were built into the slab while casting.



Figure 3-10: Typical Cage

3.3.4 Curing

For at least 72 hours after casting the slabs were kept moist and covered with burlap and plastic sheets. The side forms were removed 24 hours after casting and the slabs continually wet and kept covered for a total of at least 7 days.

3.4 Test Set-Up and Experimental Apparatus

The set-up for testing is shown in Figures 3-12 and 3-13. The set-up was built around a testing frame already on site in the University of Waterloo Structures Laboratory. The additional components added were made as rigid as possible. This was done to avoid deflections of supports. It is expected that future tests will involve application of unbalanced moments to similar specimens. Thus rigidity of the testing rig is required. The present study involves the application of pure axial load through the columns. This load was applied by means of a hydraulic actuator.

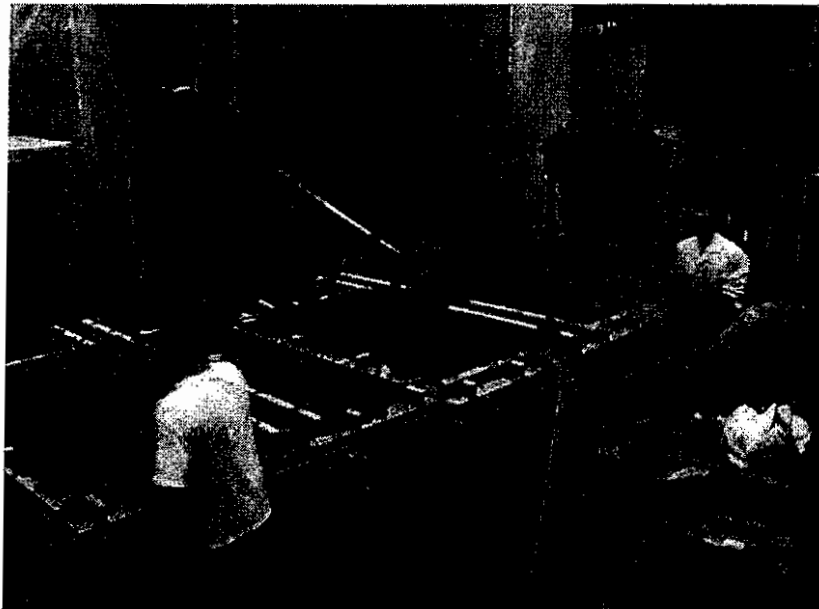


Figure 3-11: Casting by Bucket and Crane Method

3.4.1 Pedestal Support

The Pedestal Support system consisted of a series of W-sections. The steel sections conformed to CSA S16-94 (Steel Design Code) with regards to deflection and strength requirement. The pedestal system was arranged in such a way as to ensure easy access to the underside of the slabs for crack monitoring and shear bolt tightening. This was achieved by increasing the clear spans of the top W-sections within the limits on deflection from the steel code.

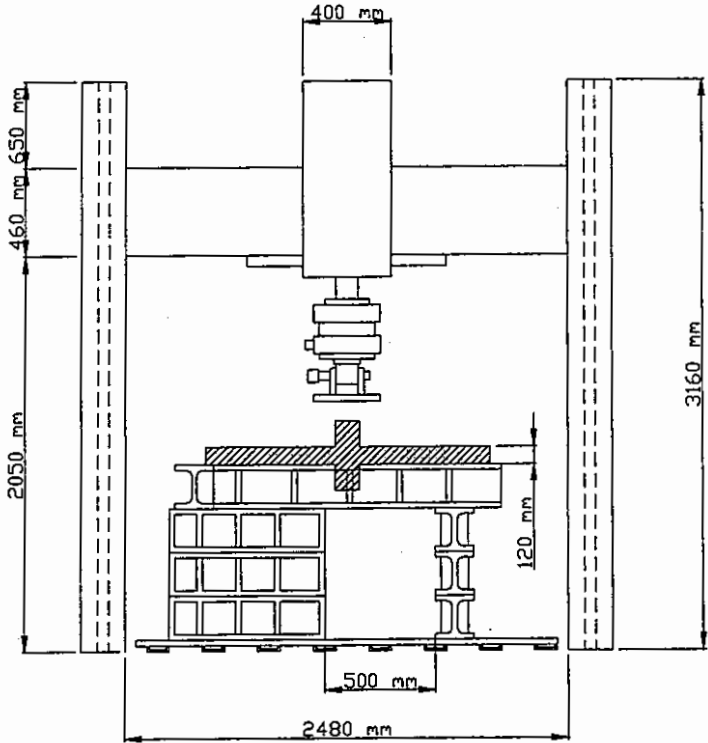


Figure 3-12: Test Set-Up with Pedestals and Slab in Place (Front)

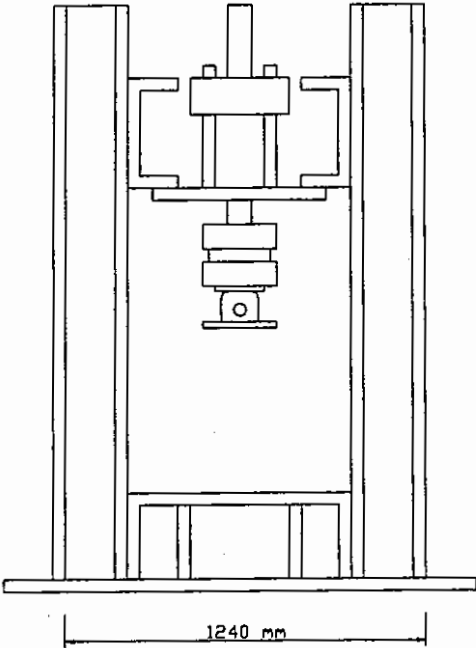


Figure 3-13: Testing Set-Up Frame Only (Side View)

3.4.2 Boundary Conditions

The specimens were designed as simply supported slabs. Simple supports at the edges were achieved by using 40 mm wide, 25 mm-thick steel plates. Placing neoprene strips between the bearing plates and the slab ensured uniformity of contact.

3.4.3 Corner Restraint

To simulate continuous slab construction and avoid the slab edges lifting during testing, tubular sections were used at each corner. The corners of the slabs were held down by sections cut out of standard tubular steel of dimension 76.2 mm square by 6.35 mm thickness (3 inch square by ¼ inch thickness). Restraint was achieved by bolting to the base plate. The restraint is to simulate the continuity of a real continuous slab system. The corner restraints used are shown in Figure 3-15.



Figure 3-14: Testing Frame, Data Acquisition and Specimen in Place

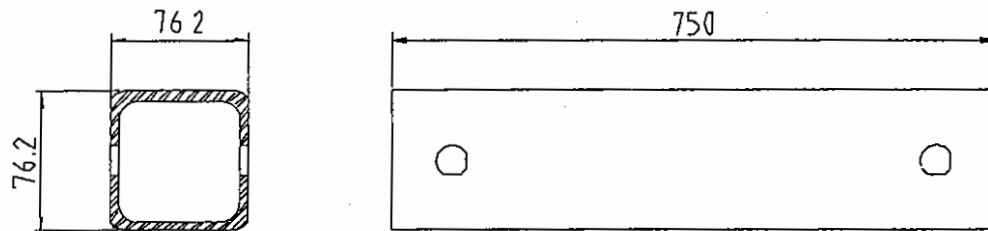


Figure 3-15: Dimensions of Corner Restraints and Connecting Rods (Dimensions in mm)

3.5 Instrumentation

3.5.1 Strain Gauges

An average of fourteen electrical resistance strain gauges per specimen was provided on the tension flexural reinforcement to measure steel strains during testing. The Strain Gauges were all made by KYOWA. The type was KFG-5-120-C1-11 for steel. Gauge length was 5 mm and resistance was 120.2 ohms. The strain gauges were bonded to the steel using an acrylate based strain gauge adhesive. The strain gauges were then connected to wires using bondable terminal Strips. The position of the strain gauges provided for all tests is shown in Figure 3-17.



Figure 3-16: Strain Gauge and Terminals

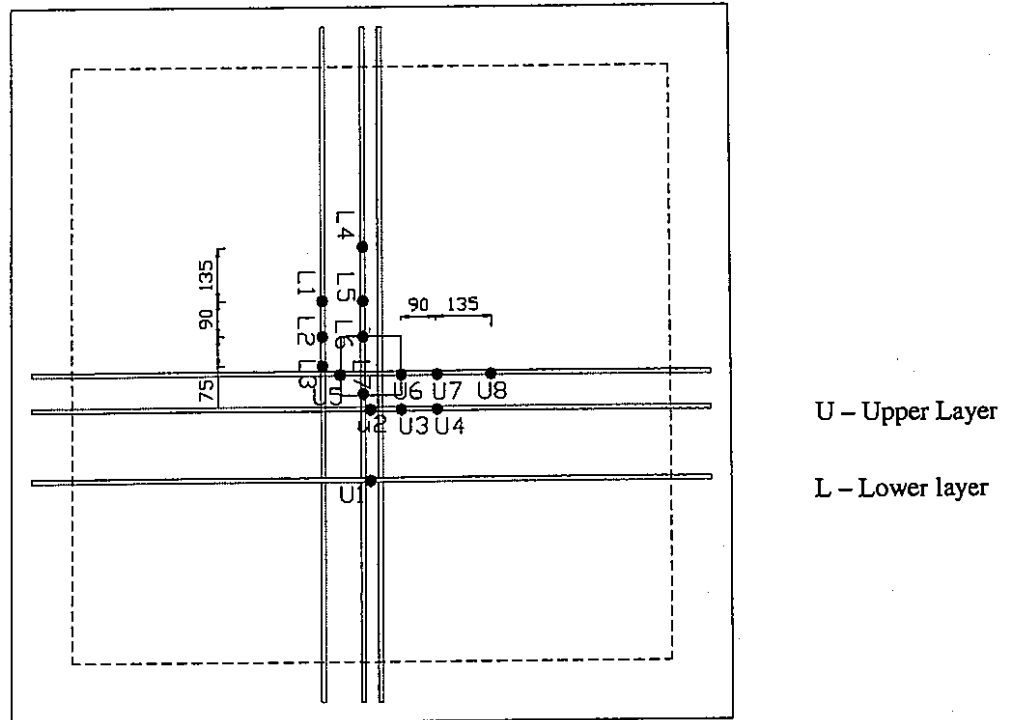
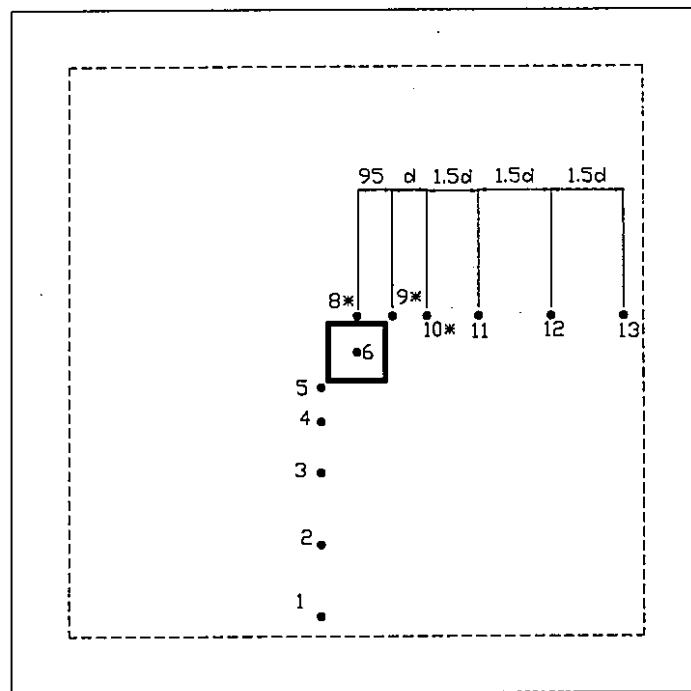


Figure 3-17: Position of Strain Gauges on Longitudinal Reinforcement (Dimensions in mm)

3.5.2 Displacement Transducers

A scheme of Linear Variable Displacement Transformers (LVDT), Direct Current Displacement Transformers (DCDT), and Potentiometers was used on each slab specimen to measure the magnitude of the deflection profile during testing. The positions of transducers are shown in Figure 3-18. At three locations, 8, 9, 10, displacement transducers were placed both on top and bottom of the slab. This was done to monitor opening of the internal inclined crack during testing. Differential displacement readings from the top and bottom pairs gave an estimate of the vertical width of the inclined shear cracks.



* LVDT pairs at top and bottom of slab

Figure 3-18: Position of LVDT on a Typical Specimen (Dimensions in mm)

3.5.3 Video Camera

A video camera was mounted underneath the slab during testing to monitor the formation of cracks. To enhance crack detection, the bottom of the slab was painted and a light source was used to increase flexural crack visibility.

Chapter 4

Design of Test Specimens

4.1 Dimension and Specimen Selection

Conventional slab-column test specimens were decided on in the early stages of the program. The conventional slab system is idealized as shown in Figure 4-1. As previously mentioned, a study was done by El-Salakawy (2003) on the use of shear bolt reinforcement at edge columns. The specimens in this program represent interior connections from the same continuous slab system used in the research by El-Salakawy. The continuous slab system was shown in Figure 3-6. In the final specimen, sufficient overhang was provided beyond the support lines of the specimen, at the lines of contraflexure, to meet anchorage provisions of CSA A23.3-94.

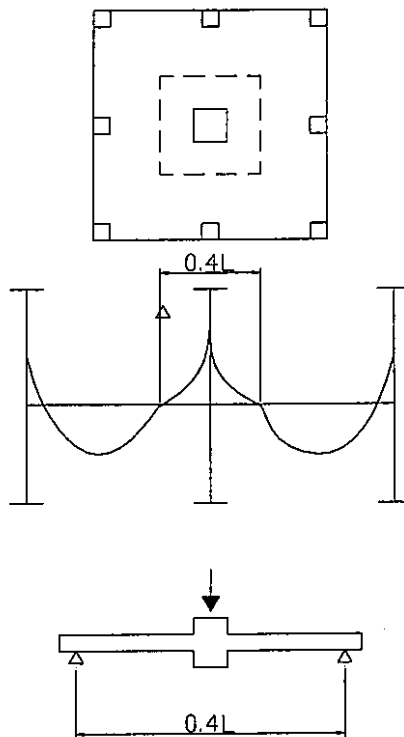


Figure 4-1: Conventional Slab-Column Specimen

4.2 Yield-Line Analysis

Yield line analysis was done to ensure that the load corresponding to the flexural capacity of specimen without shear reinforcement was higher than the load at the punching capacity as predicted by different formulas. To select the longitudinal flexural reinforcement for the specimens, a yield line analysis was carried out. It is assumed that the yield line pattern shown in Figure 4-2 forms at full yield for conventional slab-column specimens.

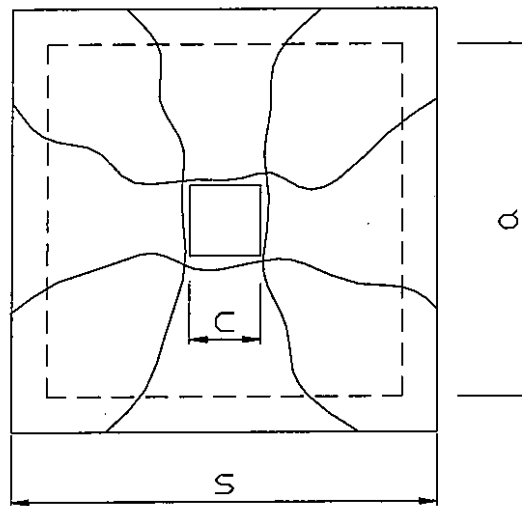


Figure 4-2: Yield-Line Pattern for Conventional Slab-Column Specimen

$$P_{flex} = K_{yl} \cdot M_b \quad (4.1)$$

$$K_{yl} = 8 \left(\frac{s}{a-c} - 0.172 \right) \quad (4.2)$$

From CSA A23.3-94

$$M_b = 39 \text{ kNm} \quad (4.3)$$

With $a = 1500 \text{ mm}$
 $c = 150 \text{ mm}$
 $s = 1800 \text{ mm}$
 $K_{yl} = 9.2907$

And with $f_y = 455$ MPa, $f'_c = 42$ MPa

Assuming 10 M bars in both layers of the tension mat, $d_{ave} = 90$ mm

$$P_{flex} = 9.2907 M_b$$

The flexural reinforcement chosen for the specimens is as follows;

10 M @ 100 in the bottom layer of the tension mat, nominal moment capacity of 39.8 MPa

10 M @ 90 in the top layer of the tension mat, nominal moment capacity of 38.1 MPa

Therefore,

$$P_{flex} = 362 \text{ kN}$$

4.3 Structural Analysis of Continuous Slab System

A structural design of an equivalent continuous slab system was carried out. As mentioned previously, it is shown that the tested slab represent portions of a slab with spans of 3.75 m in each direction. The unfactored service load was a uniformly distributed load of 18.5 kPa. The analyzed slab system consists of five spans in one direction and theoretically an infinite number of spans in the other direction. A layout of the parent slab system was shown in Figure 3-5.

CSA A23.3 –94 specifies a number of methods for analyzing a flat plate slab system. The Direct Design Method, which distributes the statical moment, M_o between positive and negative moment regions, was used as a rough initial design. Since the slab contained relatively high percentage of flexural reinforcement; it had to be designed for the high Live Loads. Therefore, to be consistent with the CSA, the elastic frame method was also used to analyze the equivalent continuous slab system. The slab was analyzed for a uniformly distributed factored load over the slab area of 18.5 kPa.

4.3.1 Direct Design Method

The coefficients given by A23.3-94 for the computation of moments in a continuous slab system without beams between columns are reproduced in Figure 4-4. For the factored load of 18.5 kPa,

a total statical moment of 113 kNm is obtained. This moment is distributed between positive and negative regions according to Figure 4-4. The moments are shown in Figure 4-5. The direct design method is recommended for structures with regularity of topology and loading.

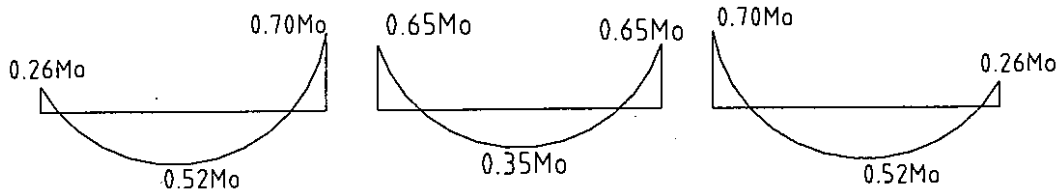


Figure 4-4: Moment Coefficients for the Direct Design Method (kNm)

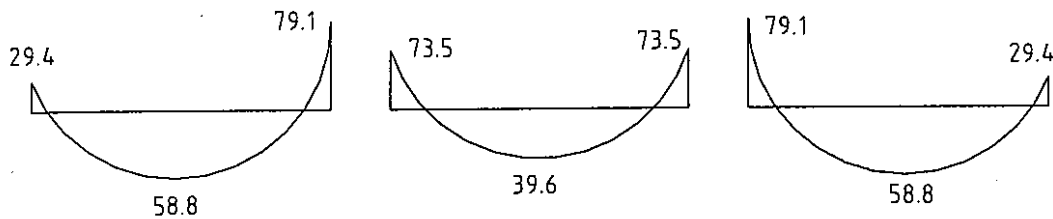


Figure 4-5: Distribution of Statical Moment by the Direct Design Method (kNm)

4.3.2 Elastic Frame Analysis

Recommended in the CSA A23.3 -94 is the elastic frame method as a more accurate method for analyzing flat plates where the ratio of the live load to dead load exceeds 1.5. The analysis of the parent slab system has been carried out using SODA®. A gravity load analysis was carried out. The idealized frame analyzed is shown with the member section properties in Figure 4-6.

A printout of the input data and analysis output has been presented in appendix A.

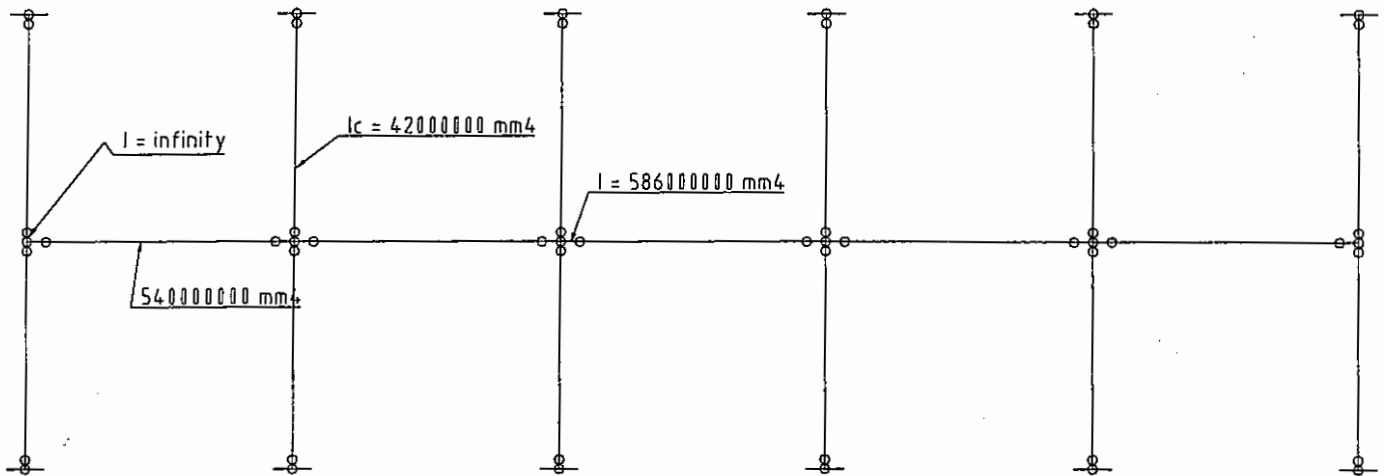


Figure 4-6: Elastic Frame Model Showing Moment of Inertia of Members

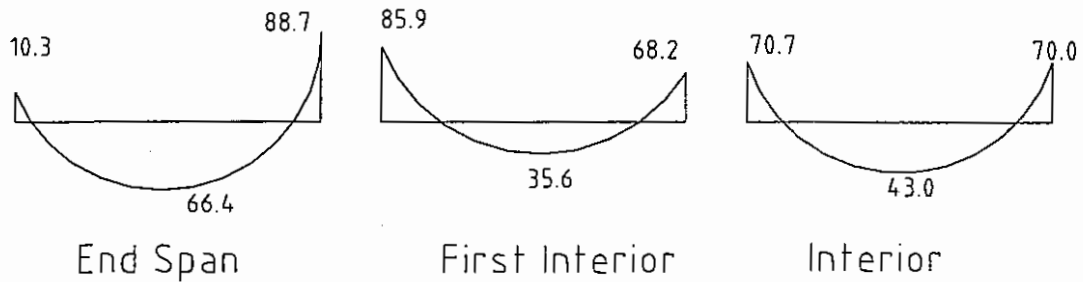


Figure 4-7: Moments from Elastic Frame Analysis

The interior support moment from an elastic frame analysis was found to be about 71 kNm as shown in Figure 4-7. This requires the approximate amount of reinforcement A_s :

$$A_s \approx \frac{M}{f_y \times 0.9d} = 1926 \text{ mm}^2$$

For a column strip width of 1875 mm, twenty 10M bars will satisfy this reinforcement requirement. This gives a ratio of 1.19 % which is equal to 1.2 % used in the specimens.

4.4 Two Step Approach to Conventional Slab Design by Rankin and Long

An analysis was carried out based on equations developed by Rankin and Long (1987). Sections 4.4.1 to 4.4.4 show the equations. Table 4-1 summarizes the analysis based on their method.

4.4.1 Full Yielding (Consideration of Yield Line) Flexural Failure

$$P_{flex} = k_{yl} M_b \quad (4.4)$$

$$k_{yl} = 8 \left(\frac{s}{a-c} - 0.172 \right) \quad (4.5)$$

This was shown earlier in section 4.2

4.4.2 Localized Compression Failure

$$P_{loc} = k_b M_{(bal)} \quad (4.6)$$

$$k_b = \frac{25}{\left(\log_e \frac{2.5a}{c} \right)^{1.5}} \quad (4.7)$$

4.4.3 Partial Yielding Flexural Failure

$$P_{par} = k_t M_b \quad (4.8)$$

$$k_t = k_b + (k_{yl} - k_b) (M_b / M_{(bal)}) \quad (4.9)$$

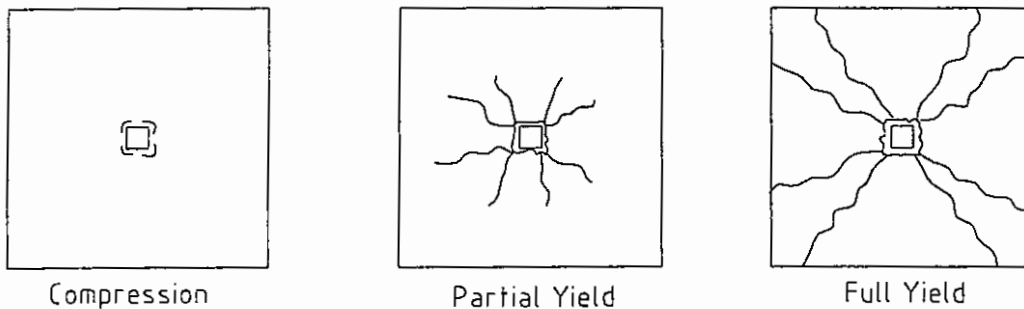


Figure 4-8: Modes of Flexural Failure (Rankin and Long, 1987)

4.4.4 Shear Punching Resistance

Shear mode of failure is precipitated by internal diagonal cracking prior to the development of yielding of the reinforcement or crushing of the concrete. Equation 4.10, determined empirically, was proposed by Rankin and Long.

$$P_{vs} = 1.66\sqrt{f'_c} (c + d)d(100\rho)^{0.25} \quad (4.10)$$

The variables in the above equations are as follows:

- M = moment per unit width
- M_b = bending moment of resistance
- $M_{(bal)}$ = balanced moment of resistance ($=0.333f'_c d^2$)
- a = distance between supports of conventional slab specimen ($=0.4L$)
- c = length of column side
- d = average effective depth to tensile reinforcement
- f'_c = cylinder compressive strength
- k_b = ratio of applied load to internal bending moment at column periphery
- k_t = ratio of applied load to ultimate moment of resistance at failure
- k_{yt} = moment factor for overall tangential yielding
- s = side length of conventional slab specimen
- ρ = reinforcement ratio

Table 4-1: Slab Capacity from Rankin and Long's Method

c (mm)	a (mm)	s (mm)	d (mm)	ρ (%)	f_y MPa	f'_c MPa	$P_{(flex)}$ (kN)	$P_{(par)}$ (kN)	$P_{(loc)}$ (kN)	P_{vs} (kN)
150	1500	1800	90	1.2	450	35	379	286	406	243

4.5 Shear Capacity by Code of Practice Approach

A review of the shear requirements from various codes of practice was examined in Chapter 2. In this chapter, a standardized form of the same design specifications equations are used as described in the FIB Bulletin (2001).

For ultimate limit state, the resistance of a section in shear needs to be greater the factored ultimate shear stress. The total punching resistance is given by Equation 4.11.

$$V_r = \phi_c V_c + \phi_s V_s \leq \phi_c V_{c, \text{outside}} \leq \phi_c V_{\text{max}} \quad (4.11)$$

The various codes give different formulae for the parameters in Equation 4.11. Generally speaking in implicit form,

$$V_c = \tau_c \cdot k \cdot f(\rho_l) \cdot u \cdot d \quad (4.12)$$

$$V_s = A_{sv} \cdot \kappa_s \cdot f_y \cdot \sin(\alpha) \quad (4.13)$$

where,

- V_r shear resistance of the reinforced concrete section
- V_c shear resistance of the reinforced concrete section without shear reinforcement or concrete contribution of the punching resistance with shear reinforcement
- V_s Contribution of shear reinforcement to the resistance of the section
- $V_{c, \text{outside}}$ shear resistance outside of the shear reinforced area
- V_{max} characteristic maximum shear resistance
- Φ_c resistance factor for concrete
- Φ_s resistance factor for steel
- τ_c concrete shear stress [MN/m²]
- k size effect factor of the effective depth
- $f(\rho_l)$ function of the tension reinforcement
- ρ_l tension reinforcement ratio [%]

u	control perimeter [mm]
d	effective depth [mm]
A_{sv}	cross section area of the shear reinforcement [mm ²]
κ_s	efficiency of the shear reinforcement
f_y	yield strength of the shear reinforcement [MPa]
α	inclination of the shear reinforcement

The following tables show the shear resistance of the slab specimens (without transverse reinforcement) according to various code provisions. Table 4-2 shows the resistances for a slab without openings, Table 4-3 with two openings and Table 4-4 with four openings.

Summarized in Table 4-5 is the shear capacity of specimens reinforced with transverse bolt reinforcement.

4.5.1 Shear Resistance without Openings/No Shear Reinforcement

Table 4-2: Shear Resistance of Specimens by Code Provisions

	τ_c (MN/m ²)	k	u (mm)	$f(\rho_l)$	V_c (kN)
Eurocode	0.423	1.511	1664	1.680	160
Model Code	0.417	2.000	2019	1.095	166
BS 8110	0.969	1.457	1664	1.063	223
ACI	2.139	1.000	955	1.000	181
CSA	2.592	1.000	955	1.000	220

4.5.2 Shear Resistance with Two openings/No Shear Reinforcement

Table 4-3: Shear Resistance of Specimens with Two Openings by Code Provisions

	τ_c (MN/m ²)	k	u (mm)	f(ρ_l)	V _c (kN)
Eurocode	0.423	1.511	1272	1.680	122
Model Code	0.417	2.000	1543	1.095	127
BS 8110	0.969	1.457	1272	1.063	17
ACI	2.139	1.000	815	1.000	156
CSA	2.592	1.000	815	1.000	189

4.5.3 Shear Resistance with Four Openings/No Shear Reinforcement

Table 4-4: Shear Resistance of Specimens with Four Openings by Code Provisions

	τ_c (MN/m ²)	k	u (mm)	f(ρ_l)	V _c (kN)
Eurocode	0.423	1.511	880	1.680	85
Model Code	0.417	2.000	1067	1.095	88
BS 8110	0.969	1.457	880	1.063	118
ACI	2.139	1.000	675	1.000	129
CSA	2.592	1.000	675	1.000	156

4.5.4 Shear Resistance of Slabs with Transverse Reinforcement by CSA-A23.3-94

Table 4-5: Shear Resistance of Specimens Reinforced with Shear Bolts

	b_o (mm)	A_{vs} (mm ²)	V_r (kN)
SB1	955	562	219
SB2	955	562	261
SB3	955	562	321
SB4	955	562	380
SB5	675	562	334
SB6	815	562	359

The area of shear reinforcement per line was found to be 567 mm² for shear bolts with yield stress of 381 MPa. A summary of the predicted capacity of the shear strengthened slab-column connection is show in Table 4-5.

Experimental Procedures and Observations

This chapter describes each test in detail. Testing procedures are presented first. Then the test observations are presented in terms of deflections, cracking and reinforcement strains. Six specimens were tested namely: SB1, SB2, SB3, SB4, SB5 and SB6. A description of each test specimen with regards to configuration and transverse reinforcement was given in Figure 3-2. Initiation and propagation of cracks in a slab-column specimen consist of the following successive stages:

- Initiation of flexural and shear cracks in the tension zone of the slab near the face of the column,
- Yielding of tension steel close to the column,
- Extension of flexural and shear cracks into the compression zone,
- Failure due to rupture of the reduced compression zone.

5.1 Testing Procedures

Slab SB1 was the first specimen to be tested. It served as a control specimen for this experimental program. SB1 is typical of all six specimens. It was without openings or transverse reinforcement. All slabs were tested by displacement control. The displacement rate was chosen to approximately follow the required load steps: 4 kN/min until about 70% of the anticipated ultimate load, and 2 kN/min from then on, until failure. While testing SB1, the equipment experienced sudden (small) jumps in the loading, which did not significantly affect the results of the test. The malfunction was corrected for subsequent tests. Test time for SB1 was 53 minutes.

Slab SB2 was the first transversely reinforced specimen with two peripheral rows of shear bolt reinforcement. All shear bolts were torqued prior to commencing the test to a strain of within a range of 5 – 15 % of yield strain (180 – 300 microstrains ($\mu\epsilon$)). While testing SB2, the slab had to be unloaded and slowly reloaded four times. This was done because the load controller had to be re-started after reaching its full range. The data between the drops in load was deleted from the load-displacement graphs. Test time for SB2 was 230 minutes.

Slab SB3 was loaded by displacement control. SB3 had three peripheral lines of shear bolts. Test time for SB3 was 182 minutes.

Slab SB4 had four peripheral lines of shear bolt reinforcement.

Slab SB 5 had two openings symmetrically positioned next to the column. It was reinforced transversely with four peripheral lines of shear bolt reinforcement. At a load of 343 kN the hydraulic lines supplying the actuator lost pressure. The load dropped down to 118 kN before picking up again. The data between the drops in load have been deleted from that presented here. Test time for SB5 was 122 minutes. While testing SB5, no deflection reading was taken at the central bottom LVDT due to malfunction of the data acquisition system.

SB6 had two openings on opposite sides of the column and was reinforced transversely with four peripheral lines of shear bolt reinforcement. At a load of 300 kN, the top displacement transducers were adjusted because the framing crossbars were in the way of the actuator and had been pushed down as the actuator went downwards. This somewhat affected the displacement readings taken from that point on. Test time for SB6 was 77 minutes.

5.2 Test Observations

5.2.1 Slab SB1

Slab SB1 failed in a sudden punching mode at a load of 253 kN. The load-displacement behavior (Figure B-1), flexural crack pattern and strain data (Figure B-3) all confirm this mode of failure. At failure, there was a complete loss of stiffness observed by the sudden drop in load. The data collected during testing for slab SB1 is presented in Appendix B, Figures B-1 to B-3.

Cracks were first noticed on the tension face of the slab along and perpendicular to the edges of the stub column. The flexural cracks became visible at about 126 kN starting from the column corners and extending a short distance towards the supports. At about 206 kN the flexural cracks had extended all the way to the supports. The crack patterns after failure for specimen SB1 are shown in Figure 5-1.

An arrangement of displacement transducers was used for measuring deflections and estimating inclined shear cracking during the test. The arrangement was shown in Figure 3-18. A central LVDT placed at the center of the bottom column, data shown in Figure B-1b, measured a maximum deflection of 10.4 mm. The value of 12 mm in Figure B-1a includes the flexing of the frame and other errors.

Displacements were measured in pairs (top and bottom of the slab) at location 8, 9, 10. The difference in these displacements enabled the monitoring of the formation of inclined shear cracking. Figure B-2 shows a plot of load against the crack vertical width. A maximum crack width of 11.5 mm observed was at location 8 next to the column. After punching, the crack width increased to 15 mm.

Strain measurements on longitudinal reinforcing steel was taken at different locations as shown in Figure 3-17. All strain gauges were placed on the tension reinforcement mat. "L" refers to lower layer and "U" refers to upper layer. First yielding occurred at 204.5 kN (81% of ultimate load) at Strain Gauge L7 in Figure B-3i. At Strain Gauges U6 and U7 yielding occurred at a load of 242 kN (95% of ultimate load) (Figure B-3g). Strain Gauges U4 and U5 in Figure B-3 show yielding in the longitudinal reinforcement after failure. No useful data was recorded at locations L1, L2, L3, L4, L5 and L6 for this specimen.

Table 5-1: Longitudinal Reinforcement Strains at Ultimate Load of Slab SB1

	U1	U2	U3	U4	U5	U6	U7	U8	L7
Strain at Ultimate Load	0.0015	0.0016	0.0015	0.002	0.002	0.002	0.002	0.001	0.002

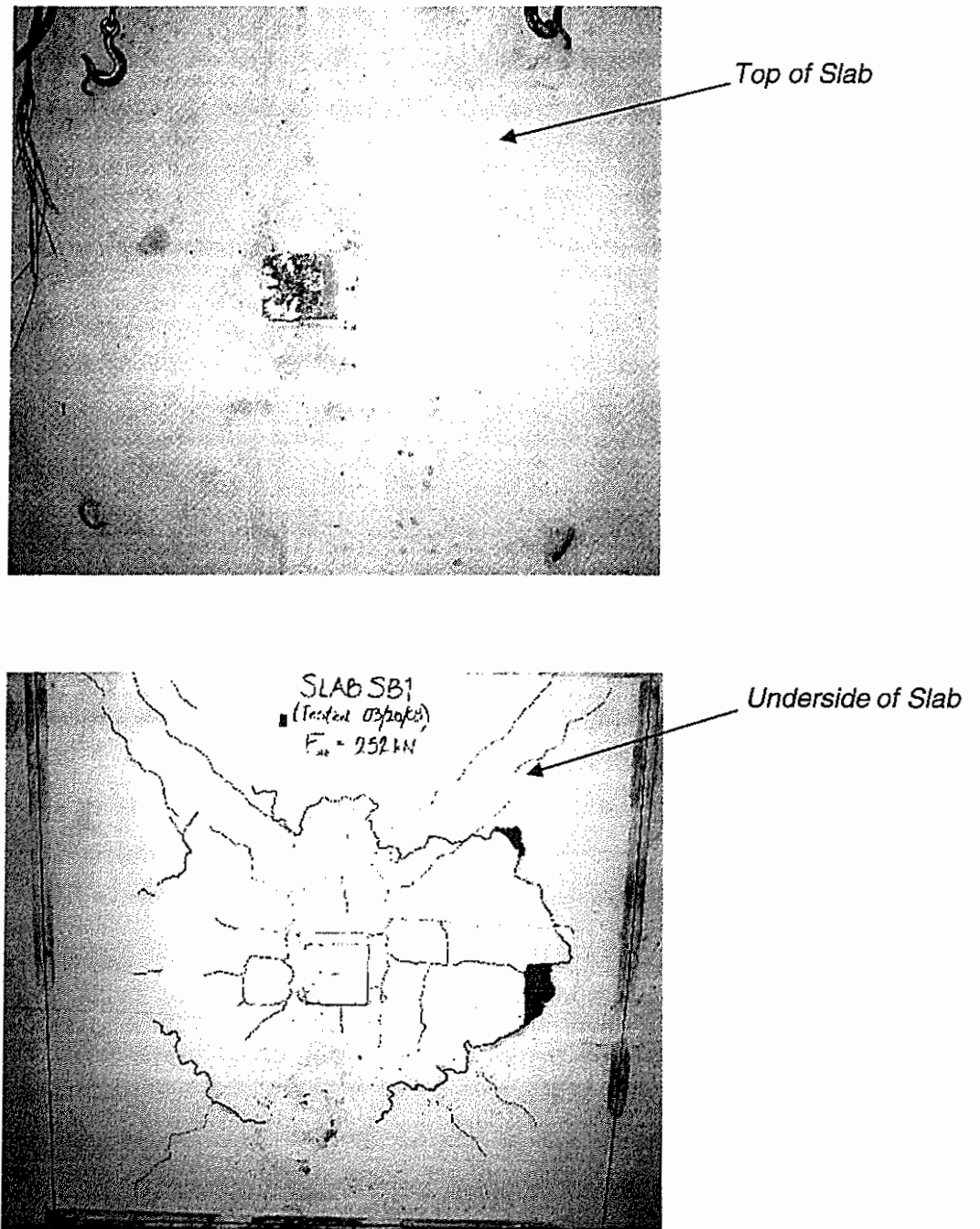


Figure 5-1: Crack Pattern after Failure of Specimen SB1

5.2.2 Slab SB2

Slab SB2 failed in a punching mode at a load of 357.7 kN. The load-displacement graph (Figure B-4), post failure crack pattern and strain measured on longitudinal reinforcement confirm this mode of failure. At failure there was a complete loss of stiffness observed by the sudden drop in load. However, though SB2 sustained a higher ultimate load and more deflection than SB1, it failed by punching outside of the shear reinforced zone. The data collected during testing for slab SB2 is presented as graphs in Appendix B, Figures B-4 to B-7.

Cracks were first noticed at a load of 116 kN on the tension face of the slab. The first cracks were parallel to the column side between the first and second peripheral line of shear bolts. The flexural cracks became visible at about 125 kN starting from the columns corners and extending a short distance towards the supports. At about 172 kN, the flexural cracks had extended all the way to the supports. Cracks were also observed, at failure, on the compression face (top) of the slab parallel to the corner restraints and offset by a distance of about 17-25 mm.

Displacements were measured during testing. Inclined shear cracking width was also estimated by measuring displacements on the top and bottom of the slab. A central LVDT placed at the center of the bottom column (Figure B-5b) measured a maximum deflection of 17.2 mm at failure. The value of 28.7 mm in Figure B-4a includes the flexing of the frame and other errors. Figure B-5 shows a plot of load against the crack vertical width. The crack width was limited to 2.5 mm during the test. This value at location 10 furthest from the column may be due to failure of a shear bolt on the outer perimeter of the bolts. At the other locations (8 and 9) the crack width did not exceed 1 mm.

First yielding of longitudinal reinforcement occurred at 166 kN (46% of ultimate load) at Strain Gauge L4 as seen in Figure B-6. Next, Strain Gauge L1 yielded at a load of 184 kN (51% of ultimate load) as shown in Figure B-6, then U4 yielded at 186 kN (52% of ultimate load). L6, U3, L3, U2, L5, U7, U5 and U1 yielded subsequently at 197 kN (55% ultimate), 200 kN (56% ultimate), 209 kN (58% ultimate), 221 kN (62% ultimate), 252 kN (70% ultimate), 274 kN (77% ultimate), 277 kN (77% ultimate) and 300 kN (84% ultimate), respectively.

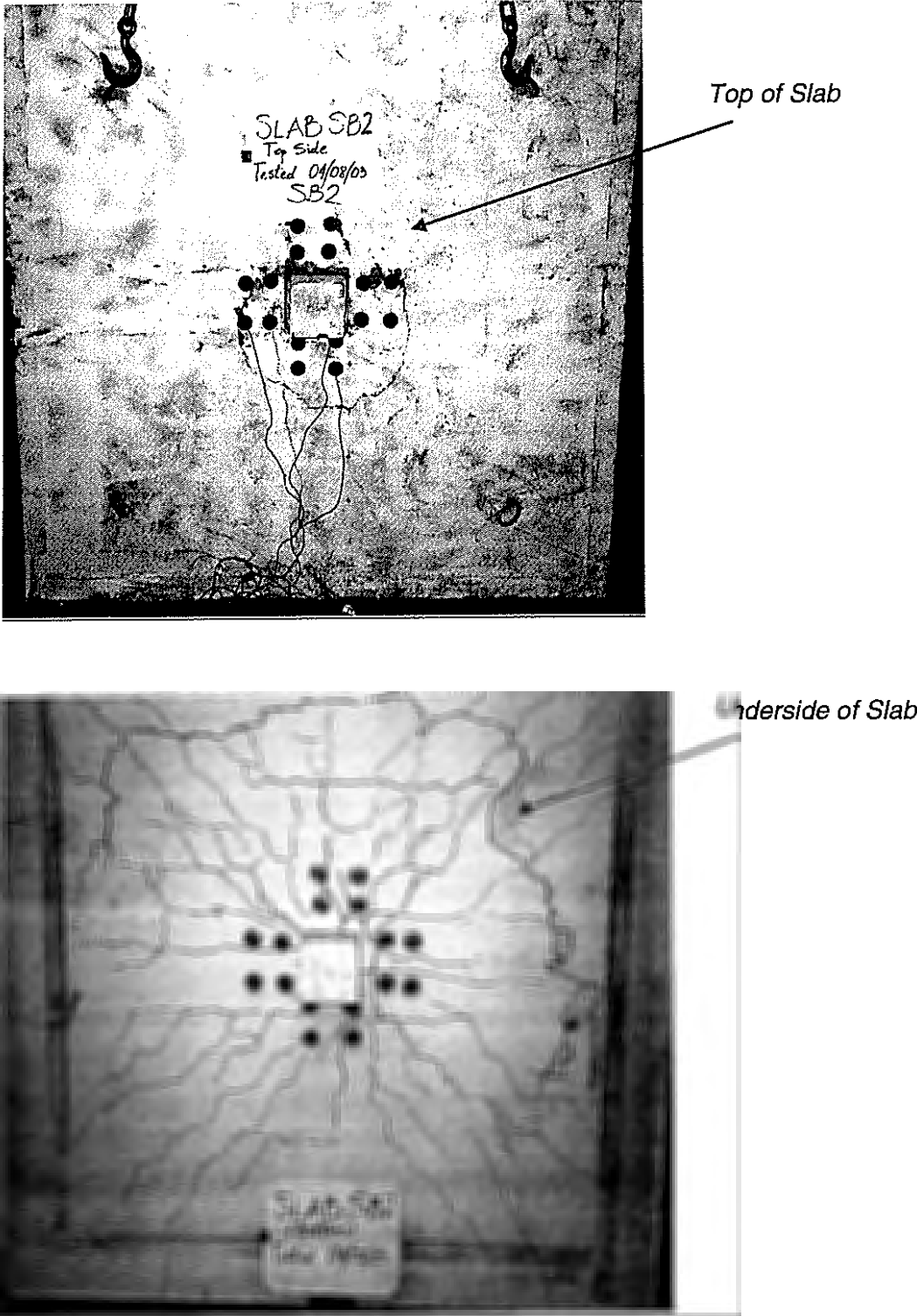


Figure 5-2: Crack Patterns after Failure of Specimen SB2

The strains at the strain gauge locations at failure load are shown in Table 5-2. For this specimen no data was collected at locations U6, U8, L2 and L7 due to damaged strain gauges.

Table 5-2: Longitudinal Reinforcement Strains at Ultimate Load of Slab SB2

	U1	U2	U3	U5	U7	L1	L3	L4	L5	L6
Failure Strain	0.002	0.004	0.007	0.003	0.003	0.003	0.004	0.003	0.006	0.021

5.2.3 Slab SB3

Slab SB3 failed at a load of 376 kN after considerable deflection. The final failure (loss of strength) happened through a punching cone. SB3 had three peripheral lines of shear bolts. The load-displacement graph in Figure B-8, post failure crack patterns, and strains measured on longitudinal reinforcement confirm this mode of failure. At failure, there was a virtually complete loss of strength observed by the sudden drop in load. The data collected during testing for slab SB3 is presented as graphs in Appendix B, Figures B-8 to B-11.

Cracks were first noticed at a load of 108 kN on the tension face of the slab. The flexural cracks became clearly visible at about 149 kN starting from the columns corners and extending a short distance towards the supports. At about 193 KN the flexural cracks had extended all the way to the supports. Final crack patterns are shown in Figure 5-3. Cracks were also observed, at failure, on the compression face (top) of the slab parallel to the corner restraints and offset at a distance of about 15-20 mm.

A central LVDT placed at the center of the bottom column (Figure B-8b) measured a maximum deflection of 26 mm at failure. The value of 33 mm deflection in Figure B-8a includes the flexing of the frame and other errors. Figure B-9 shows a plot of load against the crack vertical width. Crack width was limited to about 1 mm at all three locations during testing. The difference between crack widths at locations 8, 9 and 10 monitored during testing was very small.

Strain measurements on longitudinal reinforcing steel were done at different locations as shown in Figure 3-17. All strain gauges were placed on the tension mat. First yielding occurred at 194 kN

(52% of ultimate load) at Strain Gauge L1 as seen in Figure B-10. Next Strain Gauge L2 yielded at a load of 214 kN (57% of ultimate load) as shown in Figure B-10j, then U4 yielded at

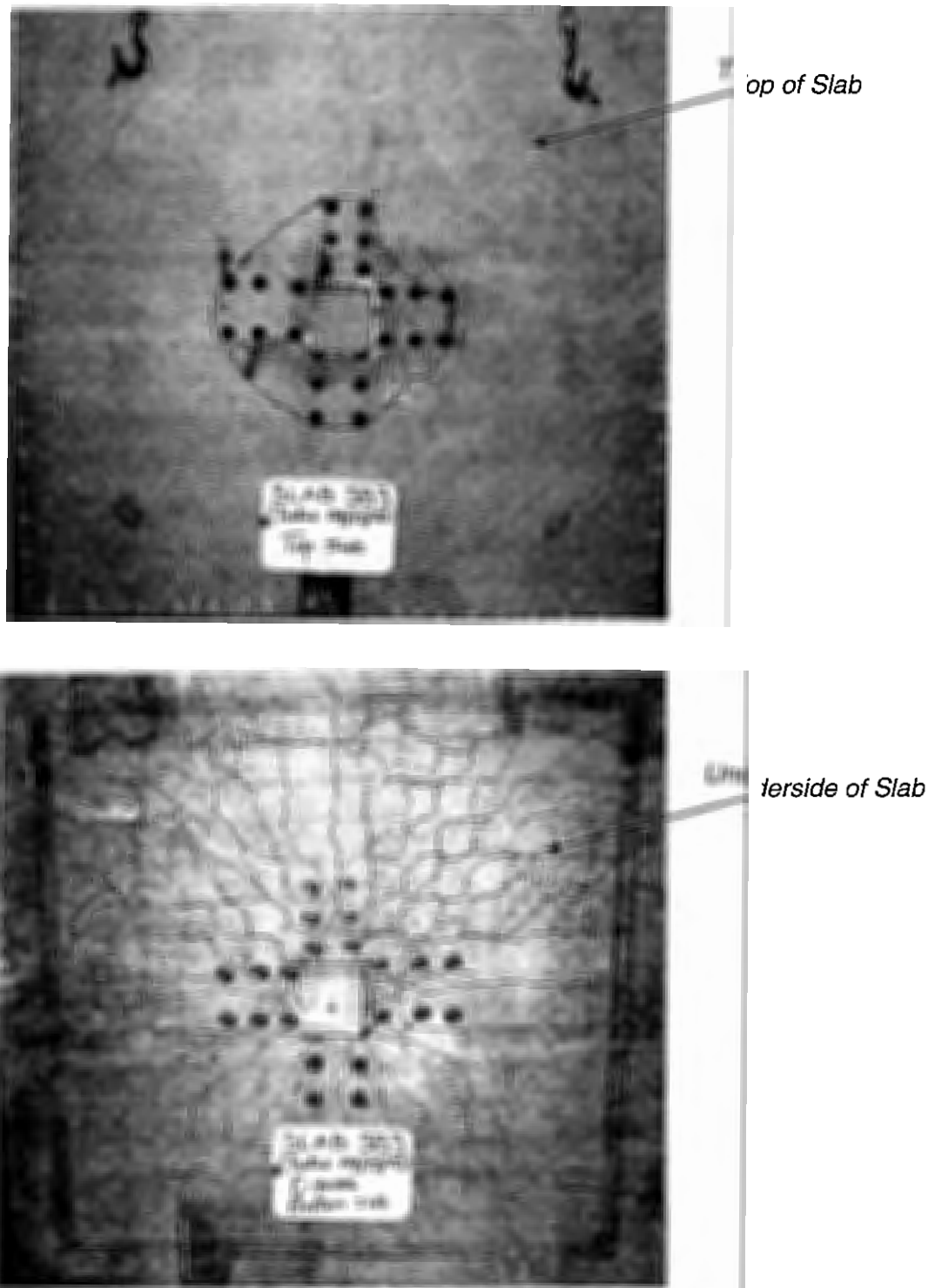


Figure 5.3: Crack Patterns after Failure of Specimen SB3

224 kN (60% of ultimate load). L3, U2, L5, U3, U8, U1, L6, U5, U6, and U7 yielded subsequently, at 225 kN (60% ultimate), 226 kN (60% ultimate), 237 kN (63% ultimate), 238 kN (63% ultimate), 245 kN (65% ultimate), 282 kN (75% ultimate), 282 kN (75% ultimate), 327 kN (87% ultimate), 327 kN (87% ultimate) and 329 kN (87% ultimate) respectively.

The strains at the respective monitoring locations at failure load are shown in Table 5-3.

For this specimen no data was collected at locations L4 and L7.

Table 5-3: Longitudinal Reinforcement Strains at Ultimate Load of Slab SB3

	U1	U2	U3	U4	U5	U6	U7	U8
Failure Strain	0.014	0.014	0.007	0.019	0.020	0.004	0.002	0.026

	L1	L2	L3	L5	L6	L7
Failure Strain	0.022	0.003	0.019	0.019	0.026	0.023

5.2.4 Slab SB 4

Slab SB4 failed in a more ductile mode at a load of about 359.5 kN evidenced by the gradual loss of stiffness after the ultimate load. SB4 was reinforced with 4 peripheral lines of shear bolts. The data collected during testing for slab SB4 is presented as graphs in Appendix B, Figures B-12 to B-15.

Cracks were first noticed at a load of about 125 kN on the tension face of the slab. The flexural cracks became clearly visible at about 132 kN. The more prominent one had formed between parallel peripheral rows of shear bolt. Subsequently at about 167 kN flexural cracks formed starting from the columns corners and extending a short distance towards the supports. At about 203 kN the flexural cracks were observed on all corners and had inched closer to the supports. At a load of about 321 kN there was widespread cracking noticeable all over the tension face of the slab. Cracks were also observed, at failure, on the compression face (top) of the slab parallel to the corner restraints and offset at a distance of about 15-20 mm.

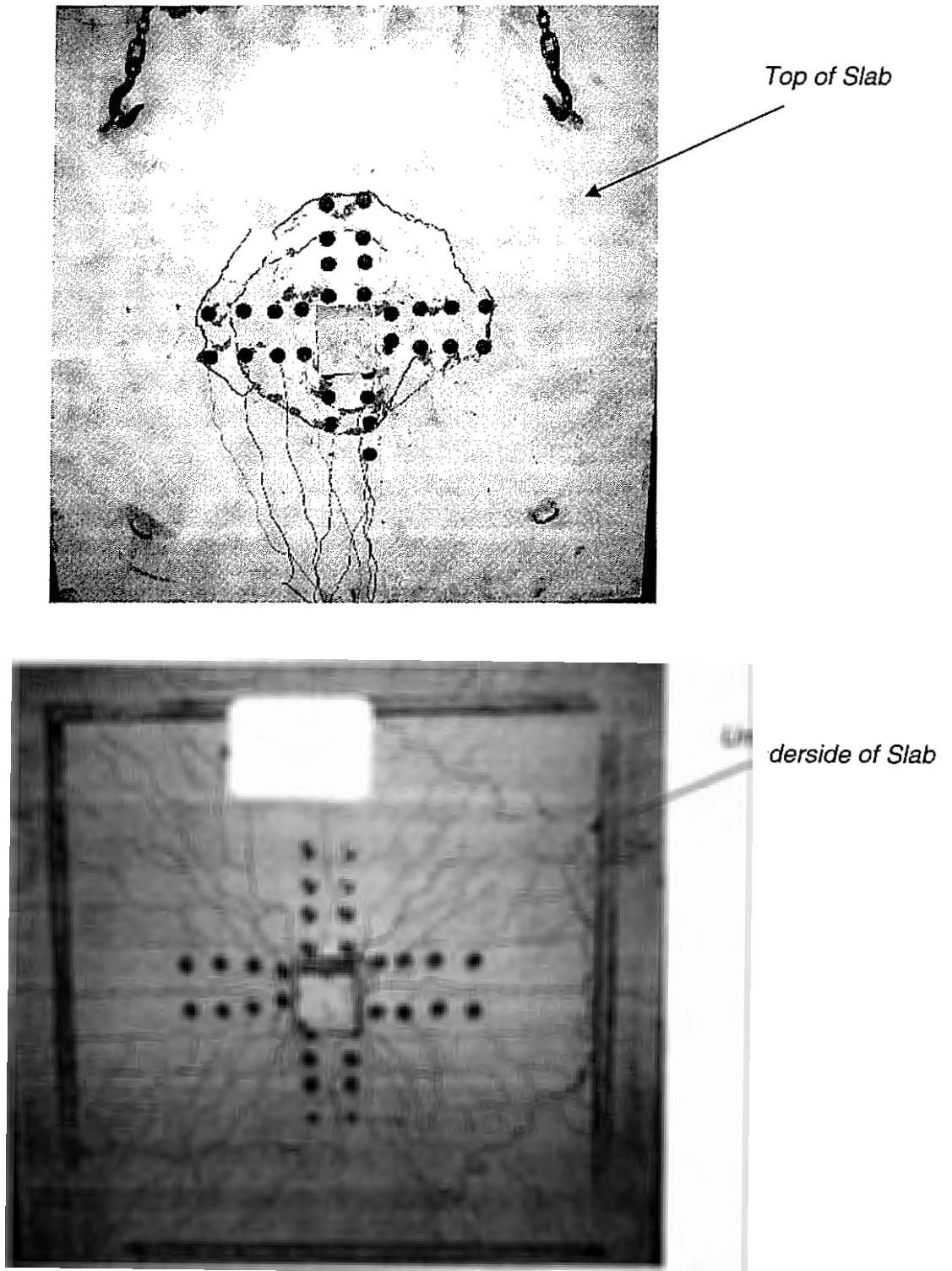


Figure 5-4: Crack Pattern after Failure of Specimen SB4

The LVDT placed at the center of the bottom column (Figure B-12b) measured a maximum deflection of 31 mm at ultimate load. Figure B-13 shows a plot of load against the crack vertical width. The crack widths at locations 8, 9, 10 were the same until about 175 kN. A maximum width of about 4 mm was observed at location 10. The lowest was at location 8.

First yielding in the longitudinal reinforcement occurred at 182 kN (51% of ultimate load) at Strain Gauge U7 as seen in Figure B-14. Next Strain Gauge U5 yielded at a load of 197 kN (55% of ultimate load) as shown in Figure B-14, then U1 yielded at 224 kN (62% of ultimate load). U6, L6, L4, L1 and L5 yielded subsequently at 241 kN (67% ultimate), 242 kN (67% ultimate), 265 kN (74% ultimate), 270 kN (75% ultimate) and 284 kN (79% ultimate) respectively. There was no yielding at U4 and U8. The strains at the strain gauge locations at ultimate load are shown in Table 5-4. No data was collected at locations U2, U3, L2 and L3.

Table 5-4: Longitudinal Reinforcement Strains at Ultimate Load of Slab SB4

	U1	U4	U5	U6	U7	U8
Failure Strain	0.011	0.026	0.006	0.006	0.025	0.002

	L1	L4	L5	L6
Failure Strain	0.003	0.026	0.020	0.018

5.2.5 Slab SB 5

Slab SB5 failed in a ductile mode at a load of about 353 kN. At ultimate load, there was a constantly increasing deflection at constant load. This is typical of a flexural failure. Load-Displacement graphs in Figure B-16, post failure crack pattern and strain measured on longitudinal reinforcement confirm a more ductile flexural failure mode. Data collected while testing slab SB5 is presented as graphs in Figures B-16 to B-19.

Cracks were first noticed at a load of about 125 kN on the tension face of the slab. At a load of 150 kN cracks were noticed to be forming from the corners of openings around the columns. Flexural

cracks became visible at about 125 kN starting from the columns and corners of the holes and extending a short distance towards the supports. At about 193.8 kN the flexural cracks were observed to be extending from the corners of the openings towards the edge of the slab. Inclined cracks became visible inside the openings at a load of about 299 kN. At a load of about 353 kN, there was a narrow punch perimeter indicating failure on the compression face of the slab roughly falling between the first and second peripheral lines of shear bolts around the openings.

The maximum central displacement of this slab measured by an internal LVDT was 30.2 mm as shown in Figure B-16a. Figure B-17 show a plot of load against the crack vertical width. Crack width was limited to a low value of 2.5 mm at all three locations during the test. Location 8 had a slightly larger vertical crack width than the two other locations.

First yielding in longitudinal reinforcement was noticed at 232 kN (65% of ultimate load) at Strain Gauge U1 as seen in Figure B-18a. Next Strain Gauge L3 yielded at a load of 236 kN (67% of ultimate load) as shown in Figure B-18h, then U4 yielded at 248 kN (70% of ultimate load). L1, U2, U3, U7, L2 and L5 yielded subsequently at 250 kN (71% ultimate), 255 kN (72% ultimate), 269 kN (76% ultimate), 319 kN (90% ultimate), 323 kN (92% ultimate) and 343 kN (97% ultimate) respectively. Yielding was noticed after ultimate load at L4, L6 and L7. The strains at the strain gauge locations at ultimate load are shown in Table 5-5. For this specimen no data was collected at locations U5, U6 and U8.

Table 5-5: Longitudinal Reinforcement Strains at Ultimate Load of Slab SB5

	U1	U2	U3	U4	U7
Strain at Ultimate Load	0.008	0.000	0.002	0.013	0.004

	L1	L2	L3	L5	L6	L7
Strain at Ultimate Load	0.015	0.000	0.001	0.003	0.000	0.000

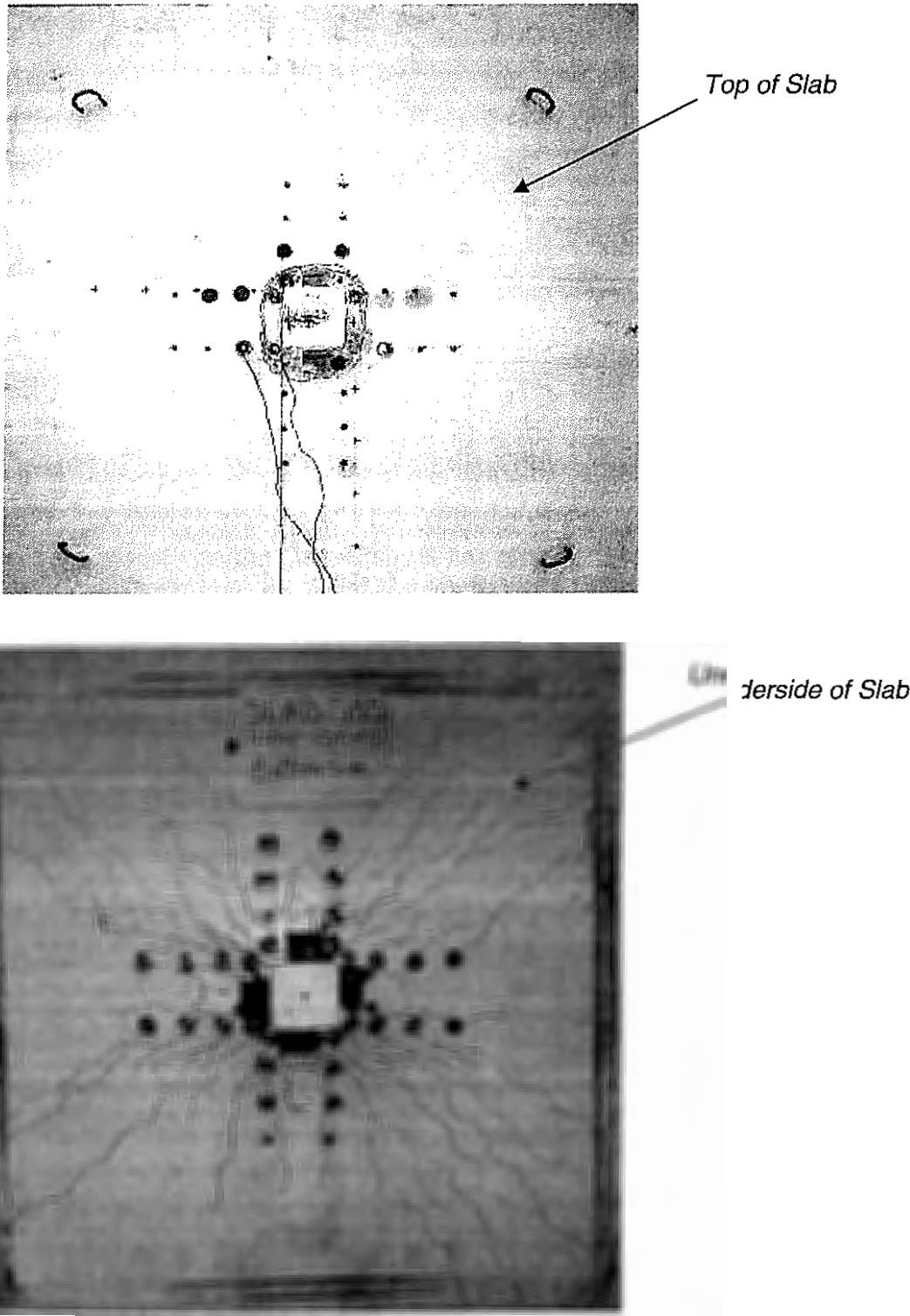


Figure 5-5: Crack Pattern after Failure of Specimen SB5

5.2.6 Slab SB 6

Slab SB6 failed in a ductile flexural mode at a load of about 336 kN evidenced by the gradual loss of stiffness after the ultimate load and more intensive formation of cracks around the column as opposed to a punch through pattern on the tension face. SB6 was the most ductile of all slabs tested. Load-displacement graphs in Figure B-20, post failure crack patterns, and strains measured on longitudinal reinforcement all indicate a flexural failure mode. Data collected while testing slab SB6 is presented as graphs in Appendix B, Figures B-20 to B-23.

Cracking was first noticed at a load of about 103 kN on the tension face of the slab. Flexural cracks were seen starting from the columns and corners of openings and extending a short distance towards the supports. At a load of 176 kN there was widespread cracking all over the tension face of this specimen. At about 250 kN the flexural cracks had extended almost all the way to the edges of the slab. At 336 kN, there was a failure evidenced by a narrow punch perimeter on the compression face of the slab almost coincident with the first peripheral line of studs. At failure the concrete closest to the column had disintegrated, had lost all strength and disintegrated exposing the longitudinal reinforcement towards the latter stages of the test.

A central LVDT placed at the center of the bottom column (Figure B-20b) measured a maximum deflection of about 22 mm at ultimate load. The value of 26 mm in Figure B-20a is the displacement of the testing frame cross piece. Figure B-21 shows a plot of load against the crack vertical width. A maximum crack width of 10-15 mm was observed at location 9. Location 8 and 10 had lower crack widths.

First yielding of longitudinal reinforcement occurred at 244 kN (73% of ultimate load) at Strain Gauge L2 as seen in Figure B-22h. Next Strain Gauge L7 yielded at a load of 250 kN (74% of ultimate load) as shown in Figure B-22m, U5 then yielded at 279 kN (83% of ultimate load). U4 yielded subsequently at 303 kN (90% ultimate). Yielding occurred after ultimate load was reached at locations U3, U6, U7, L1, L3, L4, L5 and L6. No yielding was observed at U1. The strains at the strain gauge locations at ultimate load 336 kN are shown in Table 5-6. For this specimen, because U2 and U8 were damaged, no data was collected at these locations.

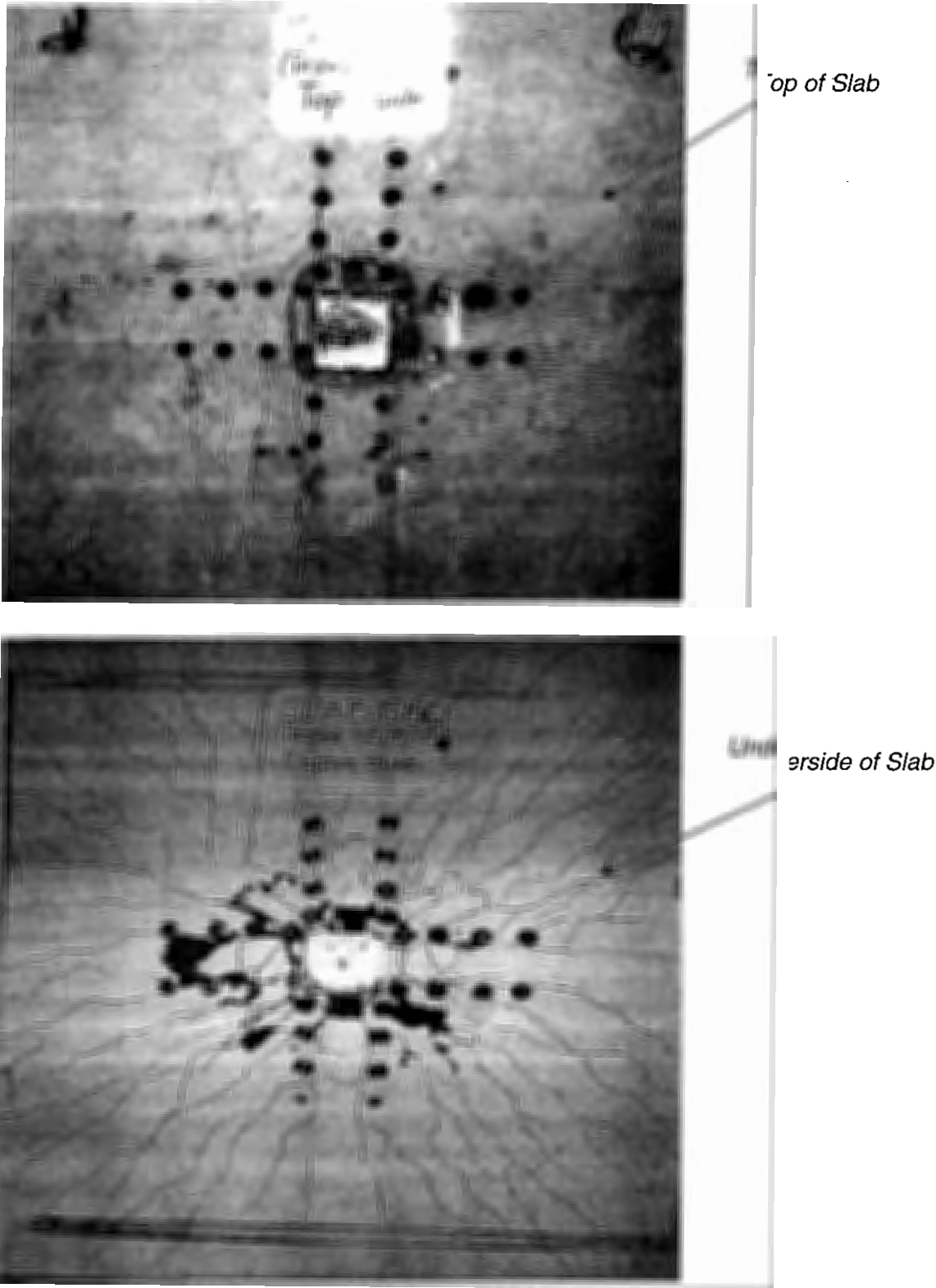


Figure 5-6: Crack Pattern after Failure of Specimen SB6

Table 5-6: Longitudinal Reinforcement Strains at Ultimate Load of Slab SB6

	U1	U3	U4	U5	U6	U7	L1	L2
Strain at Ultimate Load	0	0	0.012	0.005	0.001	0	0.001	0.003

	L3	L4	L5	L6	L7
Strain at Ultimate Load	0.001	0.001	0.001	0.001	0.001

It is important to note that the diameter and thickness of washers used as anchors on the threaded end of the shear bolts appeared to influence the distribution of cracking at the connection. Though varying sizes of washers was not investigated, it was observed that smaller (thickness and diameter) washers resulted in more cracking around the bolts and a slightly lower ultimate load at the connection. It may be that smaller size washers prevent the attainment of the yield strength of the bolts before crushing of the concrete.

Chapter 6

Analysis of Experimental Results

This chapter summarises and analyses the relevant data collected from the slab tests carried out. Inferences are drawn and comparisons made to values predicted from empirical and analytical equations presented in Chapter 2.

The data is analysed based on the crack pattern, deflection behaviour, stiffness, ductility and strain. The crack patterns at failure for the specimens tested were presented in Chapter 5. These patterns sometimes reflect the mode of failure.

6.1 Comparison of Various Code Predictions and Theoretical Analysis

The provisions from the codes of practice have been compared to the empirical failure loads in

Table 6-1: Test Specimens, Code Predictions and Experimental results

Specimen Description		SB1	SB2	SB3	SB4	SB5	SB6
	Rows of shear bolts	0	2	3	4	4	4
No of Openings	0	0	0	0	4	2	
Shear Capacity by Code Practices	Eurocode	159	259	324	375	299	337
	Model Code	164	250	305	360	345	373
	ACI	181	309	309	309	282	295
	CSA	220	361	321	380	334	358
Yield-Line	Flexural Capacity	362	362	362	362	362	362
Experimental Results	Failure Load P	253	358	376	360	353	336
	Failure Mode	Punching	Punching	Punching/ Flexure	Flexure	Flexure	Flexure

Table 6-1. Summarised in the table are the shear resistances of the specimens tested in this program.

6.2 Stiffness and Ductility

It has been previously noted in literature that ductility can be defined as the ratio of the ultimate deflection to the deflection at first yield (Marzouk and Hussein, 1991). Table 6-2 lists the ductility of the various specimens tested.

The stiffness has been defined as the slope of the load deflection curve for a typical slab-column specimen (Marzouk and Hussein, 1991). Also listed in Table 6-2 is the stiffness μ , of the various specimens tested.

Table 6-2: Stiffness, Displacement and Ductility

	Stiffness μ (kN/mm)	Ultimate Displacement (mm)	Displacement at 1st yield (mm)	Ductility (mm/mm)
SB1	19.1	10.4	7.7	1.4
SB2	20.6	17.2	9.0	1.8
SB3	24.0	25.9	12.0	2.2
SB4	26.7	33.0	10.0	3.9
SB5	22.5	30.1	11.9	2.5
SB6	22.4	22.0	10.3	2.1

6.3 Deflections

As shown in Table 6-2, there was significant improvement in the maximum deflection recorded for slabs with shear bolts before failure than for the control specimen without shear bolts. Also, in slabs with four or three peripheral lines of shear bolts more deflections were observed than in the slab with only two rows or the slab without shear bolt reinforcement.

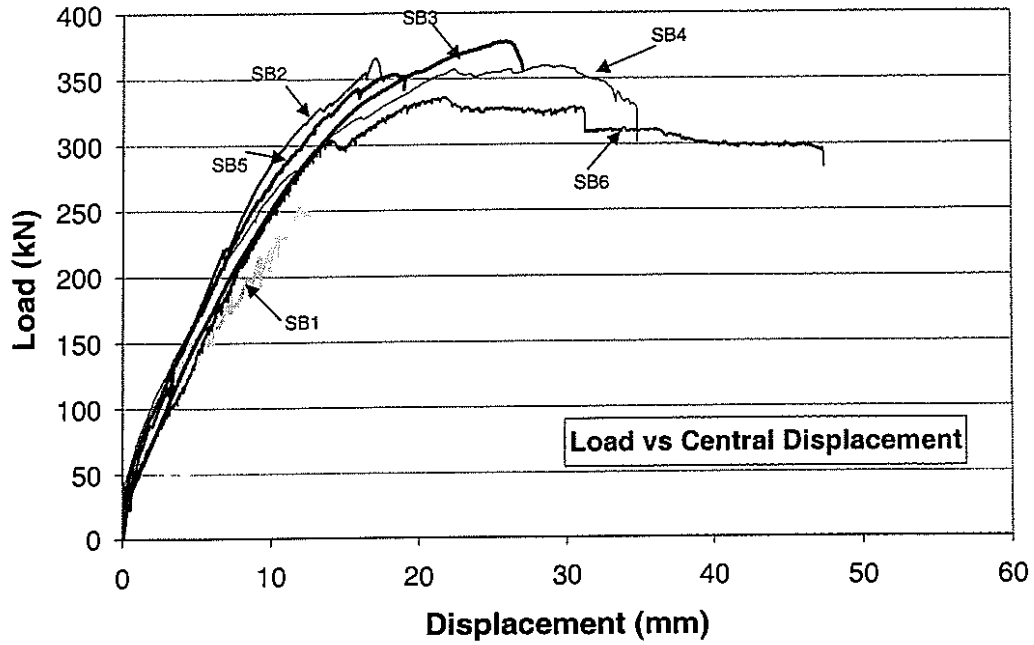


Figure 6-1: Load vs Bottom Central LVDT Displacements

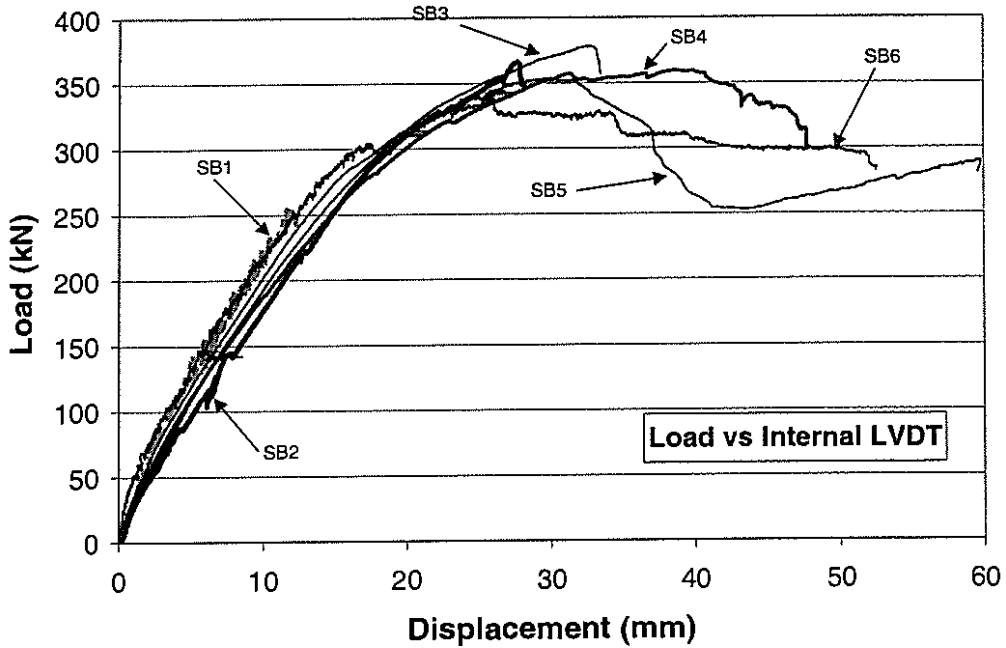


Figure 6-2: Load vs Internal LVDT Displacements

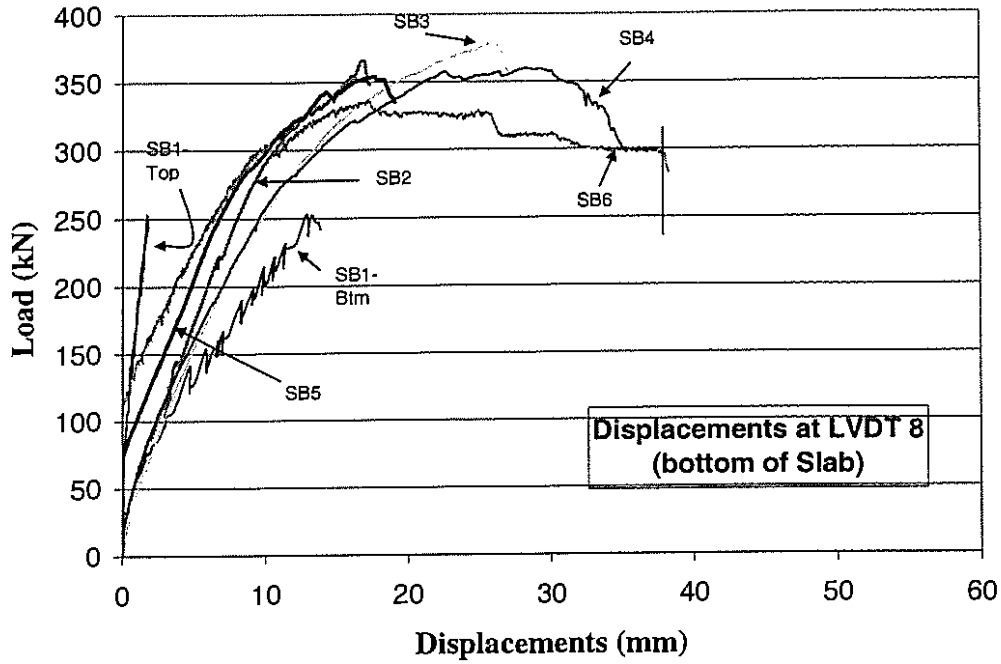


Figure 6-3: Load vs Displacement at LVDT 8

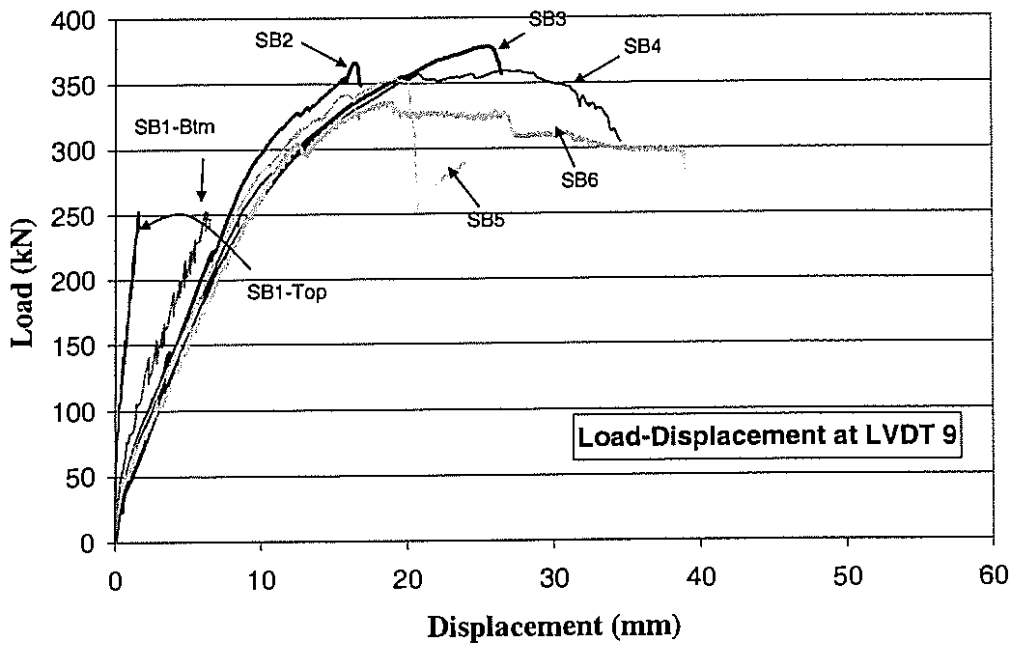


Figure 6-4: Load vs Displacement at LVDT 9

Figures 6-1 to 6-4 show the deflections for all slabs measured at the locations indicated and previously described in Chapter 3. Unless otherwise specified, the measurements are from the bottom LVDT's. In Figure 6-1, the deflection SB1 has been shifted by 2.5 mm. The LVDT did not record any deflection until the load of 80kN. Therefore, the displacement at this load was estimated as approximately 2.5 mm and the deflection data was shifted accordingly.

6.4 Strains in Longitudinal reinforcement

The strains in the longitudinal reinforcement showed some variation in the location at which first yield occurred. Table 6-3 shows the locations with respect to Figure 3-17. The loads at which yielding in the longitudinal reinforcement was first observed is also shown, as well as the other strain gauge location at which yielding was observed at ultimate load. Figure 6-5 shows the strains at the LVDT L6 location.

The load at which first yielding occurs is an indicator of the stiffness of the specimen. Also, the strain at first yield is an indicator of the ductility of the specimen being tested.

Table 6-3: Test Results: Yielding of Longitudinal Reinforcement

Specimen	Failure Load (kN)	Mode	Load at 1 st Yield (kN)	Location of first Yield	Yielding at Failure
SB1	253	Punching	204	L7	U6, U7
SB2	358	Punching	166	L4	L1,U4,L6,U3,L3, U2,L5,U7,U5
SB3	376	Flexure/ Punching	194	L1	L2,U4,L3,U2,L5, U3,U8,L6,U6,U7
SB4	360	Flexure	182	U7	U5,U1,U6,L6, L4,L1,L5
SB5	353	Flexure	232	U1	L3,U4,U3,U7,L2 ,L5
SB6	336	Flexure	250	L7	L2,U5,U4

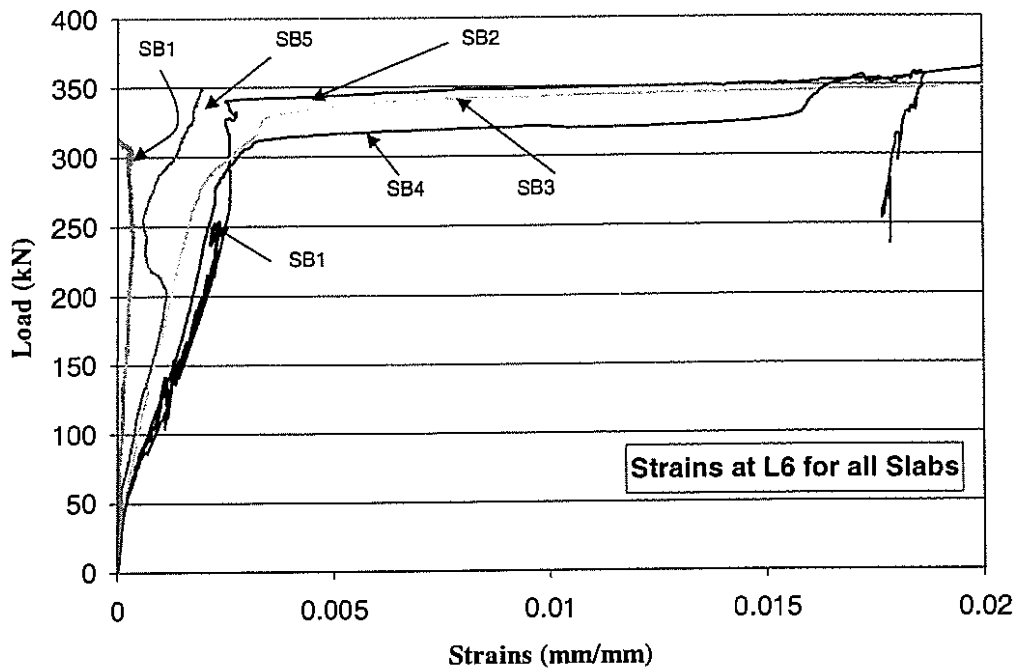


Figure 6-5: Load vs Longitudinal Reinforcement Strain at LVDT L6

6.5 Strains in Shear Bolts

For all the slabs tested, strains were larger at the strain gauges closer to the column. Figures 6-7 to 6-11 show the profile of strain in the Shear Bolts relative to their distance from the column as shown in Figure 6-6. Since individual shear bolts are installed in this method, it may be advisable to make use of steel with a bigger cross section or yield strength on the peripheral row closer to the column. Figure 6-11, showing strains for slab SB6 indicates some discrepancy with data acquisition. The strains at position 1 have been ignored.

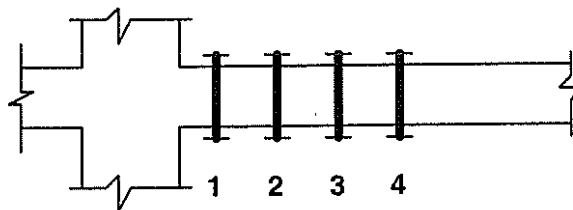


Figure 6-6: Position of Shear Bolts in Figure 6-7 to 6-11

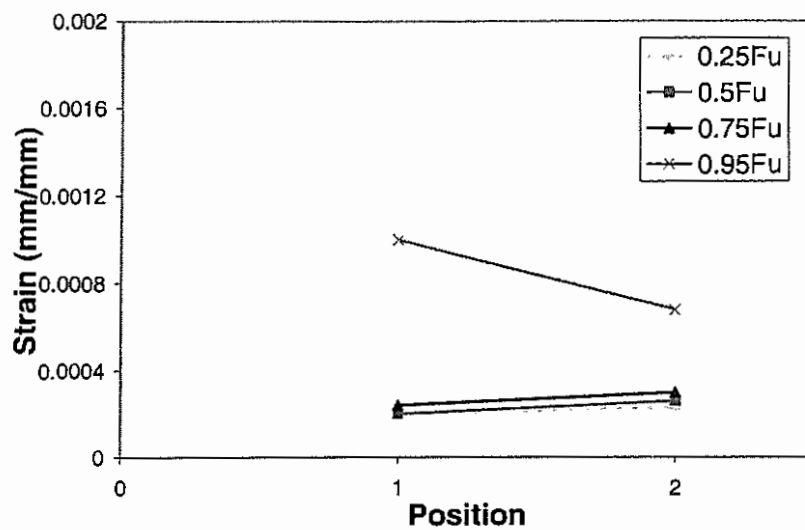


Figure 6-7: Bolt Strain Relative to Distance from the Column of Specimen SB2

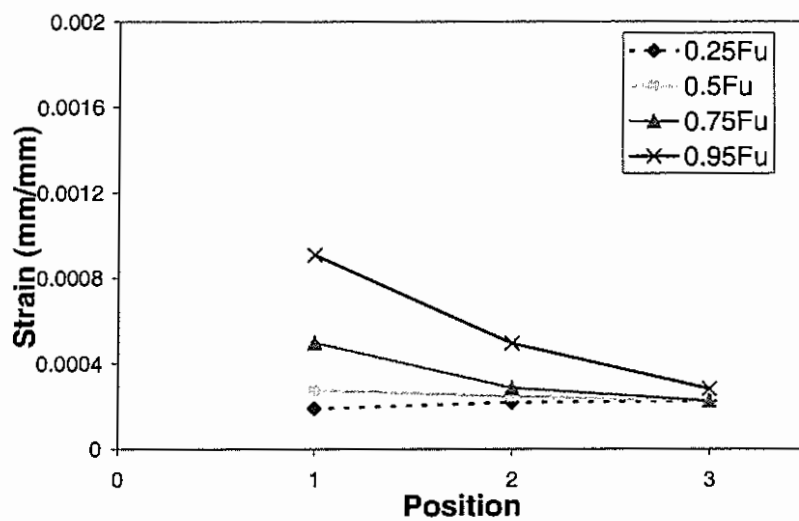


Figure 6-8: Bolt Strain Relative to Distance from the Column of Specimen SB3

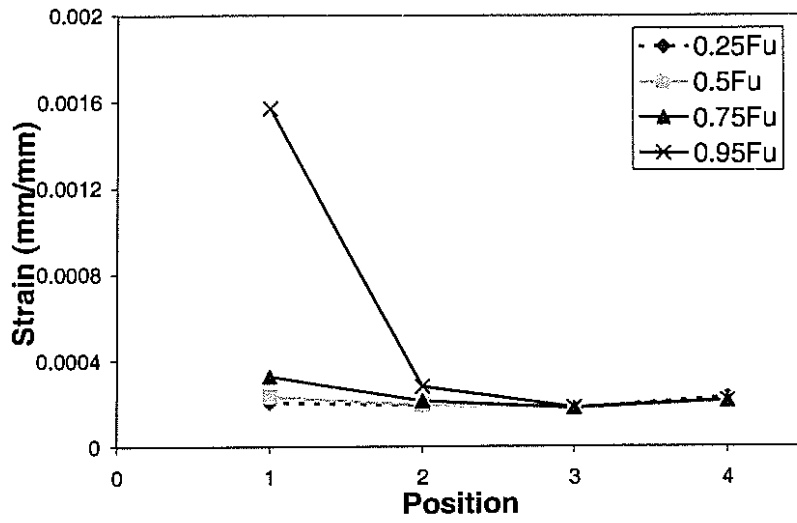


Figure 6-9: Bolt Strain Relative to Distance from the Column of Specimen SB4

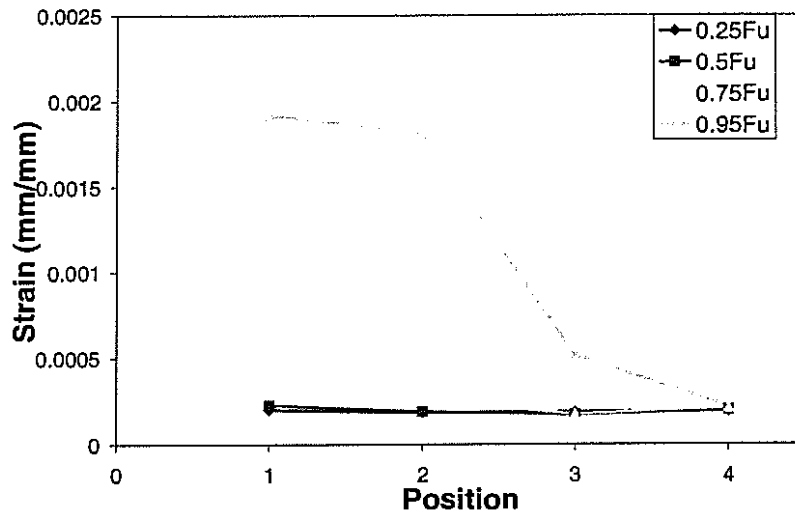


Figure 6-10: Bolt Strain Relative to Distance from the Column of Specimen SB5

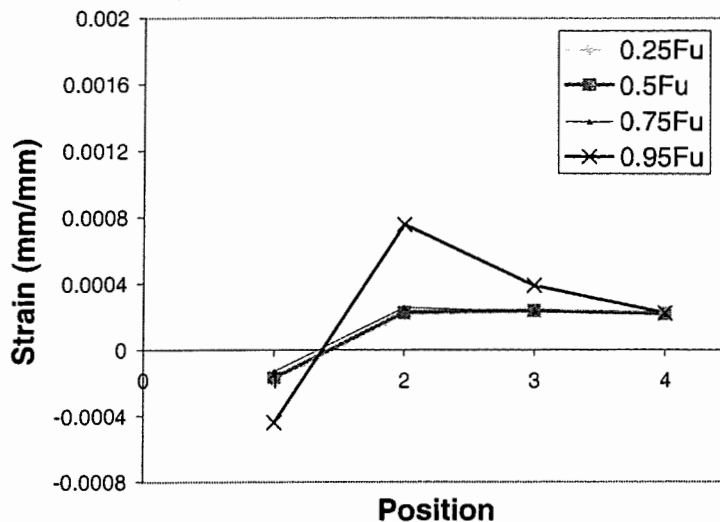


Figure 6-11: Bolt Strain Relative to Distance from the Column of Specimen SB6

6.6 Effectiveness of Shear Bolts in Reducing Crack Width

Cracks were monitored as described in Section 3.5.2. Shear bolts effectively prevented propagation of shear cracking in slabs reinforced with shear bolts. Table 6-4 gives a comparison of the shear crack width for the control specimen and the other specimens with transverse shear reinforcement. Figure 6-12 is a graph of the crack widths for SB1.

Table 6-4: Maximum Crack Widths

Specimens	Maximum Observed Crack Width
SB1	10-12 mm
SB2	<2.5 mm
SB3	<2.5 mm
SB4	<2.5 mm
SB5	1.5-2.0 mm
SB6	-

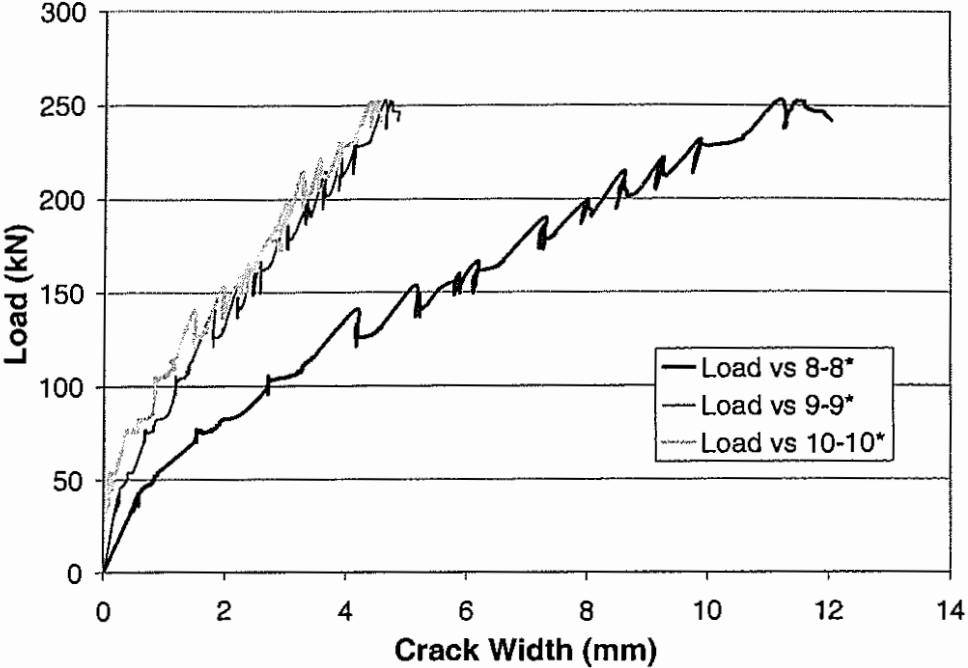


Figure 6-12: Load vs Vertical Crack Width of Specimen SB1

Chapter 7

Conclusions and Recommendations

The feasibility and effectiveness of using shear bolt as a new method of transverse reinforcement has been examined in this research program. While previous research (El-Salakawy, 2003) had verified the feasibility of the use, this program was focused on determining the behavior of an interior slab-column connection when reinforced transversely with shear bolts.

7.1 Conclusions

The data collected during testing and other visual observations made, as described in this thesis, resulted in the following inferences:

- The experimental setup and procedures that were adopted for testing the interior slab-column connections subjected to pure axial load is practical. Throughout the course of testing, there were no major failures or malfunction of equipment. The procedures gave results very consistent with predictions. The results collected for the specimens showed very little deviations.
- Shear bolts are effective in preventing punching shear failure in slab-column interior connections.
- The use of shear bolts as transverse reinforcement allowed the slab-column connection to attain flexural capacity and increased the ductility of the connection.
- Shear bolts are effective in enhancing the strength of a slab-column connection that has been subjected to a reduction in strength due to construction of openings and ducts after a structure has been built. Specimens SB5 and SB6 both failed in flexural mode.
- It was observed that the diameter of the washers (which serve as anchor plates) had an effect on the ultimate strength of the connections by affecting the ability of the shear bolt to attain yield before failure at the connection.

7.2 Recommendations

- Further testing should be carried out to collect more information on the use of shear bolts as transverse reinforcement. Different configurations and varied number of studs per peripheral row may be tested to provide more data.
- Further testing should also consider reversed cyclic loading in order to establish the effectiveness of the shear bolt in providing ductility in seismic zones.
- In future testing, code of practice requirements with regards to the minimum distance of the first row of bolts from the column ($d/2$), and the maximum spacing between rows of transverse reinforcement should be followed. If possible code of practice requirements for shear studs should be adopted for shear bolts pending additional testing to determine specific requirements for shear bolts.
- Design procedures for shear bolts should be developed. This should include size of bolt, size of the head, size of the opening drilled in the slab and layout of the shear bolts around the column.
- In future tests, the edge hold down system should have a uniform specified torque. This is to avoid inconsistencies that may have arisen from different degrees of tightening.

Appendix A

Elastic Frame Analysis in SODA®

A.1 Input File

```
*****
                        I N P U T   D A T A   E C H O
*****
```

```
PROJECT TITLE
    Continuous Slab System Design
```

```
PROJECT DESCRIPTION
2-d elastic frame analysis according to CSA A23.3-94.
The continuous slab system consists of 5 spans in one direction and infinite
number of spans in the other direction.
```

GENERAL DATA

Dimension	Structure	Action	Design Code	Output	Units

2-D	Frame	Analysis		Normal	kN;m
Analysis	Sway	Database	Foreign Sections		

First Order		None	Not Included		

STRUCTURE DATA

Members	Groups	Nodes	Load Cases	Supports

51	4	52	1	12

NODE DATA

Node Name	X-Coordinate (m)	Y-Coordinate (m)	Support Type

1 x0y0	0	0	Fixed
2 x3y0	3.75	0	Fixed
3 x6y0	7.5	0	Fixed
4 x9y0	11.25	0	Fixed
5 x12y0	15	0	Fixed
6 x15y0	18.75	0	Fixed
7 x0y1	0	0.06	
8 x0y2	0	2.64	
9 x0y4	0	2.76	
10 x0y5	0	5.34	
11 x0y6	0	5.4	Fixed
12 x1y3	0.075	2.7	
13 x2y3	3.675	2.7	
14 x3y1	3.75	0.06	
15 x3y2	3.75	2.64	
16 x3y3	3.75	2.7	
17 x3y4	3.75	2.76	
18 x9y1	11.25	0.06	

19	x9y2	11.25	2.64	
20	x9y4	11.25	2.76	
21	x9y5	11.25	5.34	
22	x9y6	11.25	5.4	Fixed
23	x10y3	11.325	2.7	
24	x11y3	14.925	2.7	
25	x12y3	15	2.7	
26	x12y1	15	0.06	
27	x12y2	15	2.64	
28	x12y4	15	2.76	
29	x12y5	15	5.34	
30	x12y6	15	5.4	Fixed
31	x13y3	15.075	2.7	
32	x14y3	18.675	2.7	
33	x15y3	18.75	2.7	
34	x15y1	18.75	0.06	
35	x15y2	18.75	2.64	
36	x15y4	18.75	2.76	
37	x15y5	18.75	5.34	
38	x15y6	18.75	5.4	Fixed
39	x0y3	0	2.7	
40	x3y5	3.75	5.34	
41	x3y6	3.75	5.4	Fixed
42	x4y3	3.825	2.7	
43	x6y3	7.5	2.7	
44	x6y1	7.5	0.06	
45	x6y2	7.5	2.64	
46	x6y4	7.5	2.76	
47	x6y5	7.5	5.34	
48	x6y6	7.5	5.4	Fixed
49	x7y3	7.56	2.7	
50	x8y3	11.175	2.7	
51	x9y3	11.25	2.7	
52	x5y3	7.425	2.7	

GROUP ANALYSIS DATA

Group Name	Shape File	X-Section Designation	Young's Modulus (MPa)	Shear Modulus (MPa)	X-Sect. Area (mm) 2	Moment of Inertia (mm) 4	
1	slab	<None>	<Unkown>	26622	77000	450000	5.4e+008
2	column	<None>	<Unkown>	26622	77000	22500	4.219e+007
3	infinite	<None>	<Unkown>	26622	77000	9e+006	1e+011
4	sconn	<None>	<Unkown>	26622	77000	450000	5.86e+008

MEMBER DATA

Member Name	Start Node	End Node	Joint Type	Beta Angle	Length Kx	Length Ky	Factors Bt	Factors Bb	Group Name
1	x0m1	x0y0	x0y1	+----+	0				infinite
2	x0m2	x0y1	x0y2	+----+	0				column
3	x0m3	x0y2	x0y3	+----+	0				infinite
4	x0m4	x0y3	x0y4	+----+	0				infinite
5	x0m5	x0y4	x0y5	+----+	0				column
6	x0m6	x0y5	x0y6	+----+	0				infinite

7	m1y3	x0y3	x1y3	+----+	0	sconn
8	m2y3	x1y3	x2y3	+----+	0	slab
9	m3y3	x2y3	x3y3	+----+	0	sconn
10	m4y3	x3y3	x4y3	+----+	0	sconn
11	x3m3	x3y2	x3y3	+----+	0	infinite
12	x3m4	x3y3	x3y4	+----+	0	infinite
13	x3m5	x3y4	x3y5	+----+	0	column
14	x3m6	x3y5	x3y6	+----+	0	infinite
15	x6m1	x6y0	x6y1	+----+	0	infinite
16	x6m2	x6y1	x6y2	+----+	0	column
17	x6m3	x6y2	x6y3	+----+	0	infinite
18	x6m4	x6y3	x6y4	+----+	0	infinite
19	x6m6	x6y5	x6y6	+----+	0	infinite
20	x6m5	x6y4	x6y5	+----+	0	column
21	x9m1	x9y0	x9y1	+----+	0	infinite
22	x9m2	x9y1	x9y2	+----+	0	column
23	x9m3	x9y2	x9y3	+----+	0	infinite
24	x9m4	x9y3	x9y4	+----+	0	infinite
25	x9m5	x9y4	x9y5	+----+	0	column
26	x9m6	x9y5	x9y6	+----+	0	infinite
27	x12m1	x12y0	x12y1	+----+	0	infinite
28	x12m2	x12y1	x12y2	+----+	0	column
29	x12m3	x12y2	x12y3	+----+	0	infinite
30	x12m4	x12y3	x12y4	+----+	0	infinite
31	x12m5	x12y4	x12y5	+----+	0	column
32	x12m6	x12y5	x12y6	+----+	0	infinite
33	x15m1	x15y0	x15y1	+----+	0	infinite
34	x15m2	x15y1	x15y2	+----+	0	column
35	x15m3	x15y2	x15y3	+----+	0	infinite
36	x15m4	x15y3	x15y4	+----+	0	infinite
37	x15m5	x15y4	x15y5	+----+	0	column
38	x15m6	x15y5	x15y6	+----+	0	infinite
39	m5y3	x4y3	x5y3	+----+	0	slab
40	m6y3	x5y3	x6y3	+----+	0	sconn
41	m7y3	x6y2	x7y3	+----+	0	sconn
42	m9y3	x8y3	x9y3	+----+	0	sconn
43	m10y3	x9y3	x10y3	+----+	0	sconn
44	m8y3	x7y3	x8y3	+----+	0	slab
45	m11y3	x10y3	x11y3	+----+	0	slab
46	m12y3	x11y3	x12y3	+----+	0	sconn
47	m13y3	x12y3	x13y3	+----+	0	sconn
48	m14y3	x13y3	x14y3	+----+	0	slab
49	m15y3	x14y3	x15y3	+----+	0	sconn
50	x3m1	x3y0	x3y1	+----+	0	infinite
51	x3m2	x3y1	x3y2	+----+	0	column

LOAD NAME DATA

Member Load: udl

Member Name	w@Start (kN / m)	Start (L/100)	w@Finish (kN / m)	Finish (L/100)	Orient- ation	Load Type	
1	m2y3	-69.4	0	-69.4	1	Y	FULL UNIDL
2	m10y3	-69.4	0	-69.4	1	Y	FULL UNIDL
3	m11y3	-69.4	0	-69.4	1	Y	FULL UNIDL
4	m12y3	-69.4	0	-69.4	1	Y	FULL UNIDL
5	m13y3	-69.4	0	-69.4	1	Y	FULL UNIDL

6	m14y3	-69.4	0	-69.4	1	Y	FULL UNIDL
7	m15y3	-69.4	0	-69.4	1	Y	FULL UNIDL
8	m1y3	-69.4	0	-69.4	1	Y	FULL UNIDL
9	m3y3	-69.4	0	-69.4	1	Y	FULL UNIDL
10	m4y3	-69.4	0	-69.4	1	Y	FULL UNIDL
11	m5y3	-69.4	0	-69.4	1	Y	FULL UNIDL
12	m6y3	-69.4	0	-69.4	1	Y	FULL UNIDL
13	m7y3	-69.4	0	-69.4	1	Y	FULL UNIDL
14	m8y3	-69.4	0	-69.4	1	Y	FULL UNIDL
15	m9y3	-69.4	0	-69.4	1	Y	FULL UNIDL

LOAD COMBINATIONS

Load Combination 1

=====

unfactored

Member Load: 'udl' with a Load Factor of 1

A.2 Analysis Printout

 ANALYSIS RESULTS

 P-Delta Effects: not included

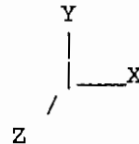
• Loads applied to SUPPORTS are ignored in Analysis and Design calculations.

Sign Convention

=====

Unless noted otherwise, the Right-Hand-Screw Rule applies.

REACTIONS & DISPLACEMENTS are with respect to the GLOBAL Axis



MEMBER-END FORCES are with respect to the LOCAL Axis



Positive Moment= tension on "top" face of member (the positive local y-axis projects from the top face).

Positive Shear = member-end shear is in the same direction as the positive local y-axis.

Axial Tension = negative axial force @ i-node, positive @ j-node.

M-stg. = bending moment about the strong (x-x) axis.

V-stg. = shear related to bending about the strong (x-x) axis.

M-weak = bending moment about the weak (y-y) axis.

V-weak = shear related to bending about the weak (y-y) axis.
 Torque = torsion about the longitudinal (z-z) axis.

Max.Span Moments: location is given as distance from i-node.

=====
 Load Combination # 1 of 1
 =====

Title: unfactored

Member - End Forces (w.r.t. local member axes)

Member Name	Node Name	axial [kN]	shear [kN]	moment [kN-m]	Max_Span_Moment & Location	LC #
x0m1	x0y0	54.177	-5.081	-4.773		1
	x0y1	-54.177	5.081	-4.468		
x0m2	x0y1	54.177	-5.081	-4.468		1
	x0y2	-54.177	5.081	8.640		
x0m3	x0y2	54.177	-5.081	8.640		1
	x0y3	-54.177	5.081	8.936		
x0m4	x0y3	-54.177	-5.072	-9.278		1
	x0y4	54.177	5.072	-8.628		
x0m5	x0y4	-54.177	-5.072	-8.628		1
	x0y5	54.177	5.072	4.457		
x0m6	x0y5	-54.177	-5.072	4.457		1
	x0y6	54.177	5.072	4.761		
m1y3	x0y3	.009	108.355	18.215	18.215	1
	x1y3	-.009	-103.150	10.282	.00 [m]	
m2y3	x1y3	.009	103.150	10.282	-66.374	1
	x2y3	-.009	146.690	88.655	1.49 [m]	
m3y3	x2y3	.009	-146.690	88.655	99.852	1
	x3y3	-.009	151.895	99.852	.08 [m]	
m4y3	x3y3	.018	135.021	95.788	95.788	1
	x4y3	-.018	-129.816	85.857	.00 [m]	
x3m3	x3y2	143.458	1.128	-1.920		1
	x3y3	-143.458	-1.128	-1.986		
x3m4	x3y3	-143.458	1.137	2.078		1
	x3y4	143.458	-1.137	1.932		
x3m5	x3y4	-143.458	1.137	1.932		1
	x3y5	143.458	-1.137	-1.001		
x3m6	x3y5	-143.458	1.137	-1.001		1
	x3y6	143.458	-1.137	-1.070		
x6m1	x6y0	127.519	-.262	-.248		1
	x6y1	-127.519	.262	-.232		
x6m2	x6y1	127.519	-.262	-.232		1
	x6y2	-127.519	.262	.444		
x6m3	x6y2	-2.283	-.233	-77.903		1
	x6y3	2.283	.233	-77.889		
x6m4	x6y3	-127.512	-.251	-.462		1
	x6y4	127.512	.251	-.429		
x6m6	x6y5	-127.512	-.251	.219		1
	x6y6	127.512	.251	.234		
x6m5	x6y4	-127.512	-.251	-.429		1
	x6y5	127.512	.251	.219		
x9m1	x9y0	128.001	.336	.317		1

	x9y1	-128.001	-.336	.297		
x9m2	x9y1	128.001	.336	.297		1
	x9y2	-128.001	-.336	-.569		
x9m3	x9y2	128.001	.336	-.569		1
	x9y3	-128.001	-.336	-.589		
x9m4	x9y3	-128.001	.326	.599		1
	x9y4	128.001	-.326	.556		
x9m5	x9y4	-128.001	.326	.556		1
	x9y5	128.001	-.326	-.285		
x9m6	x9y5	-128.001	.326	-.285		1
	x9y6	128.001	-.326	-.304		
x12m1	x12y0	143.265	-1.146	-1.074		1
	x12y1	-143.265	1.146	-1.005		
x12m2	x12y1	143.265	-1.146	-1.005		1
	x12y2	-143.265	1.146	1.951		
x12m3	x12y2	143.265	-1.146	1.951		1
	x12y3	-143.265	1.146	2.018		
x12m4	x12y3	-143.265	-1.155	-2.111		1
	x12y4	143.265	1.155	-1.963		
x12m5	x12y4	-143.265	-1.155	-1.963		1
	x12y5	143.265	1.155	1.018		
x12m6	x12y5	-143.265	-1.155	1.018		1
	x12y6	143.265	1.155	1.087		
x15m1	x15y0	54.208	5.088	4.780		1
	x15y1	-54.208	-5.088	4.475		
x15m2	x15y1	54.208	5.088	4.475		1
	x15y2	-54.208	-5.088	-8.652		
x15m3	x15y2	54.208	5.088	-8.652		1
	x15y3	-54.208	-5.088	-8.949		
x15m4	x15y3	-54.208	5.078	9.290		1
	x15y4	54.208	-5.078	8.639		
x15m5	x15y4	-54.208	5.078	8.639		1
	x15y5	54.208	-5.078	-4.462		
x15m6	x15y5	-54.208	5.078	-4.462		1
	x15y6	54.208	-5.078	-4.767		
m5y3	x4y3	.018	129.816	85.857	-35.557	1
	x5y3	-.018	120.024	68.231	1.87 [m]	
m6y3	x5y3	.018	-120.024	68.231	77.428	1
	x6y3	-.018	125.229	77.428	.08 [m]	
m7y3	x6y2	91.805	91.763	78.347	78.347	1
	x7y3	-88.860	-88.818	70.686	.00 [m]	
m9y3	x8y3	.029	-125.243	69.973	79.561	1
	x9y3	-.029	130.448	79.561	.08 [m]	
m10y3	x9y3	.019	125.553	78.374	78.374	1
	x10y3	-.019	-120.348	69.153	.00 [m]	
m8y3	x7y3	.029	125.638	70.686	-43.038	1
	x8y3	-.029	125.243	69.973	1.81 [m]	
m11y3	x10y3	.019	120.348	69.153	-35.197	1
	x11y3	-.019	129.492	85.611	1.73 [m]	
m12y3	x11y3	.019	-129.492	85.611	95.518	1
	x12y3	-.019	134.697	95.518	.08 [m]	
m13y3	x12y3	.010	151.834	99.646	99.646	1
	x13y3	-.010	-146.629	88.454	.00 [m]	
m14y3	x13y3	.010	146.629	88.454	-66.445	1
	x14y3	-.010	103.211	10.303	2.11 [m]	
m15y3	x14y3	.010	-103.211	10.303	18.239	1

	x15y3	-.010	108.416	18.239	.08 [m]	
x3m1	x3y0	143.458	1.128	1.057		1
	x3y1	-143.458	-1.128	.990		
x3m2	x3y1	143.458	1.128	.990		1
	x3y2	-143.458	-1.128	-1.920		

D i s p l a c e m e n t s & S u p p o r t R e a c t i o n s

Node Name	disp-X [mm]	disp-Y [mm]	rotn-Z [rad]	force-X [kN]	force-Y [kN]	moment-Z [kN-m]	LC #
x0y0	.0000	.0000	.0000	5.08	54.18	-4.773	1
x3y0	.0000	.0000	.0000	-1.13	143.46	1.057	1
x6y0	.0000	.0000	.0000	.26	127.52	-.248	1
x9y0	.0000	.0000	.0000	-.34	128.00	.317	1
x12y0	.0000	.0000	.0000	1.15	143.27	-1.074	1
x15y0	.0000	.0000	.0000	-5.09	54.21	4.780	1
x0y1	.0000	.0000	.0000				1
x0y2	-.2932	-.2334	-.0048				1
x0y4	.2817	-.2334	-.0048				1
x0y5	.0000	.0000	.0000				1
x0y6	.0000	.0000	.0000	-5.07	54.18	-4.761	1
x1y3	-.0058	-.5955	-.0049				1
x2y3	-.0058	-.7155	.0015				1
x3y1	.0000	.0000	.0000				1
x3y2	.0584	-.6179	.0011				1
x3y3	-.0058	-.6180	.0011				1
x3y4	-.0699	-.6179	.0011				1
x9y1	.0000	.0000	.0000				1
x9y2	.0249	-.5514	.0003				1
x9y4	-.0126	-.5514	.0003				1
x9y5	.0000	.0000	.0000				1
x9y6	.0000	.0000	.0000	.33	128.00	.304	1
x10y3	.0062	-.5415	.0000				1
x11y3	.0062	-.5523	-.0007				1
x12y3	.0062	-.6171	-.0011				1
x12y1	.0000	.0000	.0000				1
x12y2	-.0590	-.6171	-.0011				1
x12y4	.0713	-.6171	-.0011				1
x12y5	.0000	.0000	.0000				1
x12y6	.0000	.0000	.0000	-1.16	143.27	-1.087	1
x13y3	.0062	-.7159	-.0015				1
x14y3	.0062	-.5961	.0049				1
x15y3	.0062	-.2335	.0048				1
x15y1	.0000	.0000	.0000				1
x15y2	.2940	-.2335	.0048				1
x15y4	-.2817	-.2335	.0048				1
x15y5	.0000	.0000	.0000				1
x15y6	.0000	.0000	.0000	5.08	54.21	4.767	1
x0y3	-.0058	-.2334	-.0048				1
x3y5	.0000	.0000	.0000				1
x3y6	.0000	.0000	.0000	1.14	143.46	1.070	1
x4y3	-.0058	-.5545	.0006				1
x6y3	-.0058	-.5493	-.0002				1
x6y1	.0000	.0000	.0000				1
x6y2	-.0203	-.5493	-.0002				1

x6y4	.0087	-.5493	-.0002				1
x6y5	.0000	.0000	.0000				1
x6y6	.0000	.0000	.0000	-.25	127.51	-.234	1
x7y3	.0062	-.5767	-.0006				1
x8y3	.0062	-.5886	.0007				1
x9y3	.0062	-.5514	.0003				1
x5y3	-.0058	-.5446	.0001				1

Sum of Input Loads | Sum of Reactions [kN]

```
-----
force-X =           .00 |           .00
force-Y =        -1301.25 |        1301.25
=====
```

For ALL Load Combinations

MAXIMUM Member - End Forces (w.r.t. local member axes)

Member Name	tension [kN] (LC)	comp'n [kN] (LC)	shear [kN] (LC)	end-moment [kN-m] (LC)
x0m1	.0 (0)	-54.2 (1)	5.1 (1)	4.8 (1)
x0m2	.0 (0)	-54.2 (1)	5.1 (1)	8.6 (1)
x0m3	.0 (0)	-54.2 (1)	5.1 (1)	8.9 (1)
x0m4	54.2 (1)	.0 (0)	5.1 (1)	9.3 (1)
x0m5	54.2 (1)	.0 (0)	5.1 (1)	8.6 (1)
x0m6	54.2 (1)	.0 (0)	5.1 (1)	4.8 (1)
m1y3	.0 (0)	.0 (1)	108.4 (1)	18.2 (1)
m2y3	.0 (0)	.0 (1)	146.7 (1)	88.7 (1)
m3y3	.0 (0)	.0 (1)	151.9 (1)	99.9 (1)
m4y3	.0 (0)	.0 (1)	135.0 (1)	95.8 (1)
x3m3	.0 (0)	-143.5 (1)	1.1 (1)	2.0 (1)
x3m4	143.5 (1)	.0 (0)	1.1 (1)	2.1 (1)
x3m5	143.5 (1)	.0 (0)	1.1 (1)	1.9 (1)
x3m6	143.5 (1)	.0 (0)	1.1 (1)	1.1 (1)
x6m1	.0 (0)	-127.5 (1)	.3 (1)	.2 (1)
x6m2	.0 (0)	-127.5 (1)	.3 (1)	.4 (1)
x6m3	2.3 (1)	.0 (0)	.2 (1)	77.9 (1)
x6m4	127.5 (1)	.0 (0)	.3 (1)	.5 (1)
x6m6	127.5 (1)	.0 (0)	.3 (1)	.2 (1)
x6m5	127.5 (1)	.0 (0)	.3 (1)	.4 (1)
x9m1	.0 (0)	-128.0 (1)	.3 (1)	.3 (1)
x9m2	.0 (0)	-128.0 (1)	.3 (1)	.6 (1)
x9m3	.0 (0)	-128.0 (1)	.3 (1)	.6 (1)
x9m4	128.0 (1)	.0 (0)	.3 (1)	.6 (1)
x9m5	128.0 (1)	.0 (0)	.3 (1)	.6 (1)
x9m6	128.0 (1)	.0 (0)	.3 (1)	.3 (1)
x12m1	.0 (0)	-143.3 (1)	1.1 (1)	1.1 (1)
x12m2	.0 (0)	-143.3 (1)	1.1 (1)	2.0 (1)
x12m3	.0 (0)	-143.3 (1)	1.1 (1)	2.0 (1)
x12m4	143.3 (1)	.0 (0)	1.2 (1)	2.1 (1)
x12m5	143.3 (1)	.0 (0)	1.2 (1)	2.0 (1)

x12m6	143.3 (1)	.0 (0)	1.2 (1)	1.1 (1)
x15m1	.0 (0)	-54.2 (1)	5.1 (1)	4.8 (1)
x15m2	.0 (0)	-54.2 (1)	5.1 (1)	8.7 (1)
x15m3	.0 (0)	-54.2 (1)	5.1 (1)	8.9 (1)
x15m4	54.2 (1)	.0 (0)	5.1 (1)	9.3 (1)
x15m5	54.2 (1)	.0 (0)	5.1 (1)	8.6 (1)
x15m6	54.2 (1)	.0 (0)	5.1 (1)	4.8 (1)
m5y3	.0 (0)	.0 (1)	129.8 (1)	85.9 (1)
m6y3	.0 (0)	.0 (1)	125.2 (1)	77.4 (1)
m7y3	.0 (0)	-91.8 (1)	91.8 (1)	78.3 (1)
m9y3	.0 (0)	.0 (1)	130.4 (1)	79.6 (1)
m10y3	.0 (0)	.0 (1)	125.6 (1)	78.4 (1)
m8y3	.0 (0)	.0 (1)	125.6 (1)	70.7 (1)
m11y3	.0 (0)	.0 (1)	129.5 (1)	85.6 (1)
m12y3	.0 (0)	.0 (1)	134.7 (1)	95.5 (1)
m13y3	.0 (0)	.0 (1)	151.8 (1)	99.6 (1)
m14y3	.0 (0)	.0 (1)	146.6 (1)	88.5 (1)
m15y3	.0 (0)	.0 (1)	108.4 (1)	18.2 (1)
x3m1	.0 (0)	-143.5 (1)	1.1 (1)	1.1 (1)
x3m2	.0 (0)	-143.5 (1)	1.1 (1)	1.9 (1)

A.3 Node Labels in Elastic Frame Model

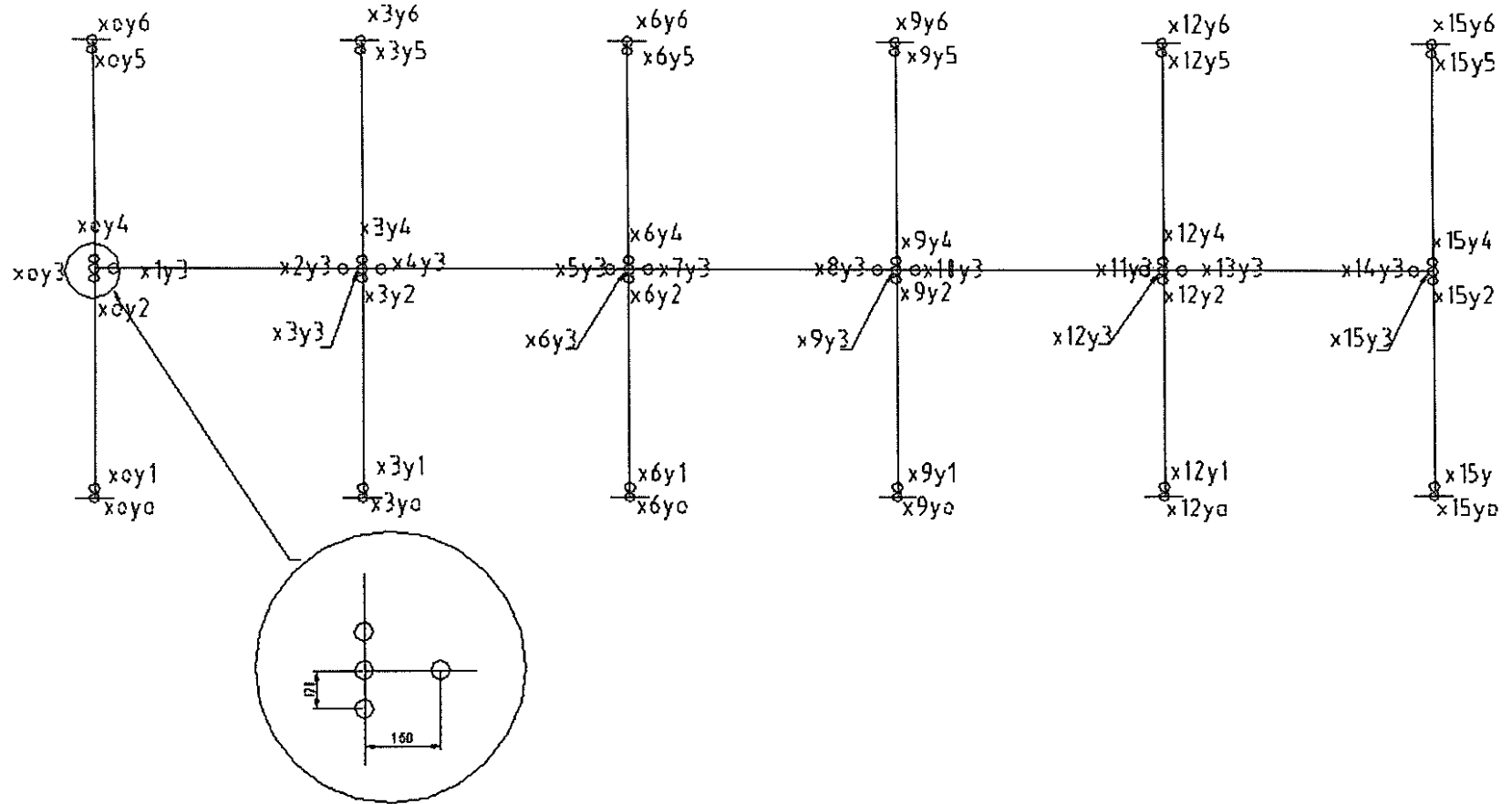


Figure A-1: Node Labels

A.4 Member Labels in Elastic Frame Model

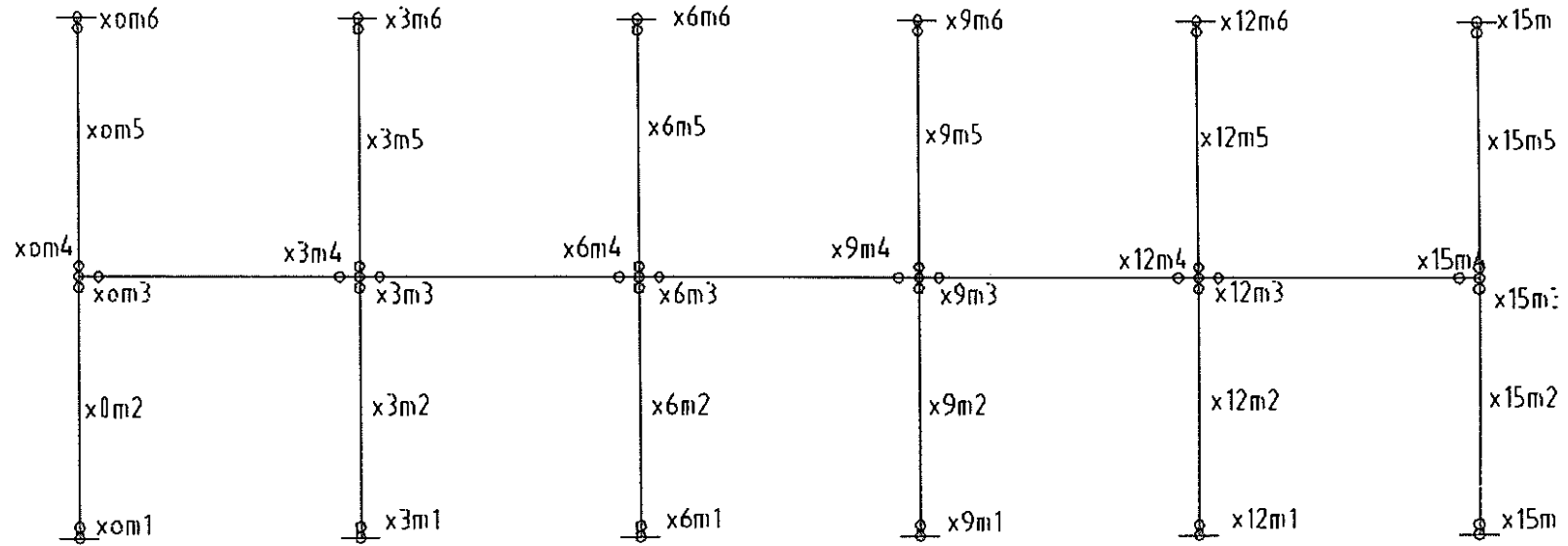
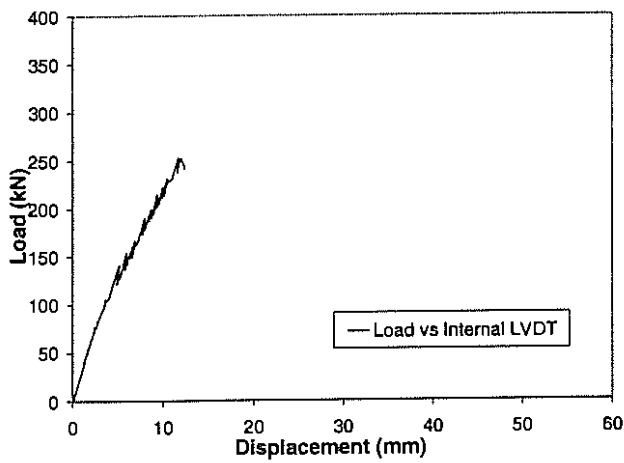


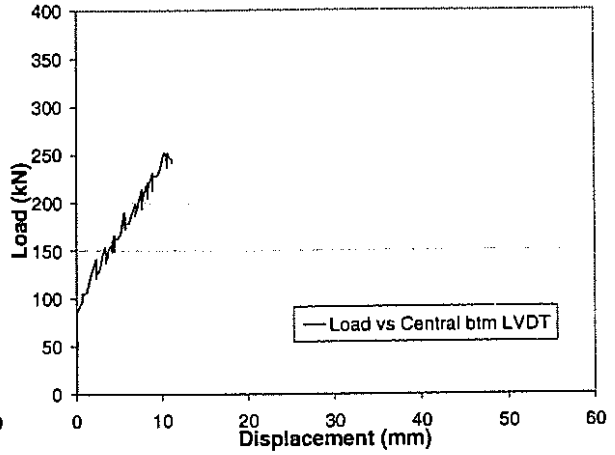
Figure A-2: Member Labels

Appendix B

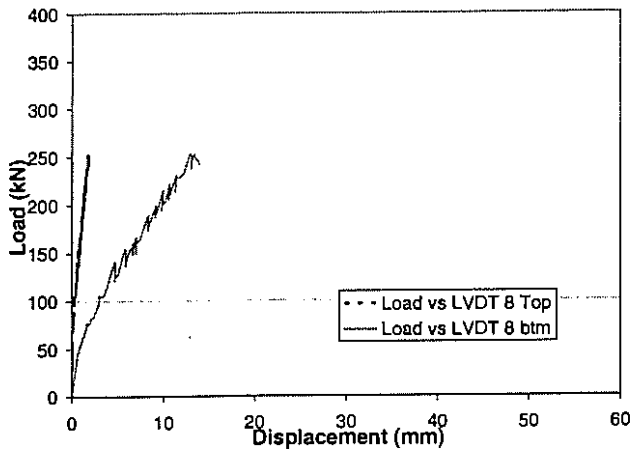
Experimental Results



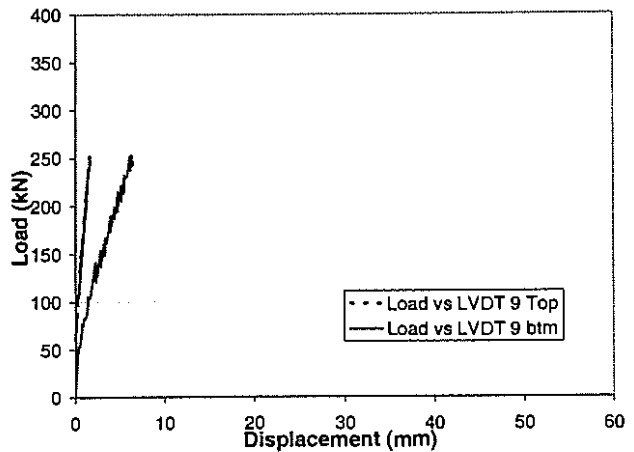
(a.) Load vs Internal LVDT



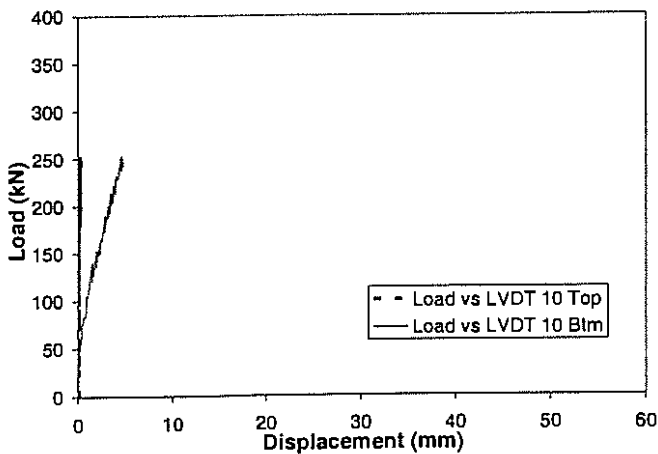
(b.) Load vs Central LVDT



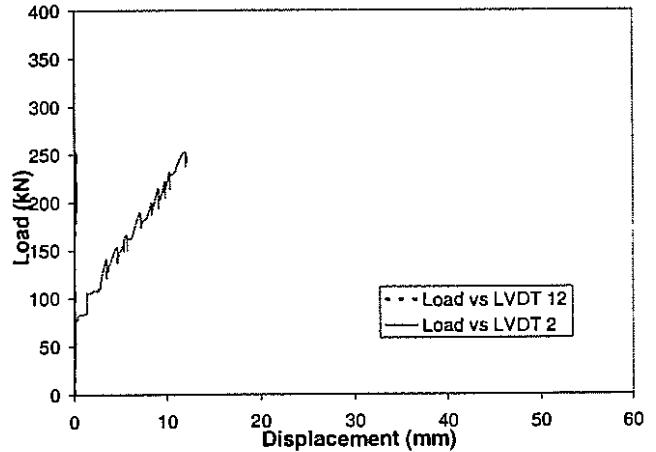
(c.) Load vs LVDT 8 Top, 8 Btm



(d.) Load vs LVDT 9 Top, 9 Btm

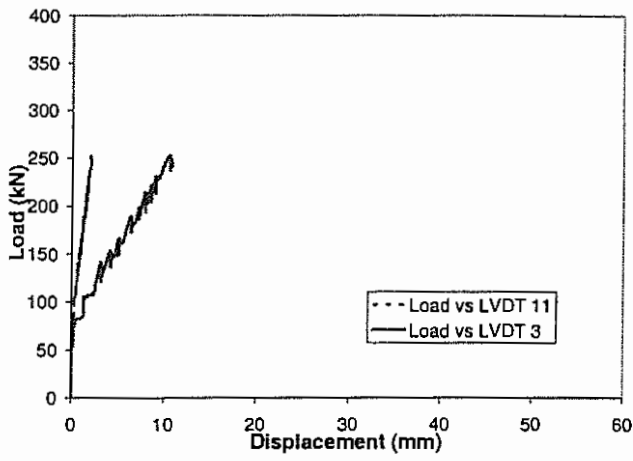


(e.) Load vs LVDT 10 Top, 10 Btm

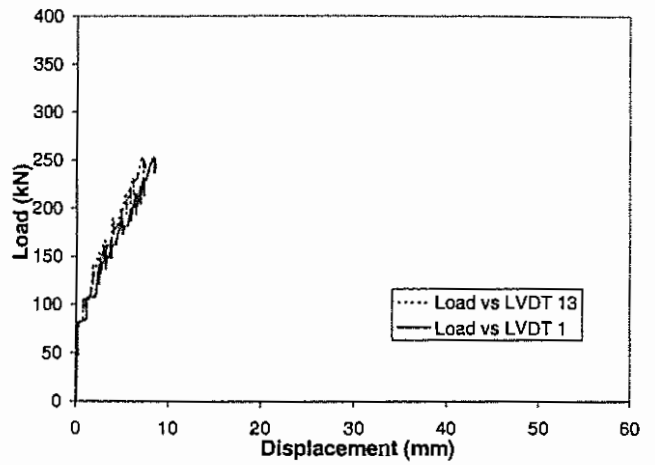


(f.) Load vs LVDT 12, 2

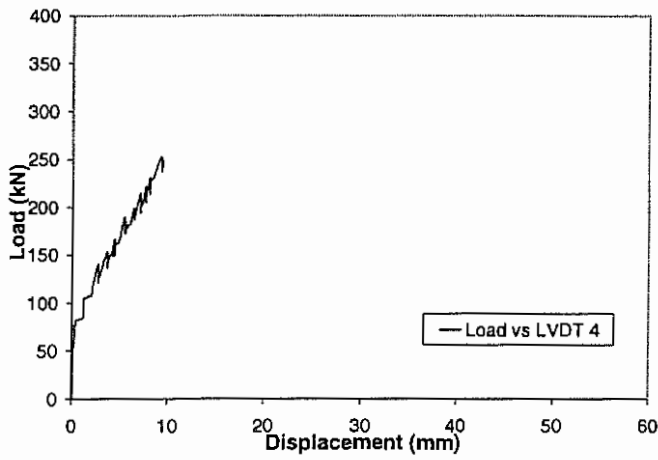
Figure B-1: Load-Displacement Graphs of Specimen SB1



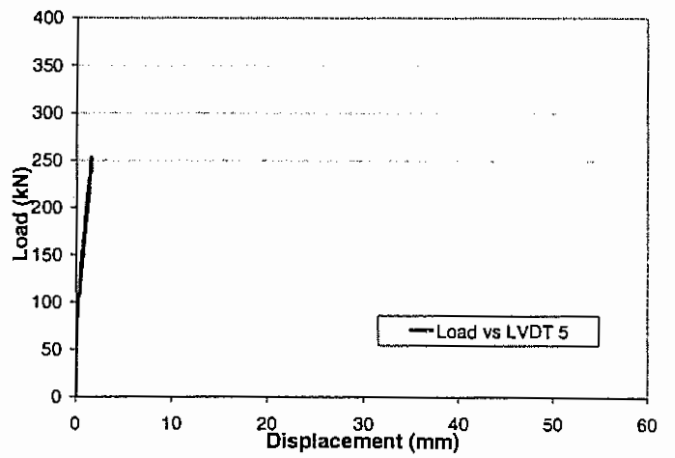
(g.) Load vs LVDT 11, 3



(h.) Load vs LVDT 13, 1

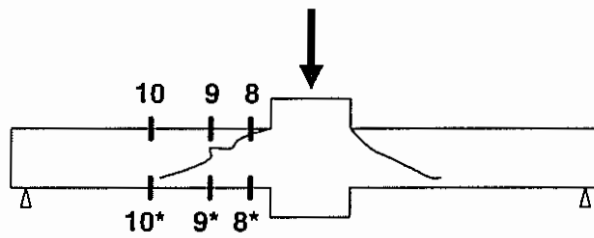
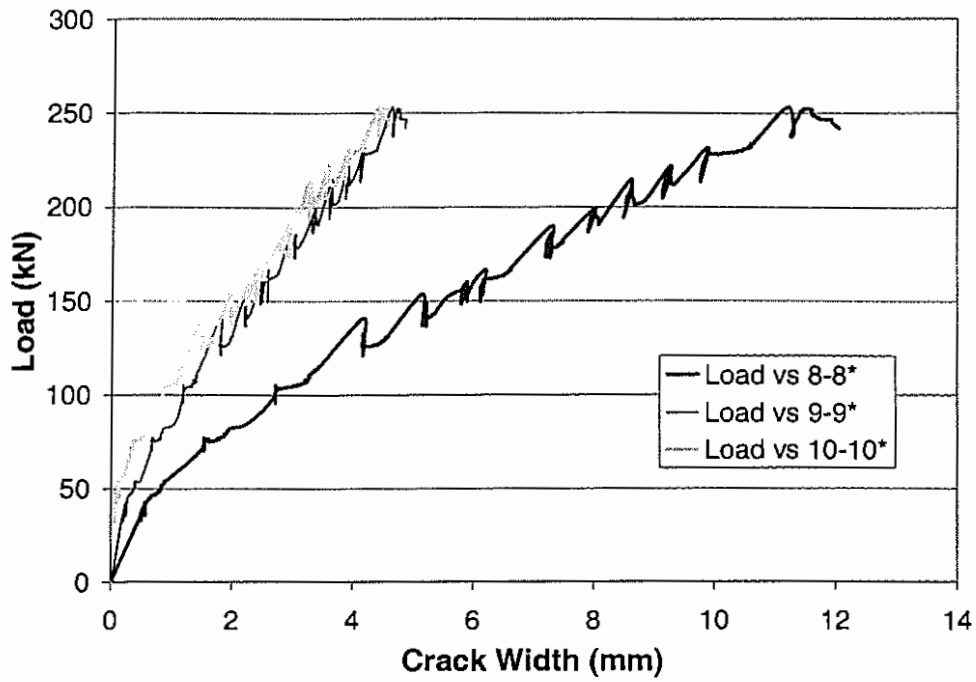


(i.) Load vs LVDT 4



(j.) Load vs LVDT 5

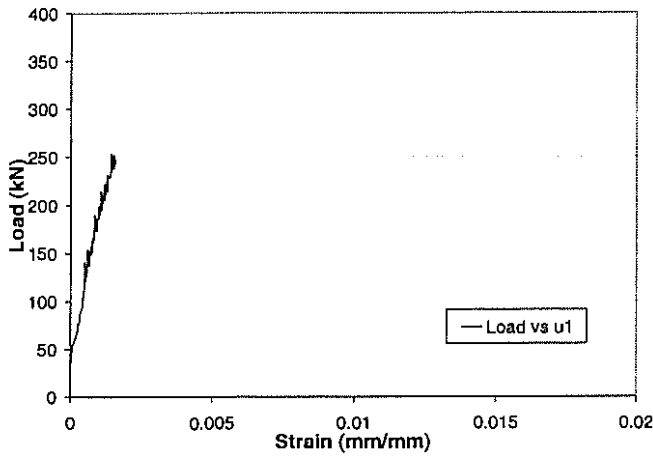
Figure B-1: Continued



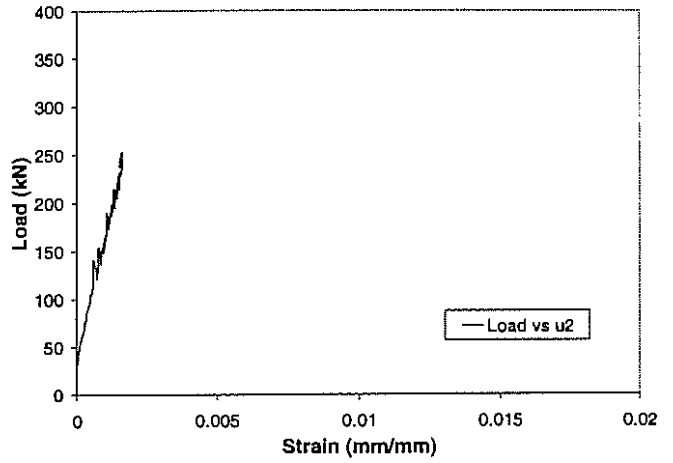
Positions of LVDT pairs around the column

Figure B-2: Load vs Vertical Crack Width of Specimen SB1

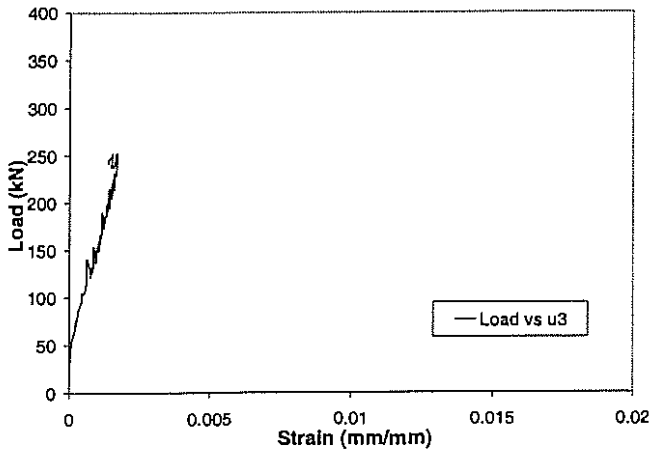
Note: * see Figure 3-18



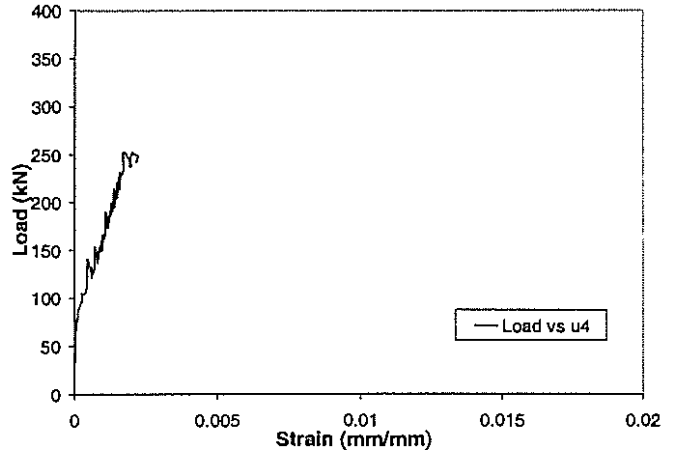
(a.) Load vs U1 Strain Gauge



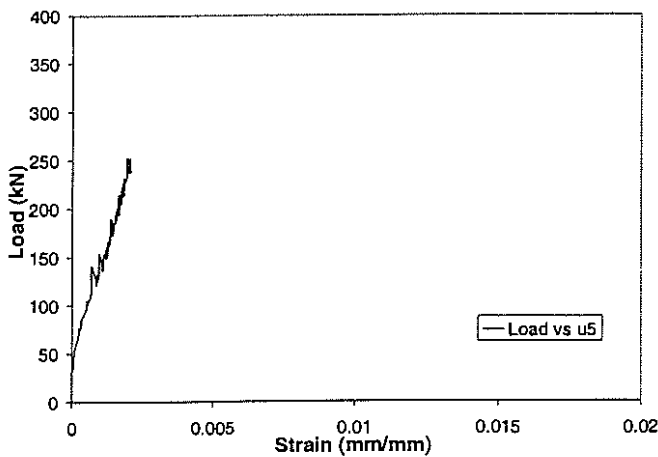
(b.) Load vs U2 Strain Gauge



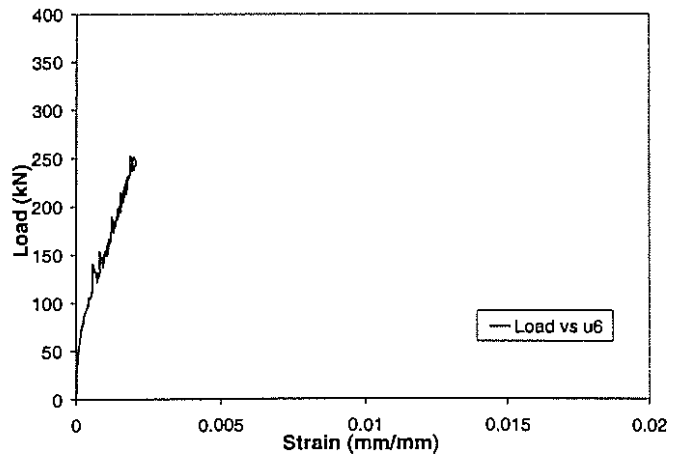
(c.) Load vs U3 Strain Gauge



(d.) Load vs U4 Strain Gauge

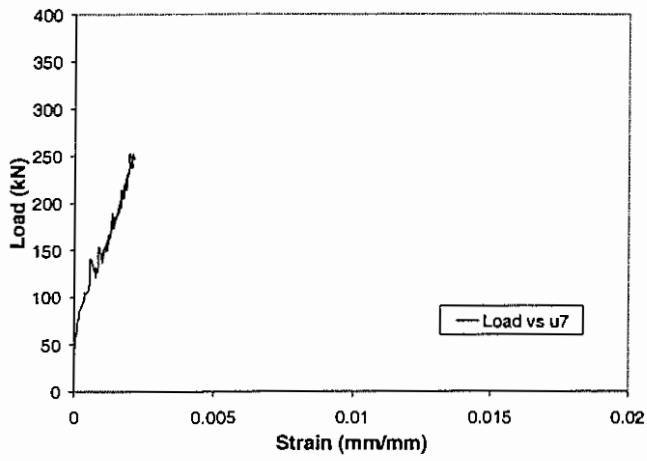


(e.) Load vs U5 Strain Gauge

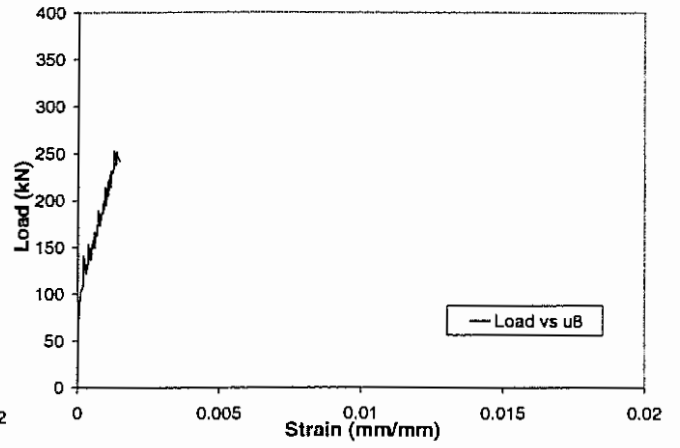


(f.) Load vs U6 Strain Gauge

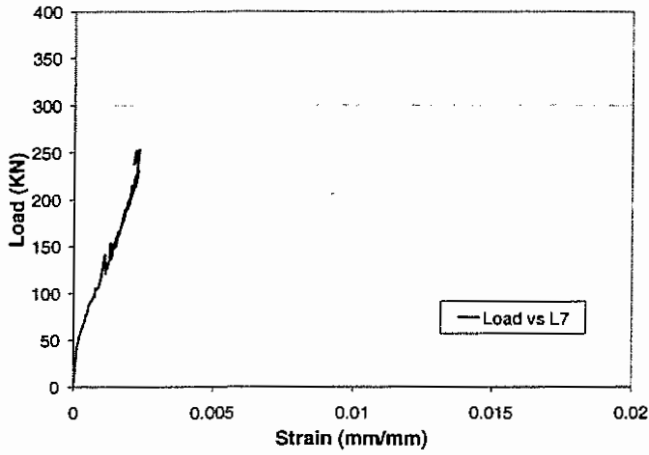
Figure B-3: Load-Longitudinal Reinforcement Strain Graphs of Specimen SB1



(g.) Load vs U7 Strain Gauge

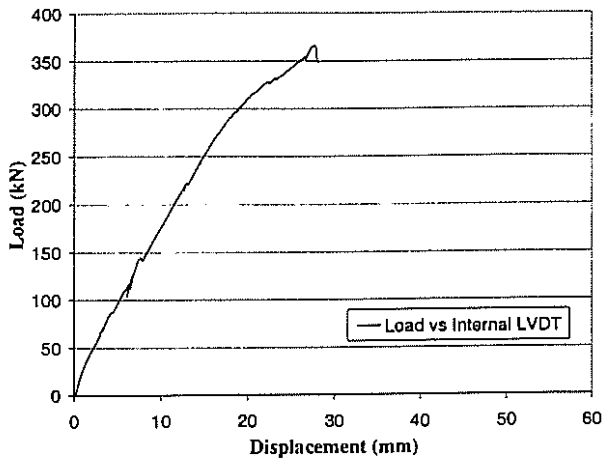


(h.) Load vs U8 Strain Gauge

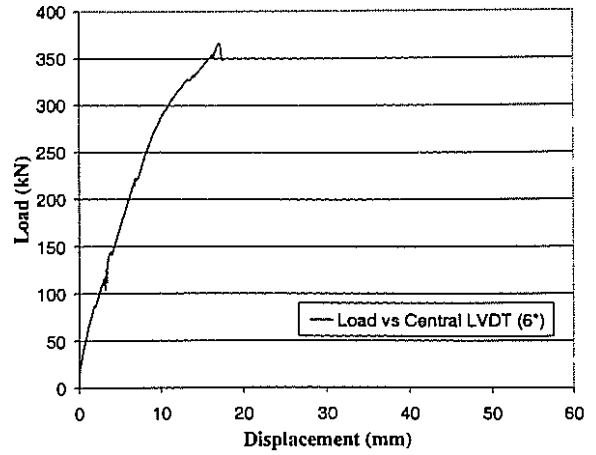


(i.) Load vs L7 Strain Gauge

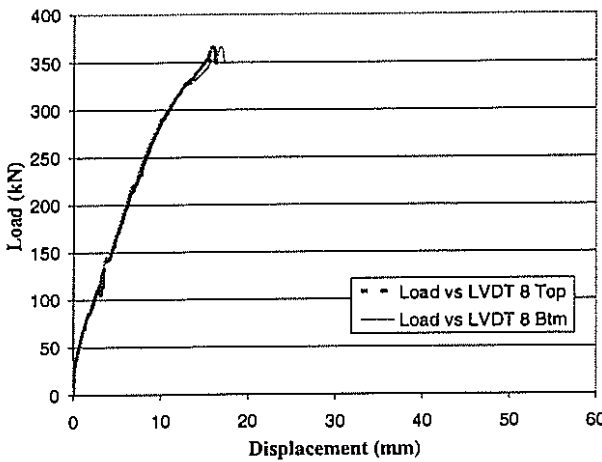
Figure B-3: Continued



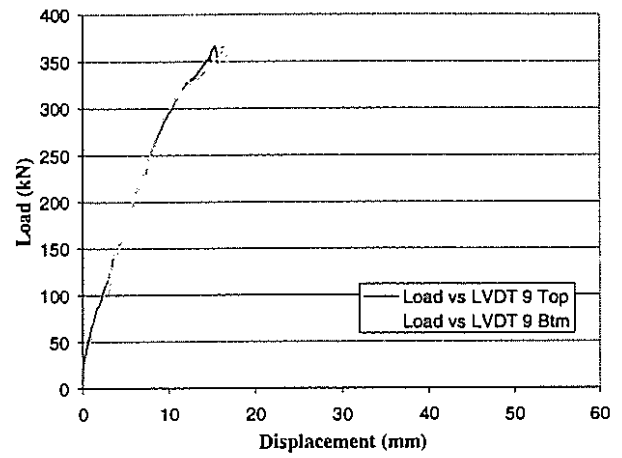
(a.) Load vs Internal LVDT



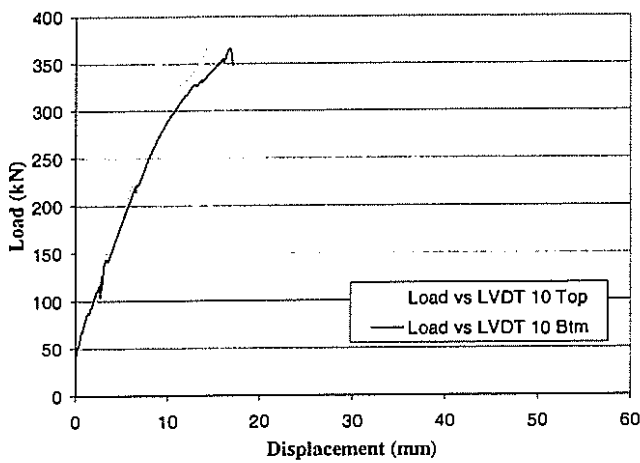
(b.) Load vs Central LVDT



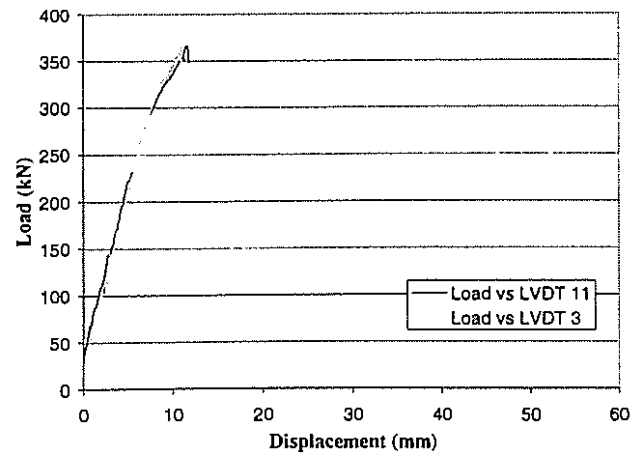
(c.) Load vs LVDT 8 Top, 8 Btm



(d.) Load vs LVDT 9 Top, 9 Btm

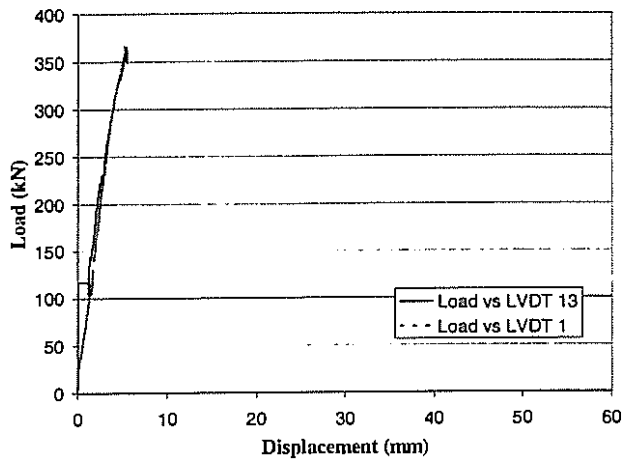


(e.) Load vs LVDT 10 Top, 10 Btm

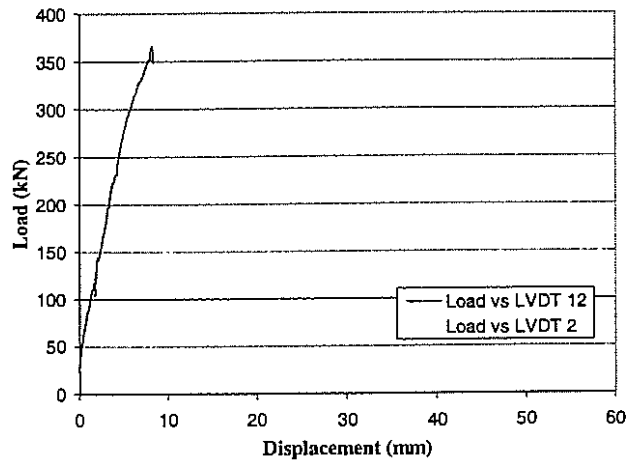


(f.) Load vs LVDT 11, 3

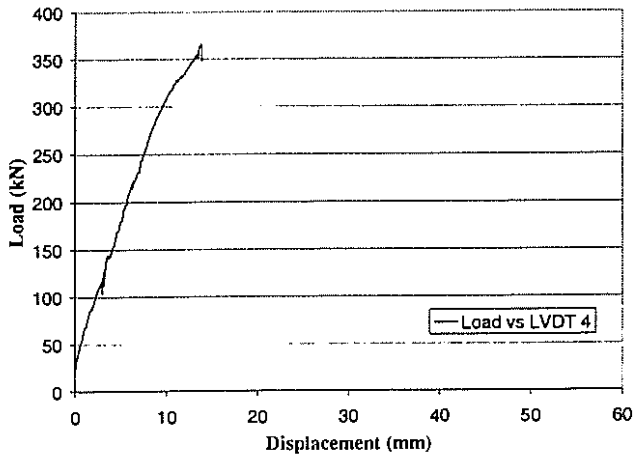
Figure B-4: Load-Displacement Graphs of Specimen SB2



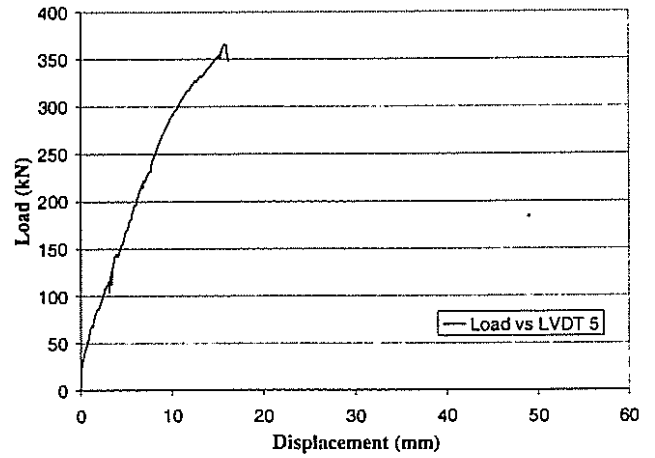
(g.) Load vs LVDT 13, 1



(h.) Load vs LVDT 12, 2



(i.) Load vs LVDT 4



(j.) Load vs LVDT 5

Figure B-4: Continued

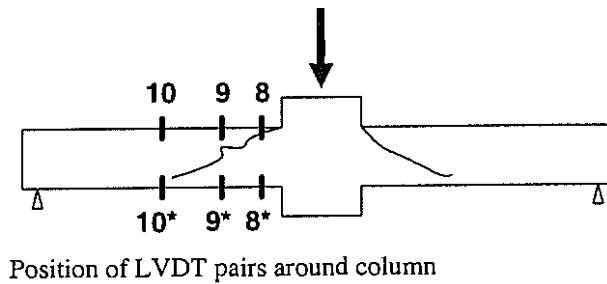
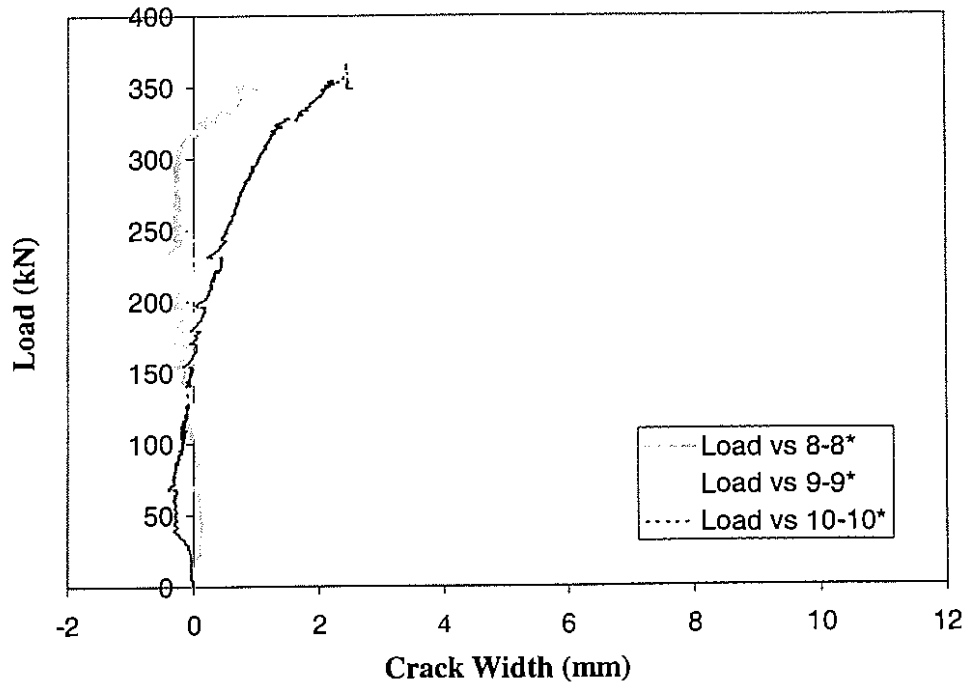
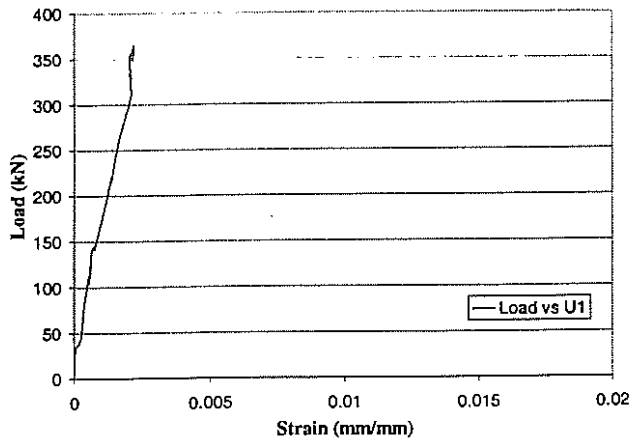


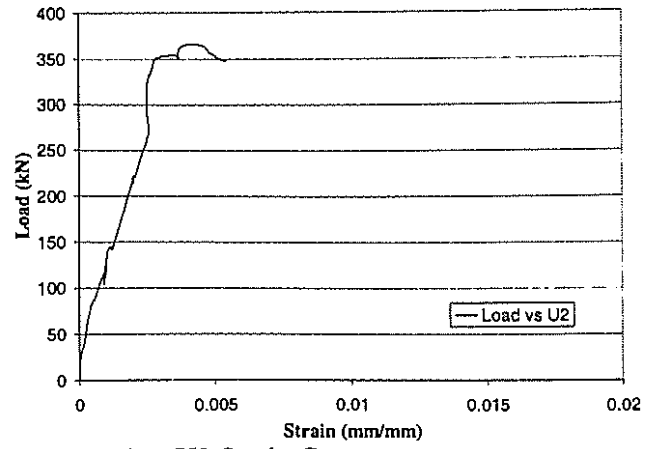
Figure B-5: Load vs Vertical Crack Width of Specimen SB2

Note: * see Figure 3-18

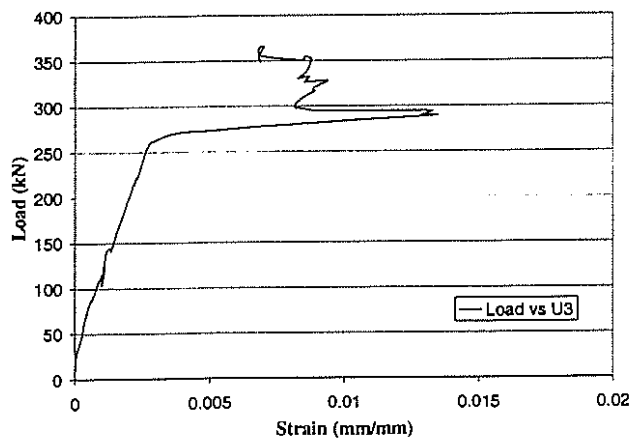
Crack width was obtained as the absolute difference between LVDT at top and bottom. Negative crack width may be due to instrumentation noise.



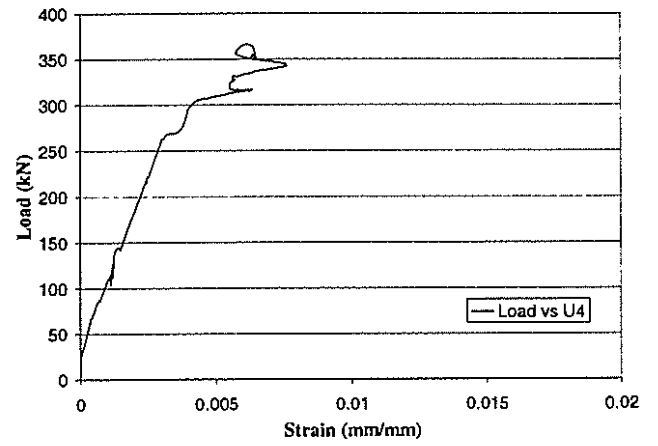
(a.) Load vs U1 Strain Gauge



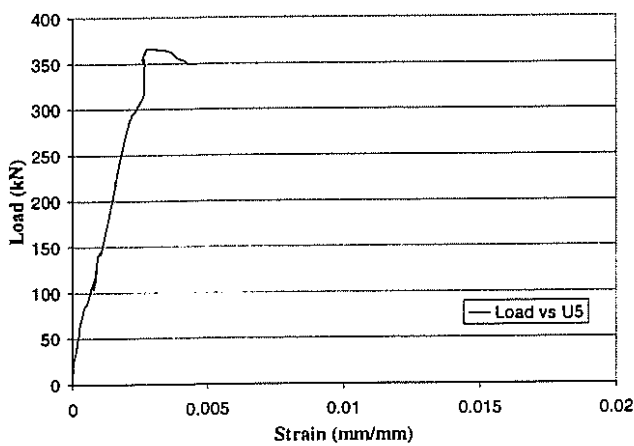
(b.) Load vs U2 Strain Gauge



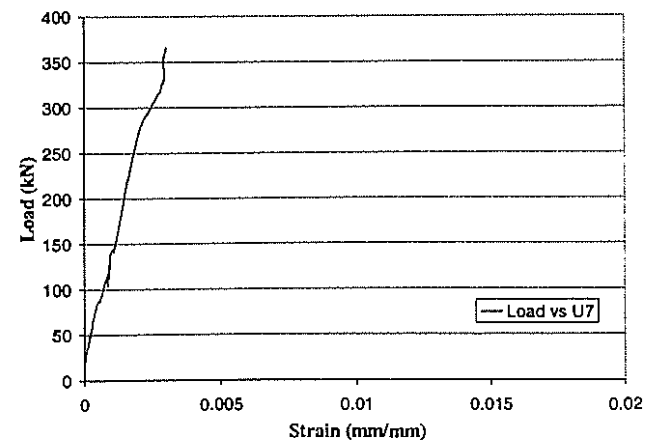
(c.) Load vs U3 Strain Gauge



(d.) Load vs U4 Strain Gauge

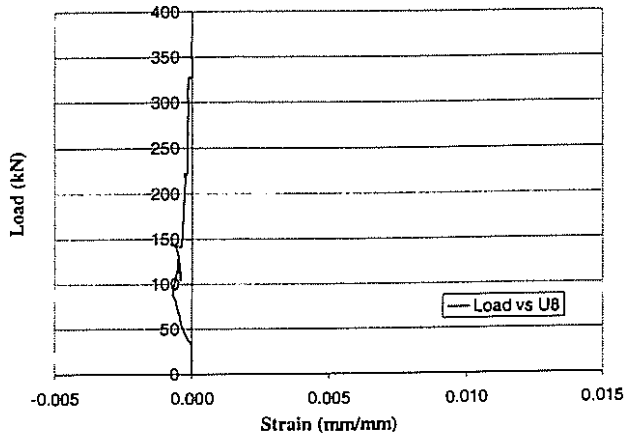


(e.) Load vs U5 Strain Gauge

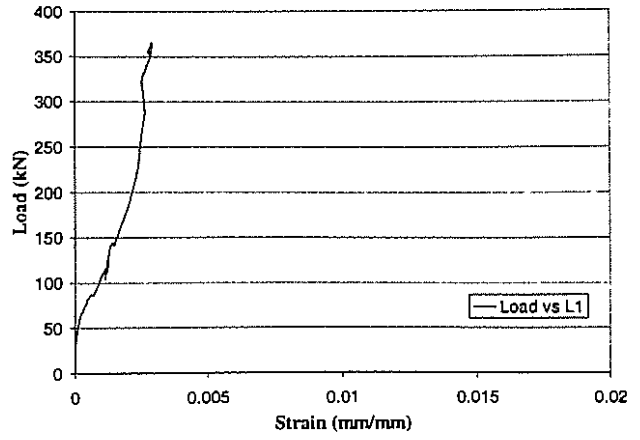


(f.) Load vs U7 Strain Gauge

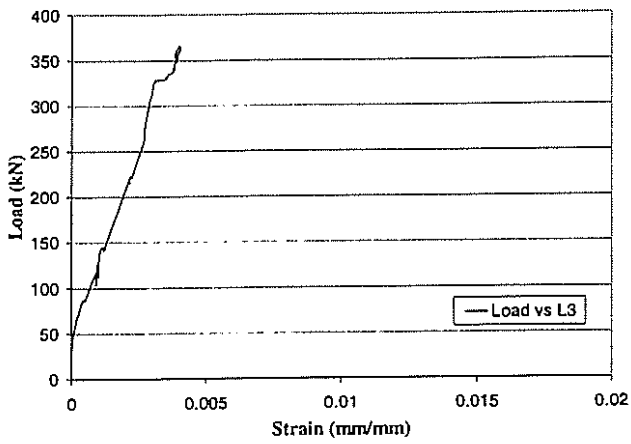
Figure B-6: Load-Longitudinal Reinforcement Strain Graphs of Specimen SB2



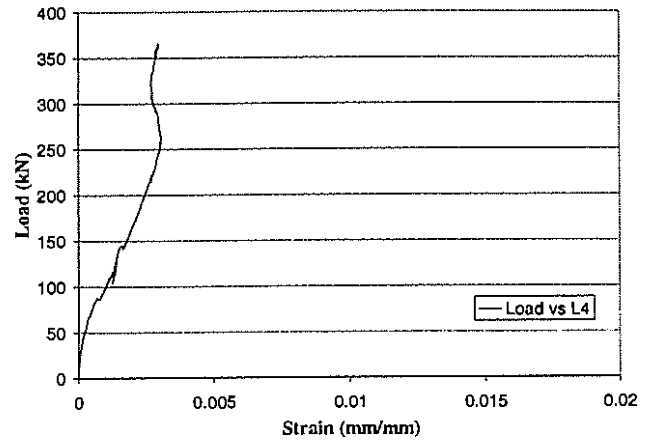
(a.) Load vs U8 Strain Gauge



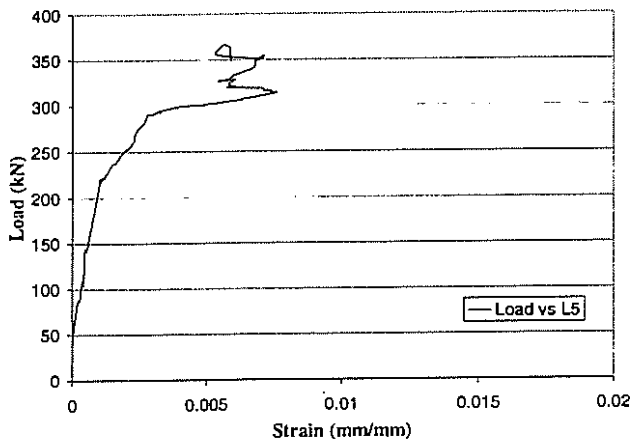
(b.) Load vs L1 Strain Gauge



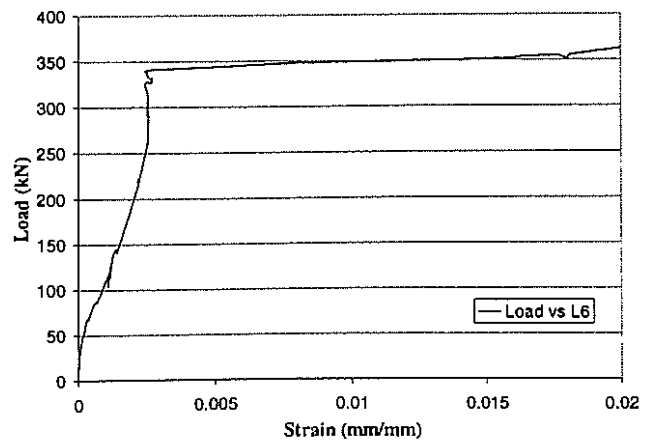
(c.) Load vs L3 Strain Gauge



(d.) Load vs L4 Strain Gauge



(e.) Load vs L5 Strain Gauge



(f.) Load vs L6 Strain Gauge

Figure B-6: Continued

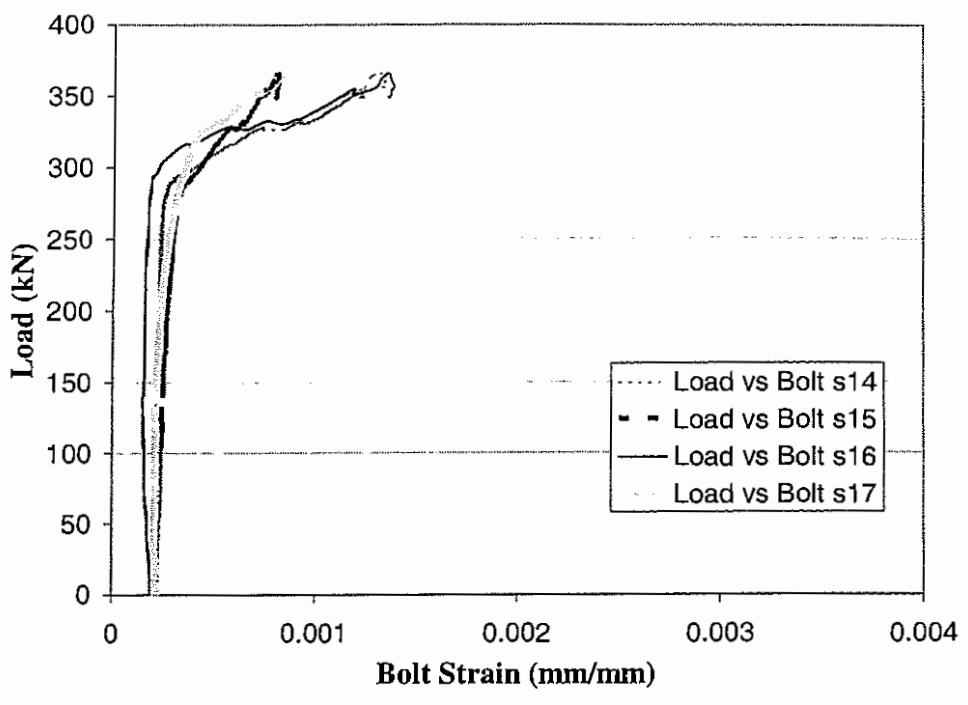
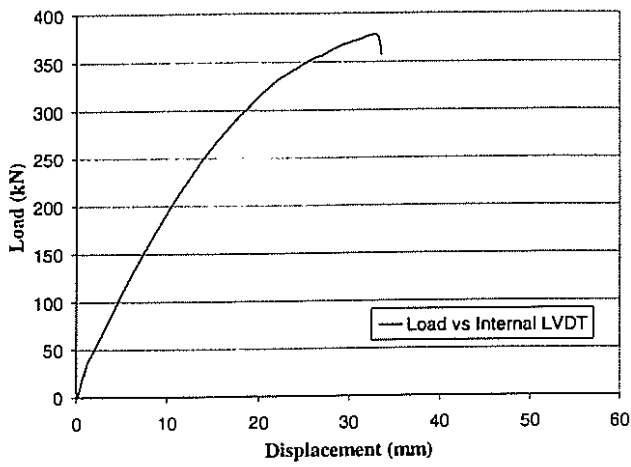
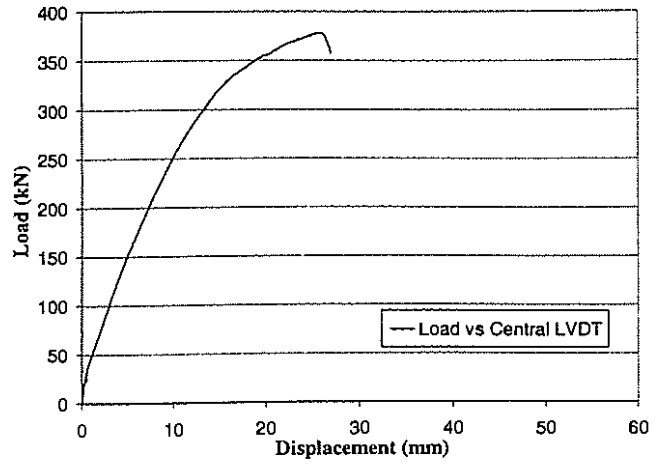


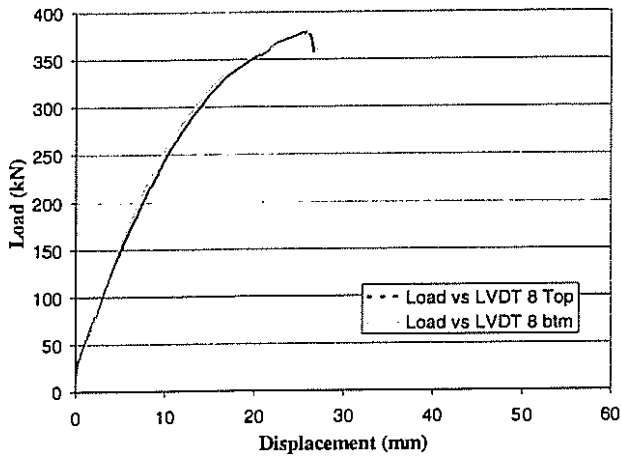
Figure B-7: Load-Bolt Strain Graphs of Specimen SB2



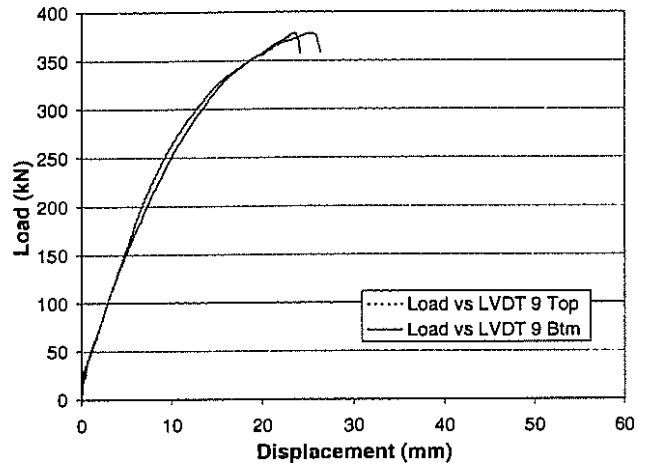
(a.) Load vs Internal LVDT



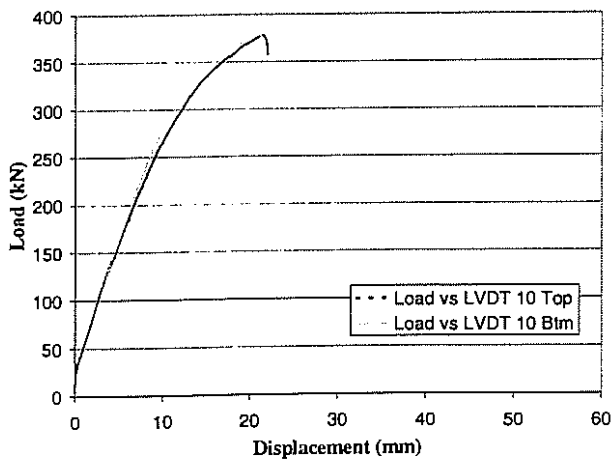
(b.) Load vs Central LVDT



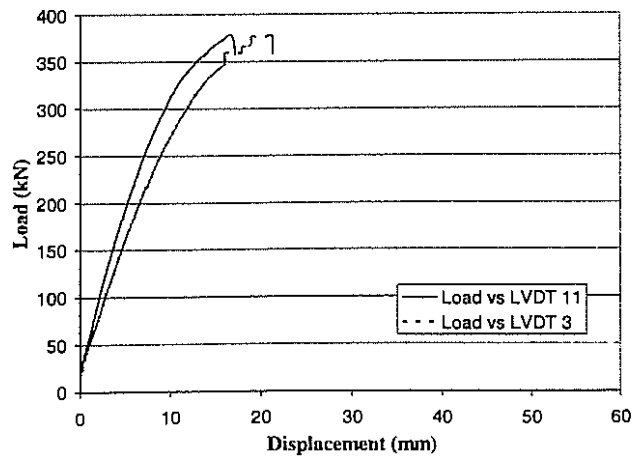
(c.) Load vs LVDT 8 Top, 8 Btm



(d.) Load vs LVDT 9 Top, 9 Btm

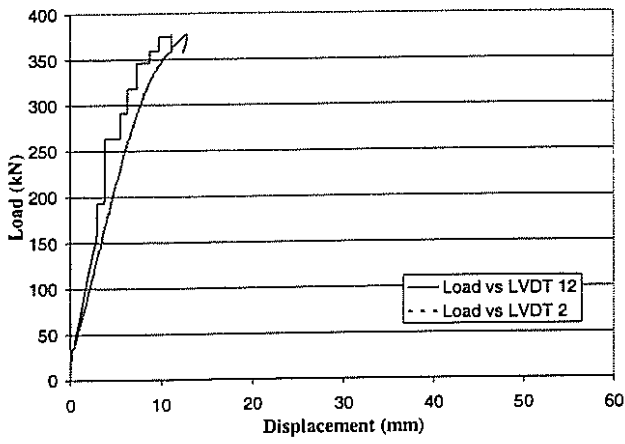


(e.) Load vs LVDT 10 Top, 10 Btm

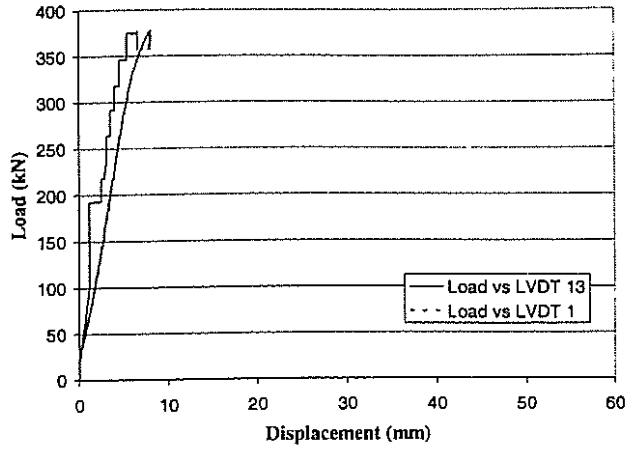


(f.) Load vs LVDT 11, 3

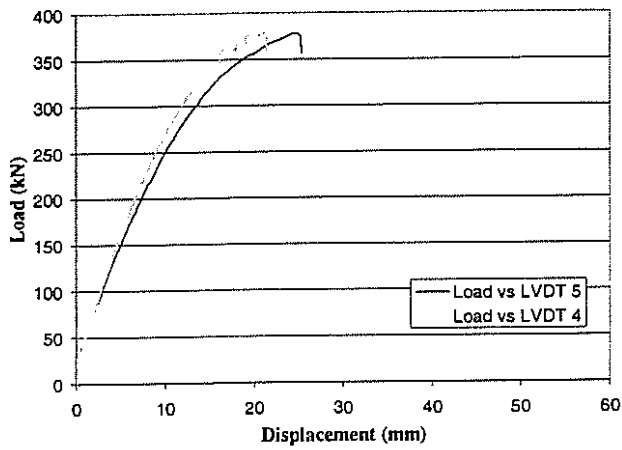
Figure B-8: Load-Displacement Graphs of Specimen SB3



(g.) Load vs LVDT 12, 2

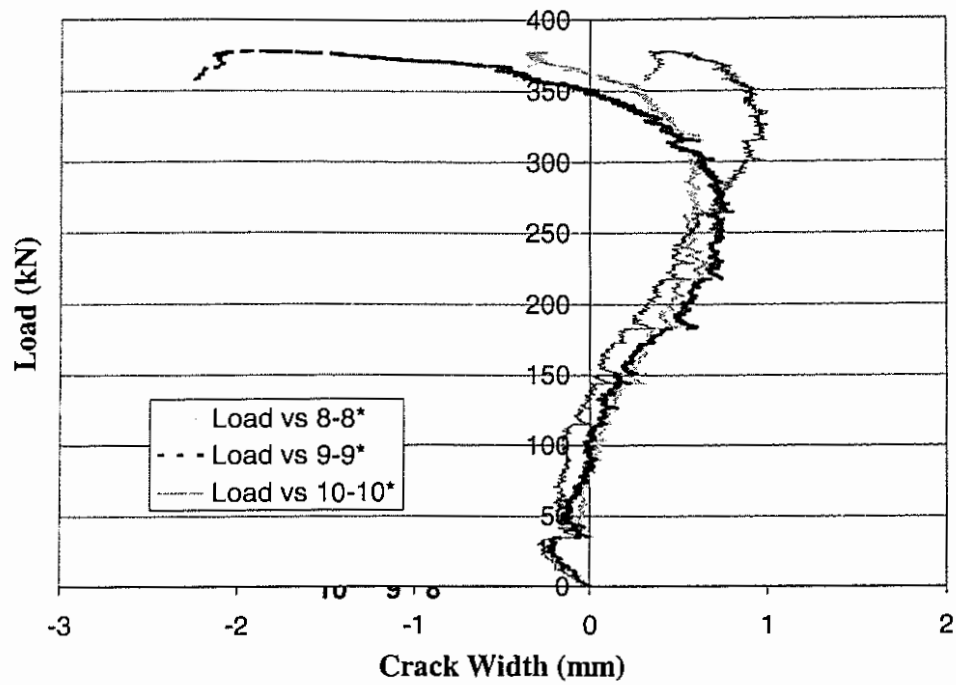


(h.) Load vs LVDT 13, 1



(i.) Load vs LVDT 4, 5

Figure B-8: Continued

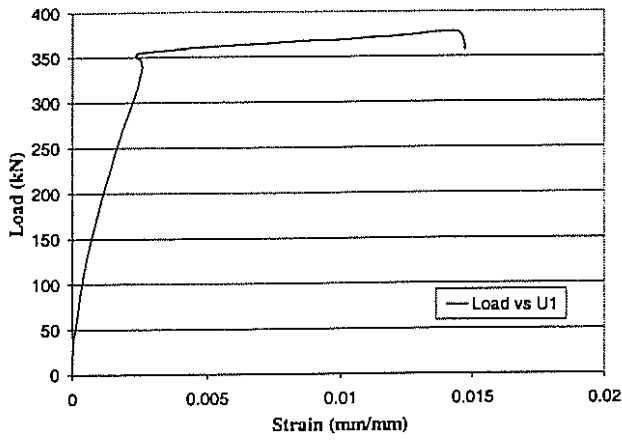


Positions of LVDT pairs around the column

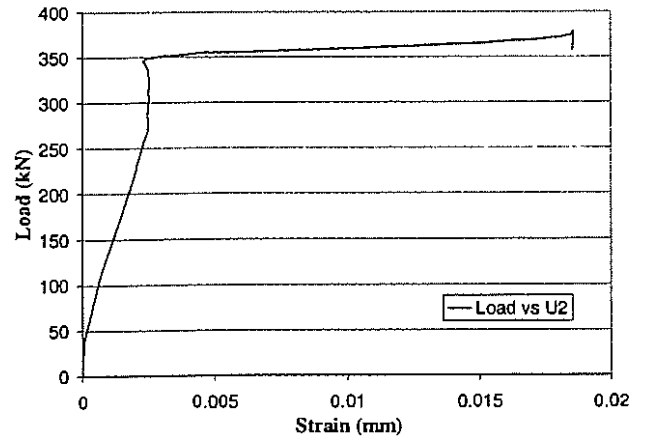
Figure B-9: Load vs Vertical Crack Width of Specimen SB3

Note: *See Figure 3-18

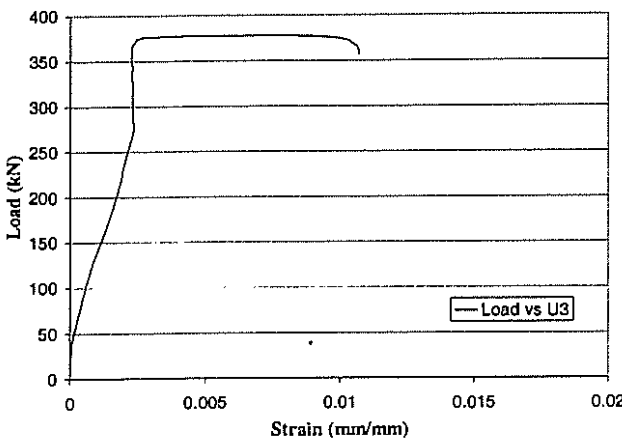
Crack width was obtained as the absolute difference between LVDT at top and bottom.
Negative crack width may be due to instrumentation noise.



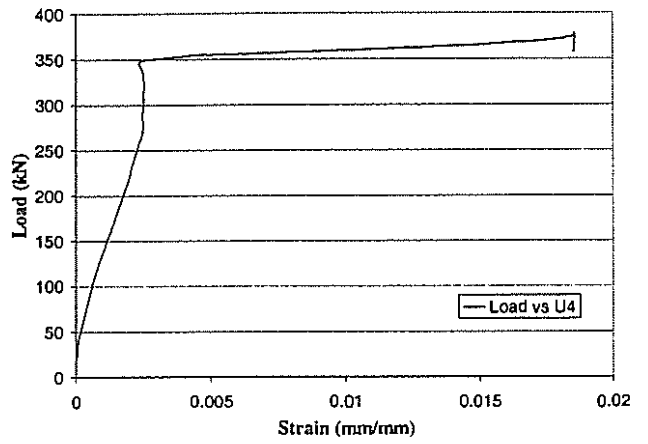
(a.) Load vs U1 Strain Gauge



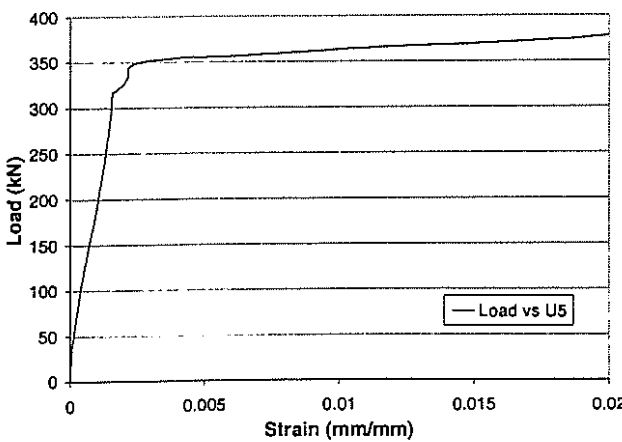
(b.) Load vs U2 Strain Gauge



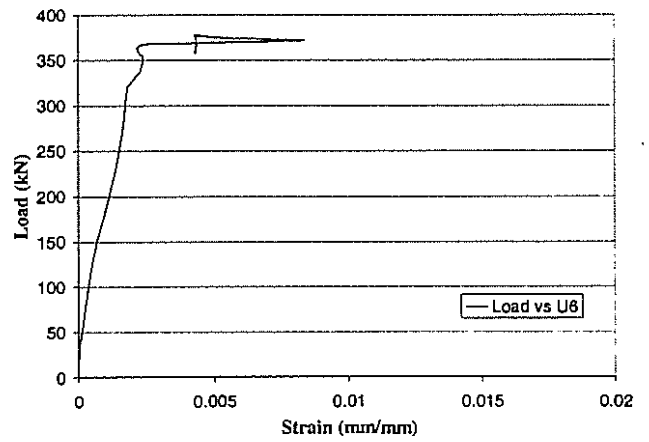
(c.) Load vs U3 Strain Gauge



(d.) Load vs U4 Strain Gauge

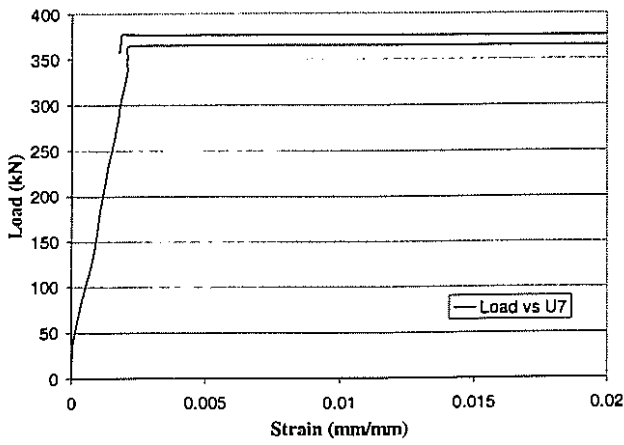


(e.) Load vs U5 Strain Gauge

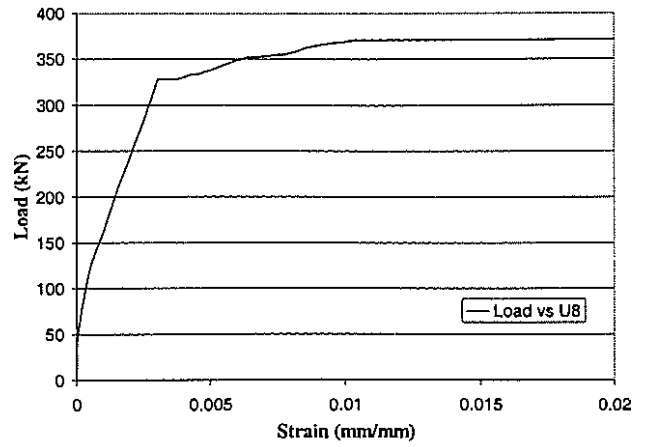


(f.) Load vs U6 Strain Gauge

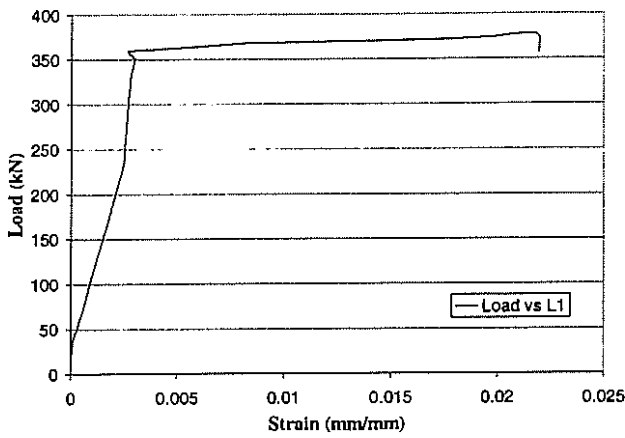
Figure B-10: Load-Longitudinal Reinforcement Strain Graphs of Specimen SB3



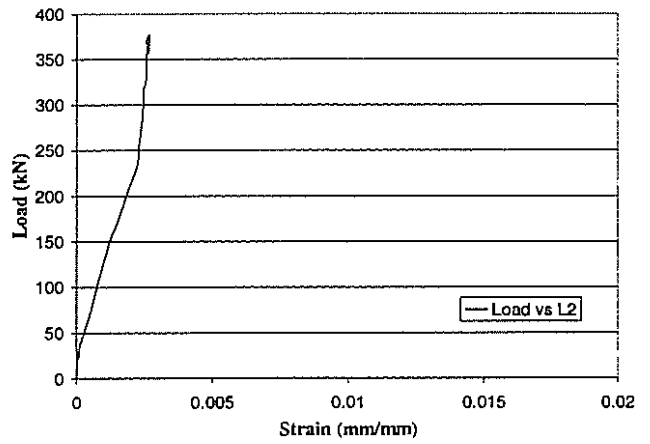
(g.) Load vs U7 Strain Gauge



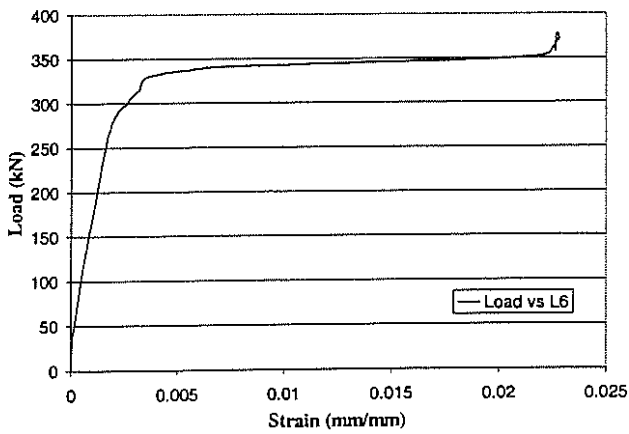
(h.) Load vs U8 Strain Gauge



(i.) Load vs L1 Strain Gauge



(j.) Load vs L2 Strain Gauge



(k.) Load vs L6 Strain Gauge

Figure B-10: Continued

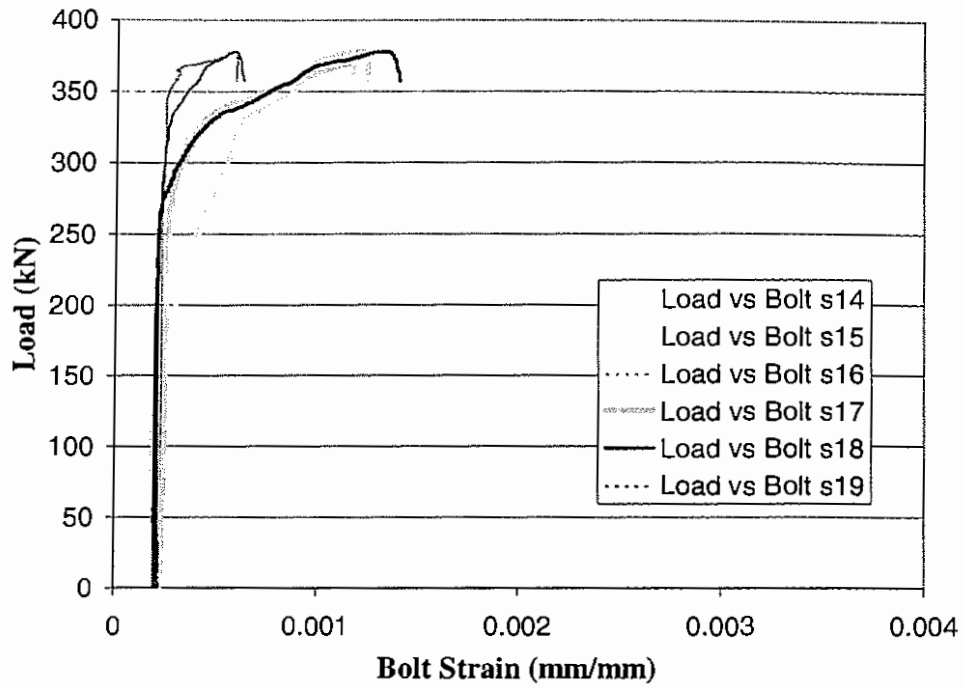
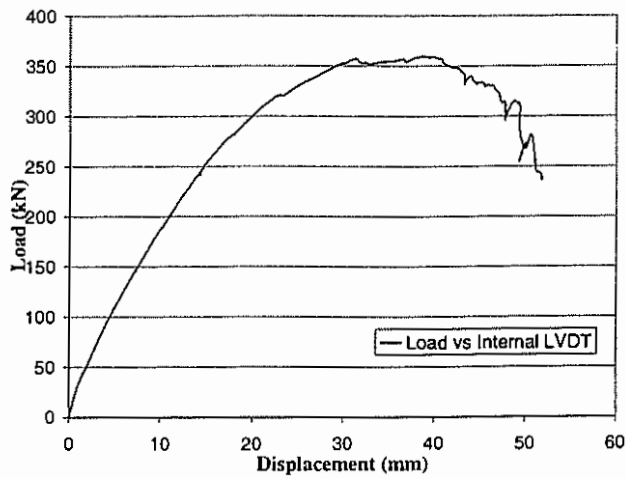
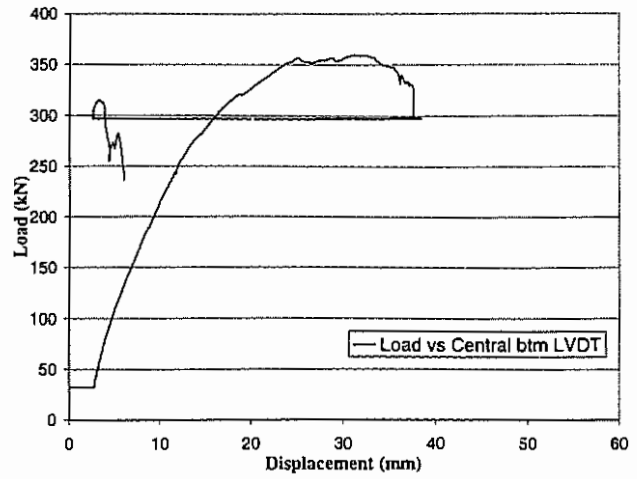


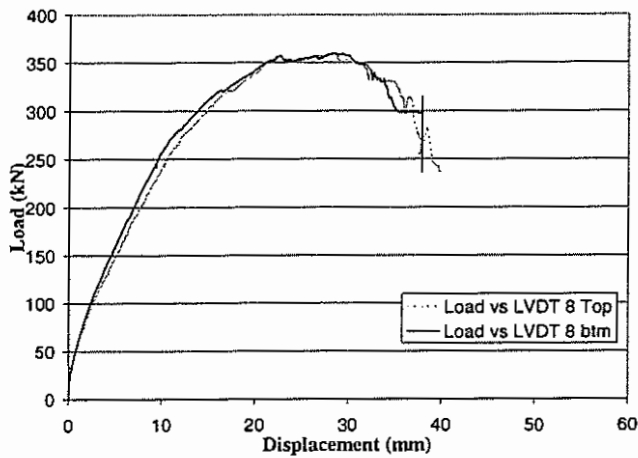
Figure B-11: Load-Bolt Strain Graphs of Specimen SB3



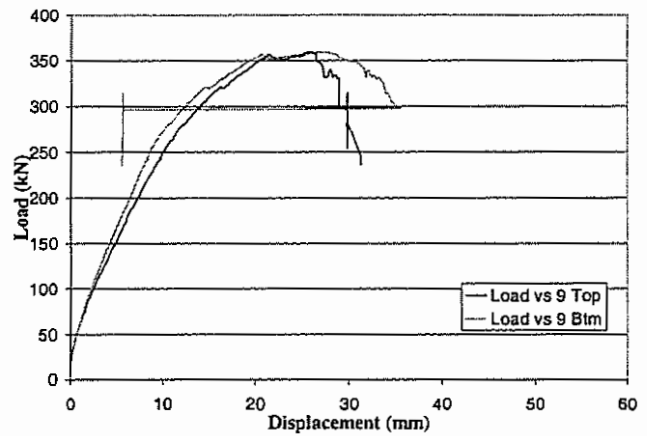
(a.) Load vs Internal LVDT



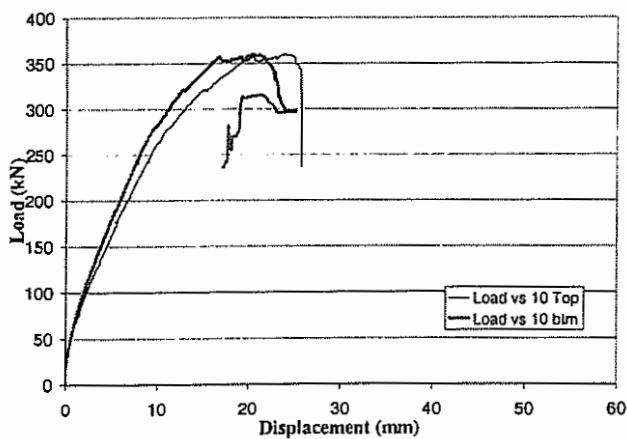
(b.) Load vs Central LVDT



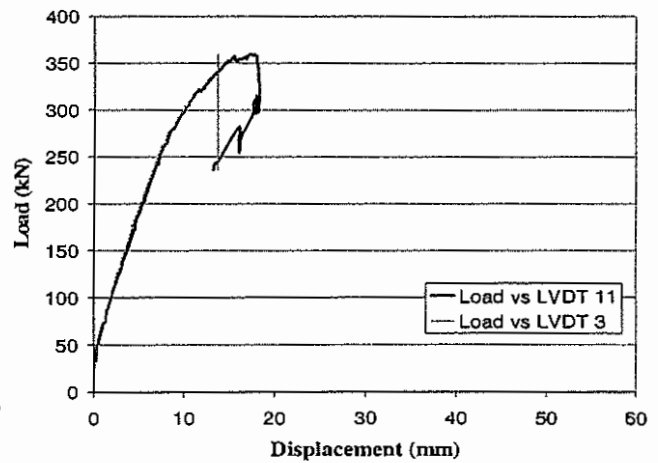
(c.) Load vs LVDT 8 Top, 8 Btm



(d.) Load vs LVDT 9 Top, 9 Btm

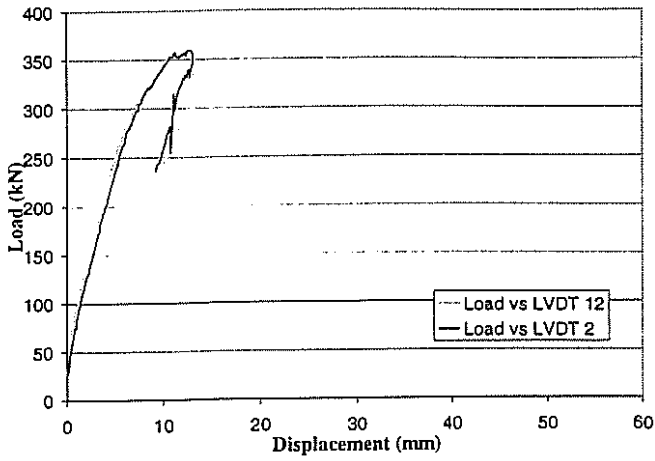


(e.) Load vs LVDT 10 Top, 10 Btm

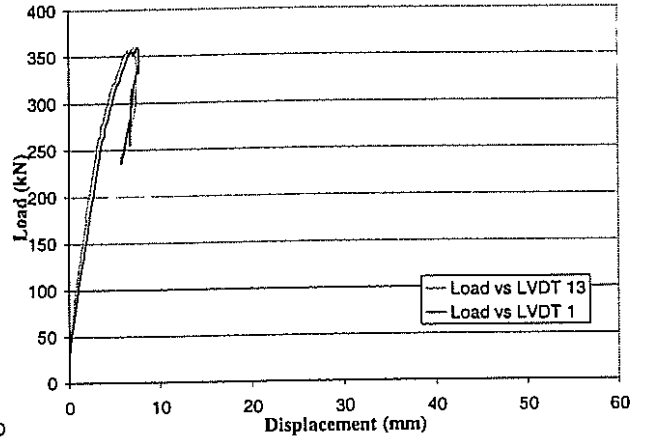


(f.) Load vs LVDT 11, 3

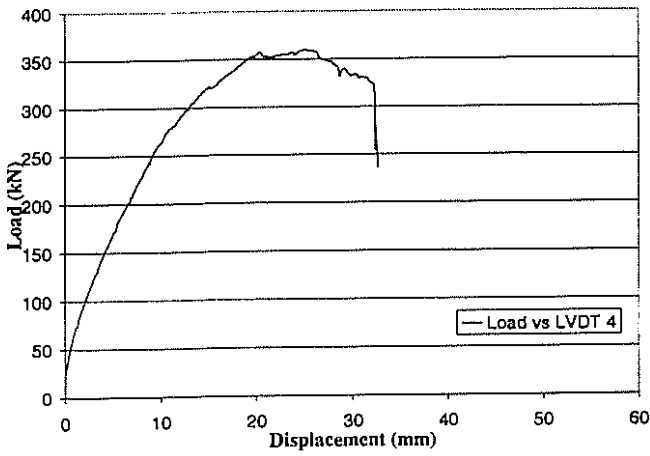
Figure B-12: Load-Displacement Graphs of Specimen SB4



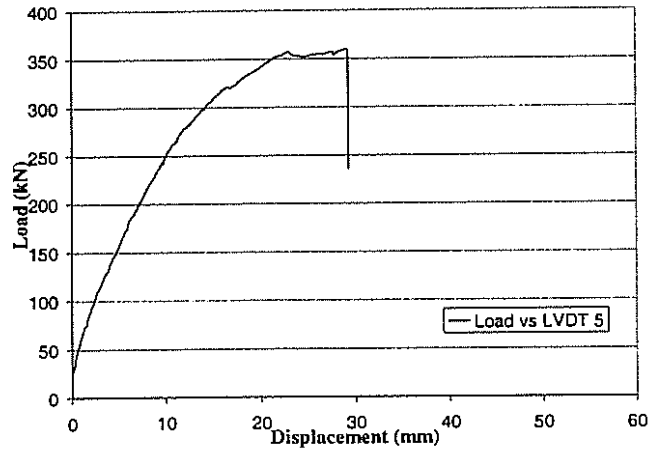
(g.) Load vs LVDT 12, 2



(h.) Load vs LVDT 13, 1

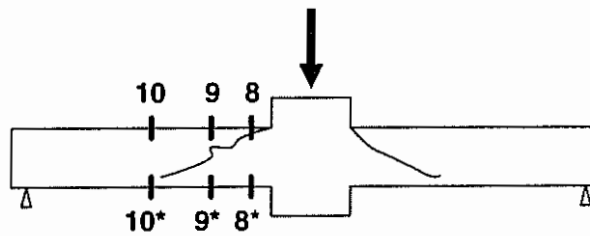
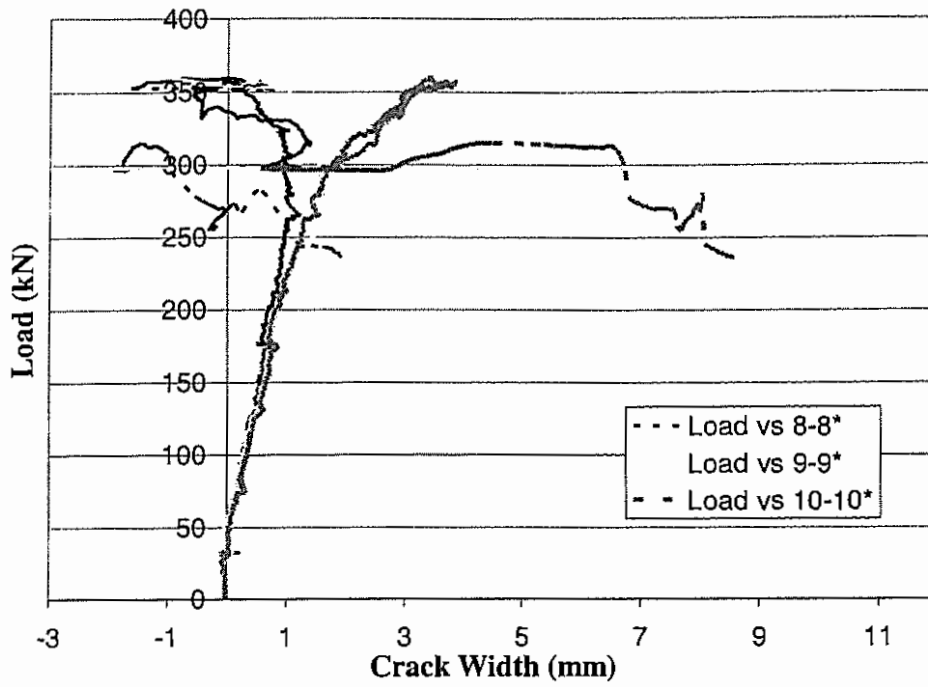


(i.) Load vs LVDT 4



(j.) Load vs LVDT 5

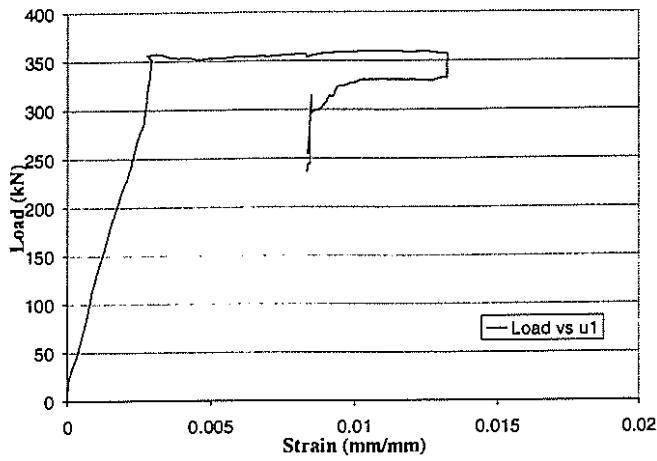
Figure B-12: Continued



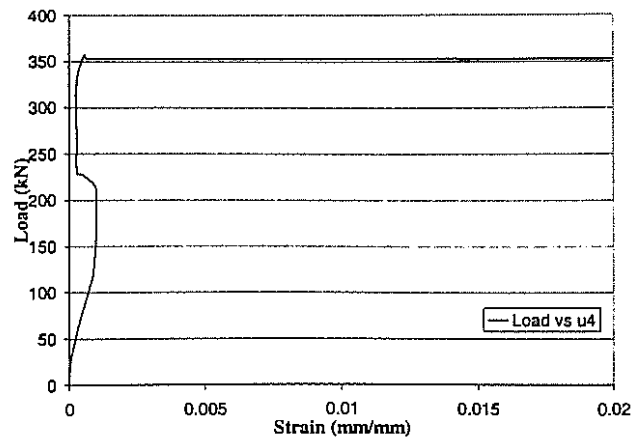
Positions of LVDT pairs around the column

Figure B-13: Load vs Vertical Crack Width of Specimen SB4

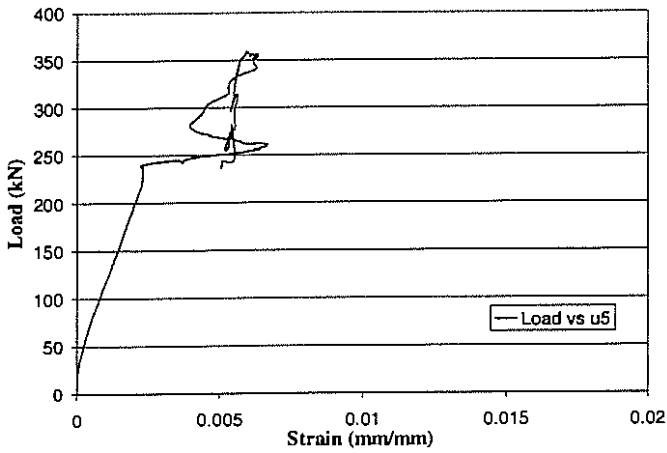
Note: *See Figure 3-18



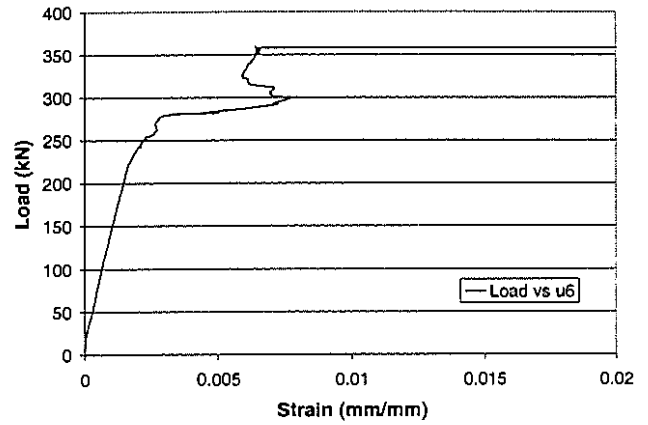
(a.) Load vs U1 Strain Gauge



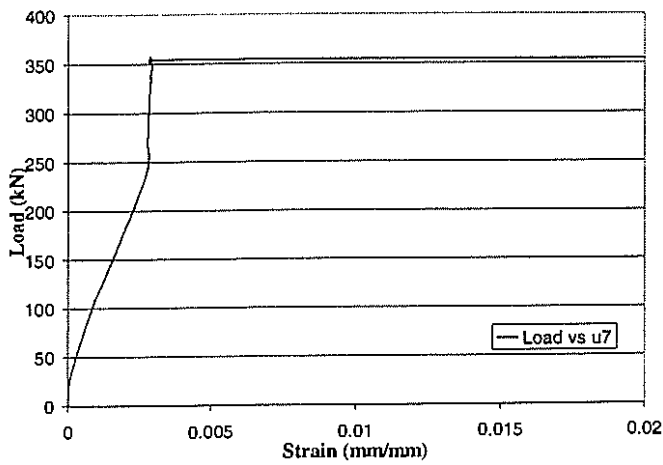
(b.) Load vs U4 Strain Gauge



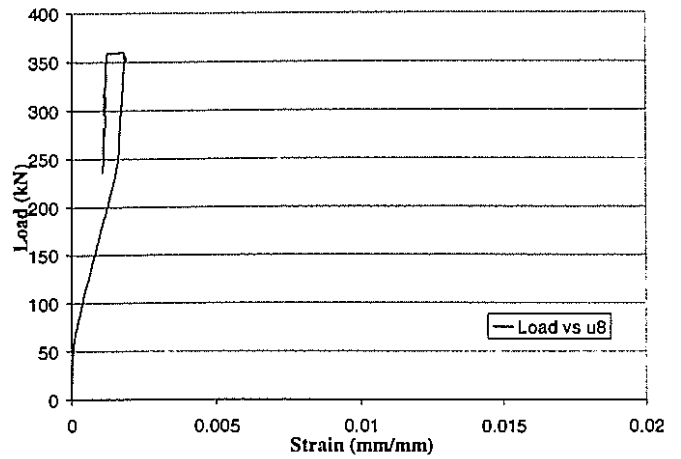
(c.) Load vs U5 Strain Gauge



(d.) Load vs U6 Strain Gauge

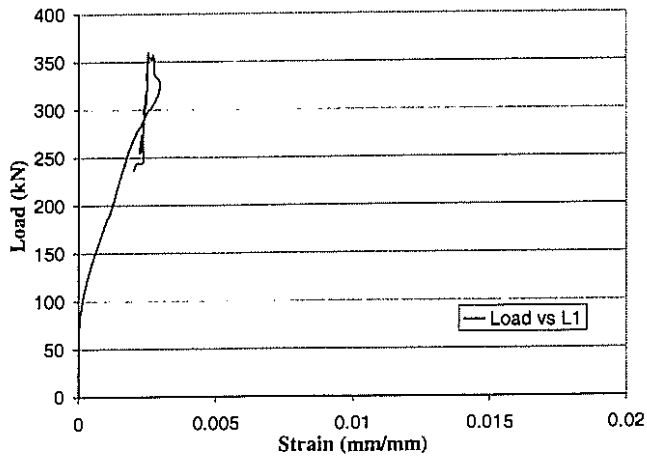


(e.) Load vs U7 Strain Gauge

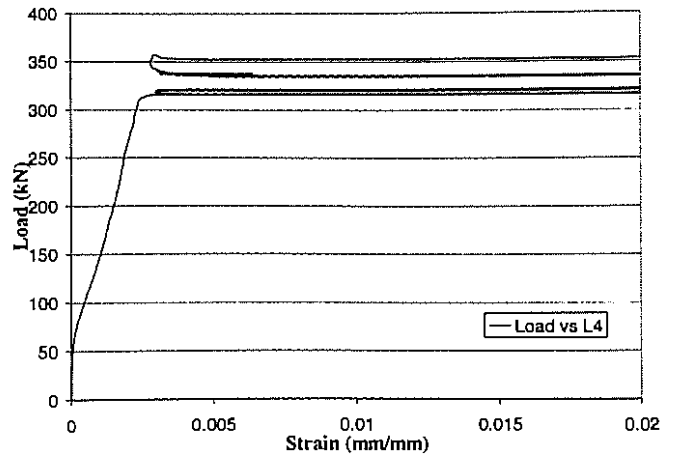


(f.) Load vs U8 Strain Gauge

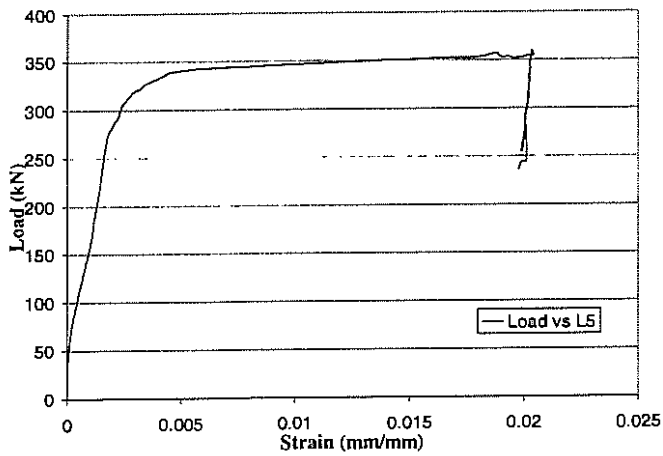
Figure B-14: Load-Longitudinal Reinforcement Strain Graphs of Specimen SB4



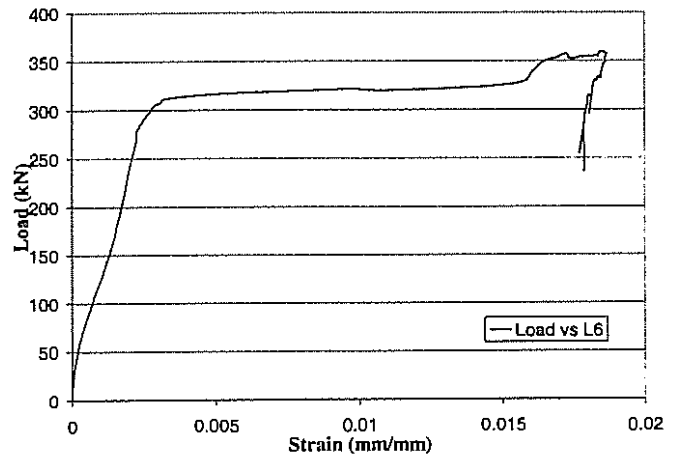
(g.) Load vs L1 Strain Gauge



(h.) Load vs L4 Strain Gauge



(i.) Load vs L5 Strain Gauge



(j.) Load vs L6 Strain Gauge

Figure B-14: Continued

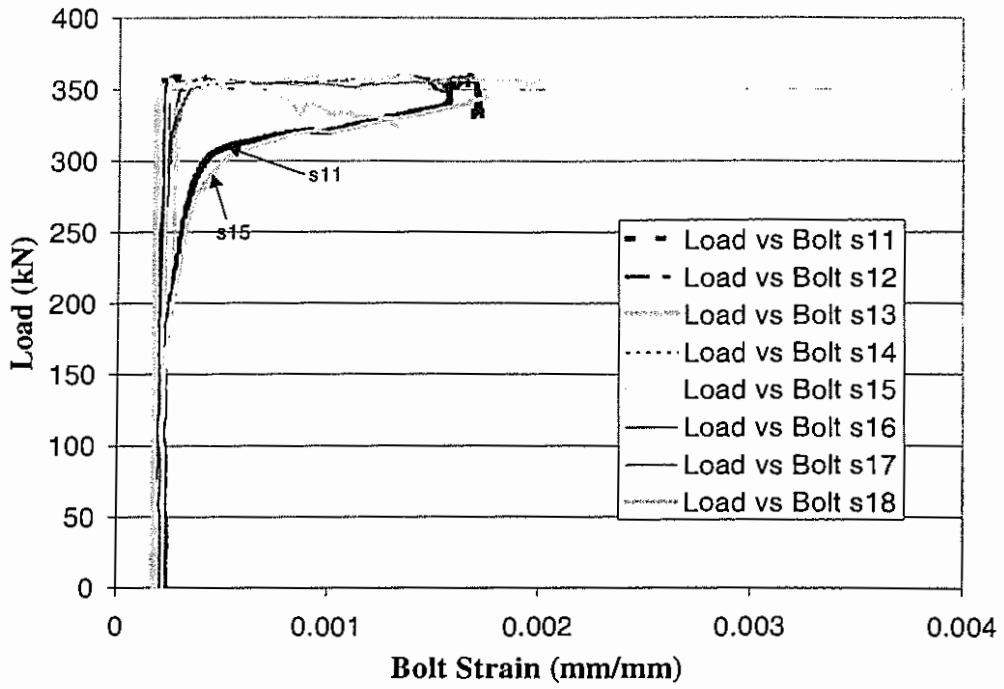
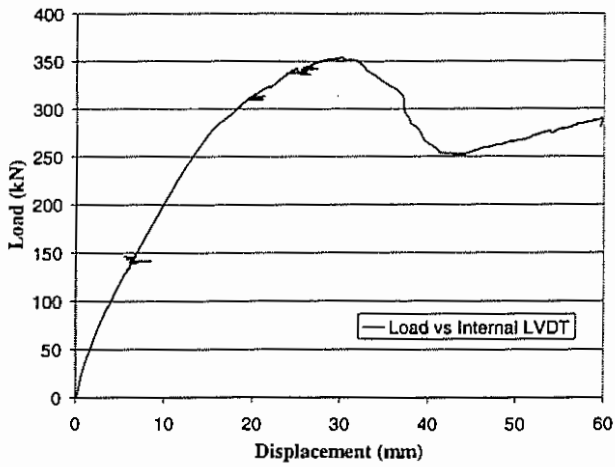
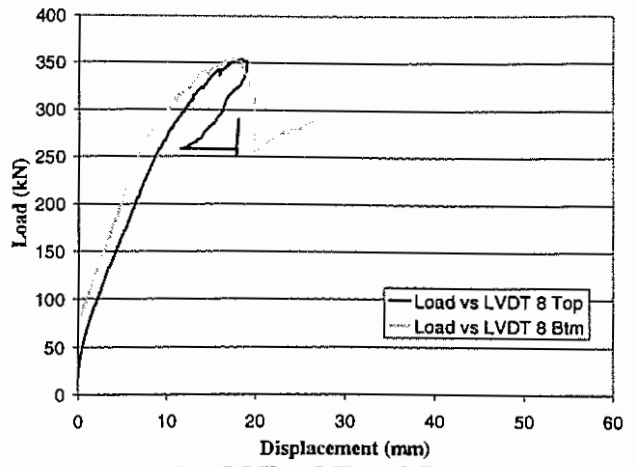


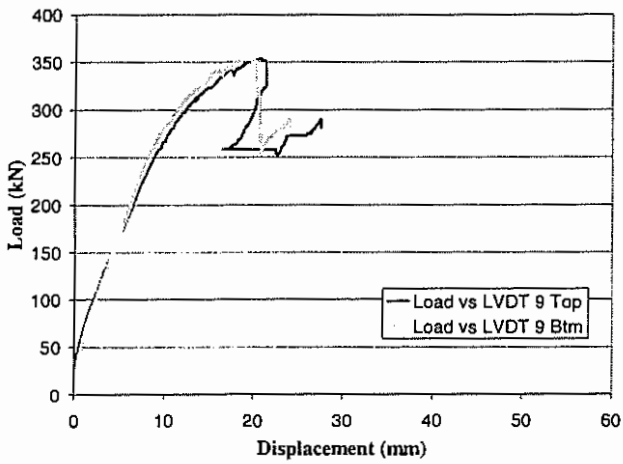
Figure B-15: Load vs Bolt Strain Graphs of Specimen SB4



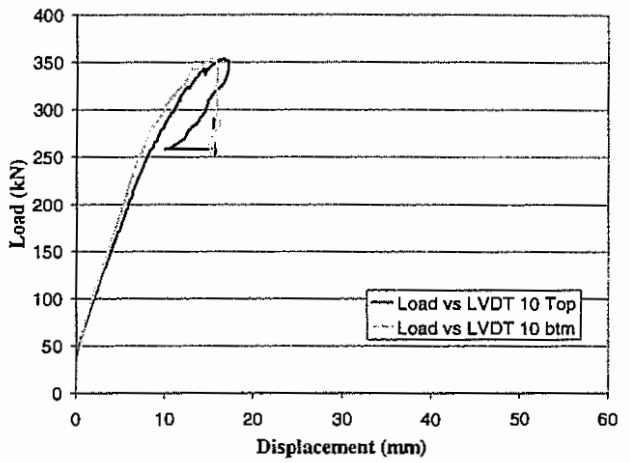
(a.) Load vs Internal LVDT



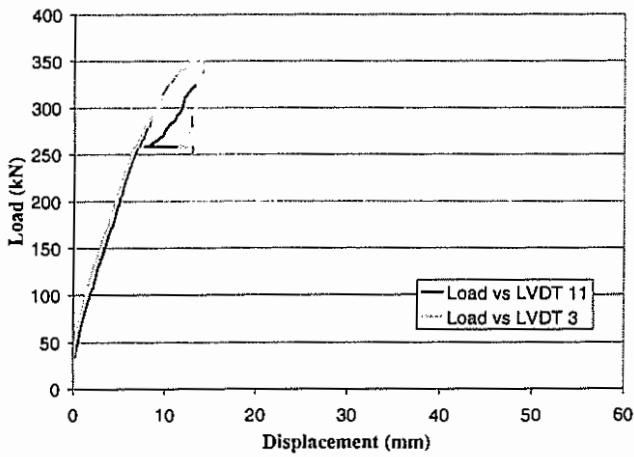
(b.) Load vs LVDT 8 Top, 8 Btm



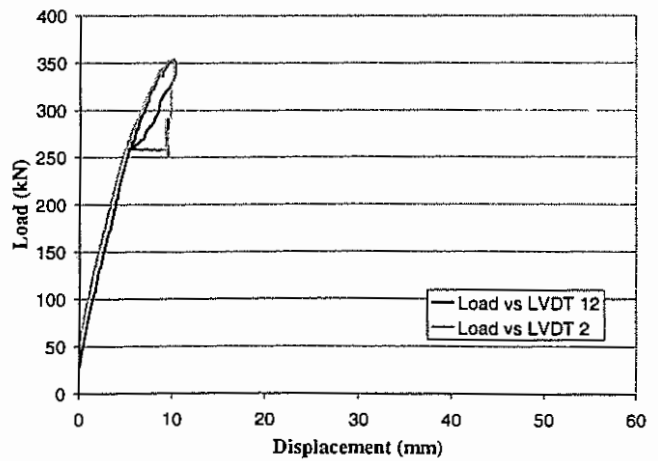
(c.) Load vs LVDT 9 Top, 9 Btm



(d.) Load vs LVDT 10 Top, 10 Btm

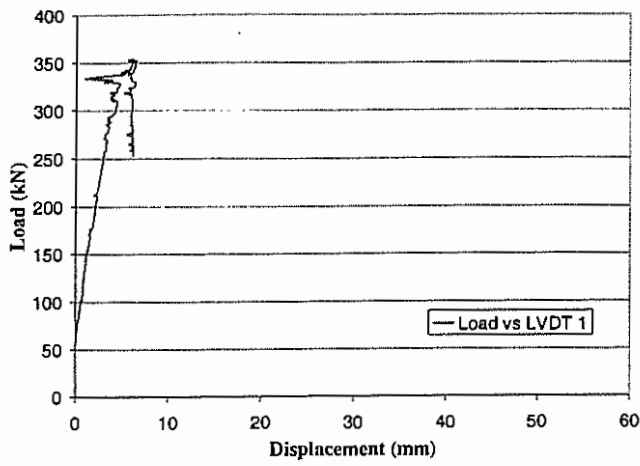


(e.) Load vs LVDT 11, 3

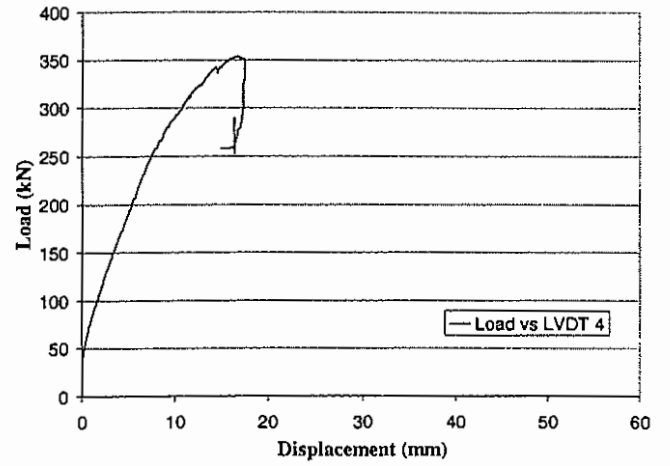


(f.) Load vs LVDT 12, 2

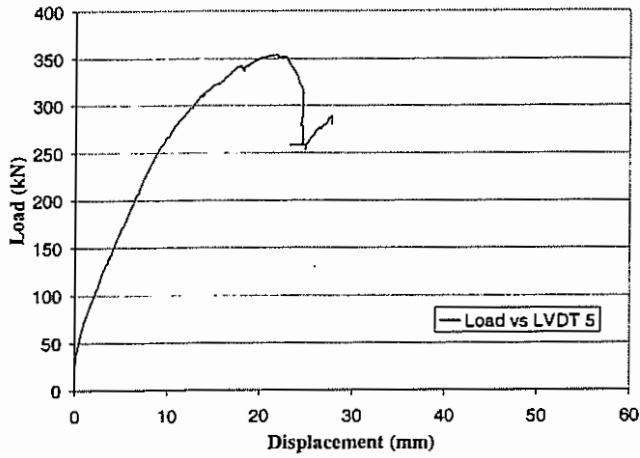
Figure B-16: Load-Displacement Graphs of Specimen SB5



(g.) Load vs LVDT1

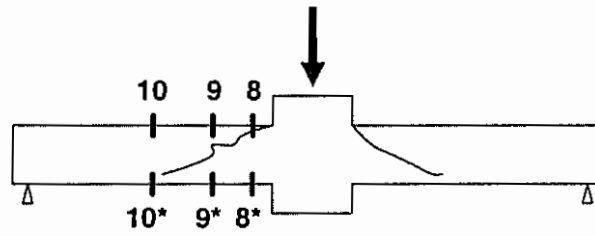
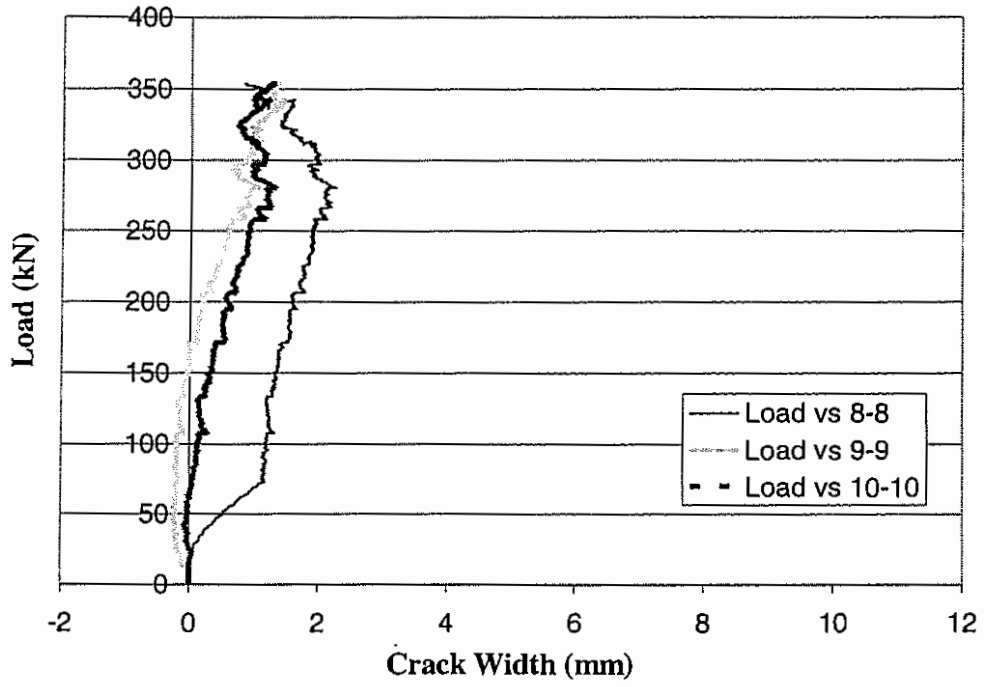


(h.) Load vs LVDT 4



(i.) Load vs LVDT 5

Figure B-16: Continued

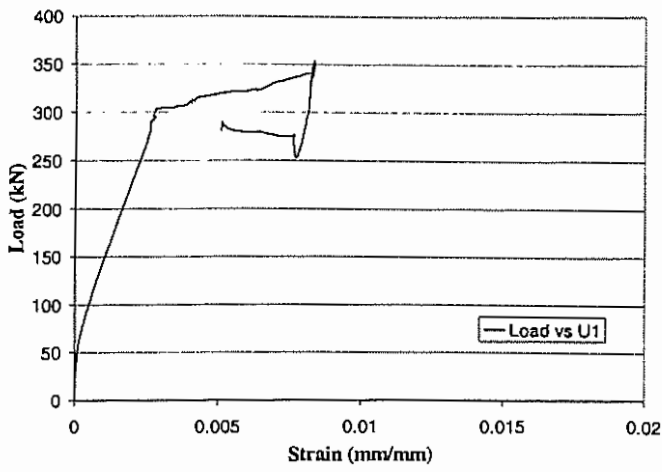


Positions of LVDT pairs around the column

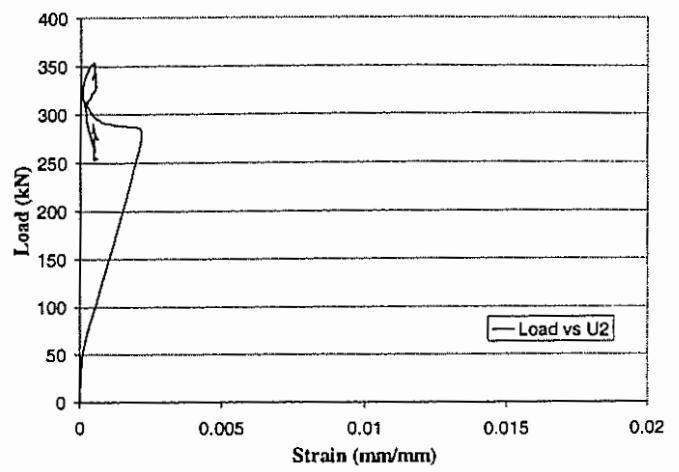
Figure B-17: Load vs Vertical Crack Width of Specimen SB5

Note: *See Figure 3-18

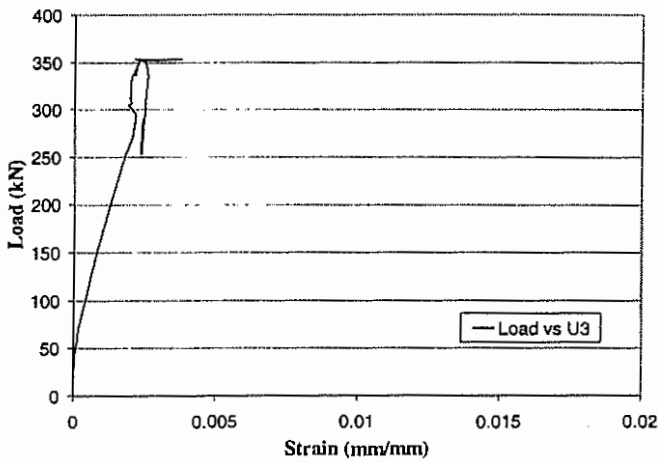
Crack width was obtained as the absolute difference between LVDT at top and bottom. Negative crack width may be due to instrumentation noise.



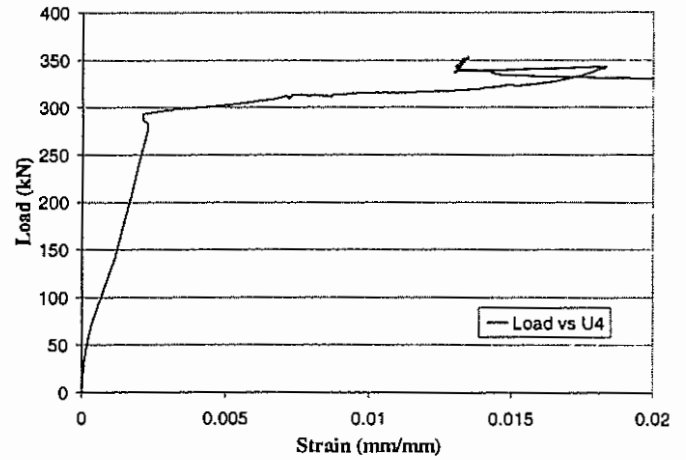
(a.) Load vs U1 Strain Gauge



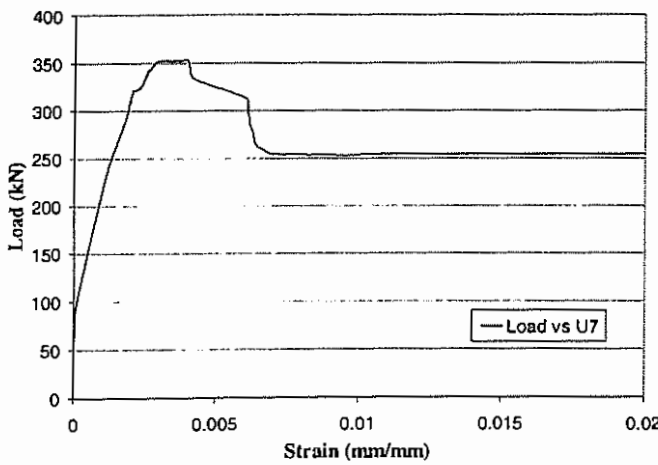
(b.) Load vs U2 Strain Gauge



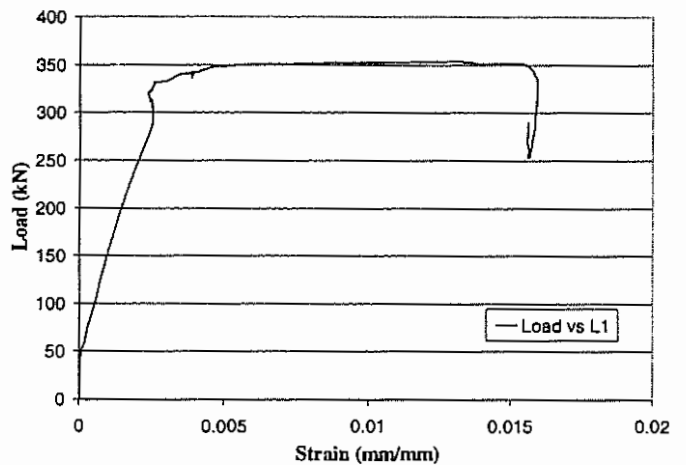
(c.) Load vs U3 Strain Gauge



(d.) Load vs U4 Strain Gauge

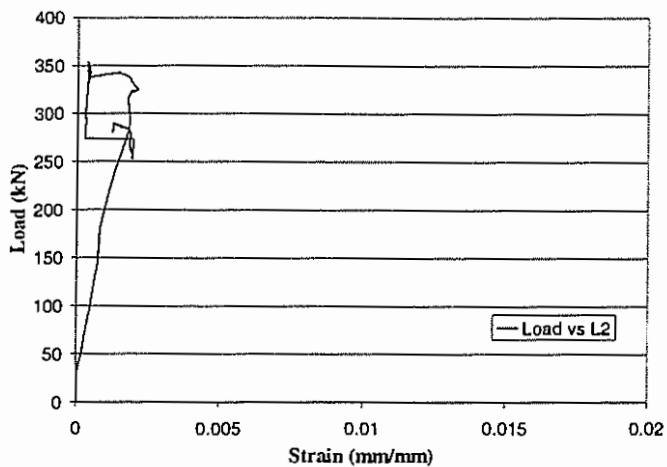


(e.) Load vs U7 Strain Gauge

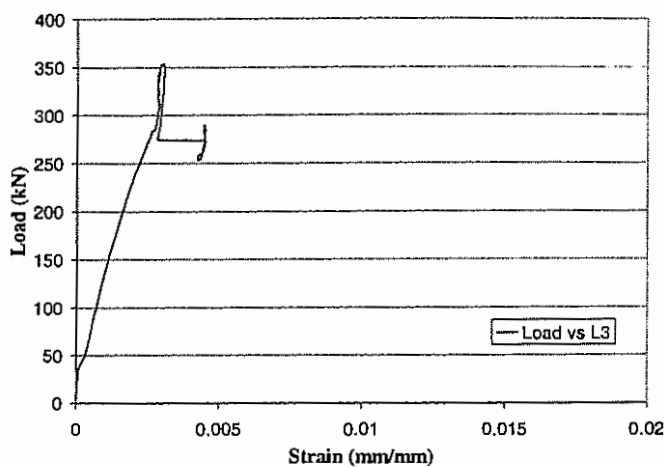


(f.) Load vs L1 Strain Gauge

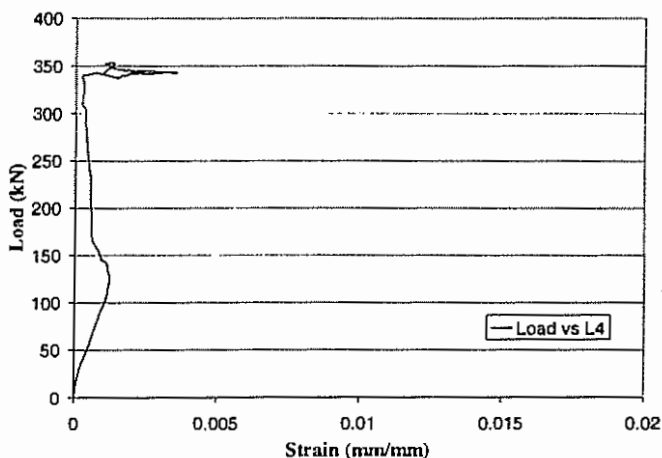
Figure B-18: Load-Longitudinal Reinforcement Strain Graphs of Specimen SB5



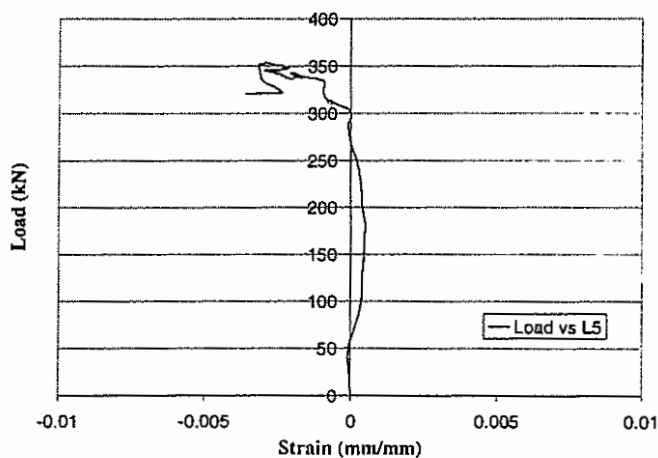
(a.) Load vs L2 Strain Gauge



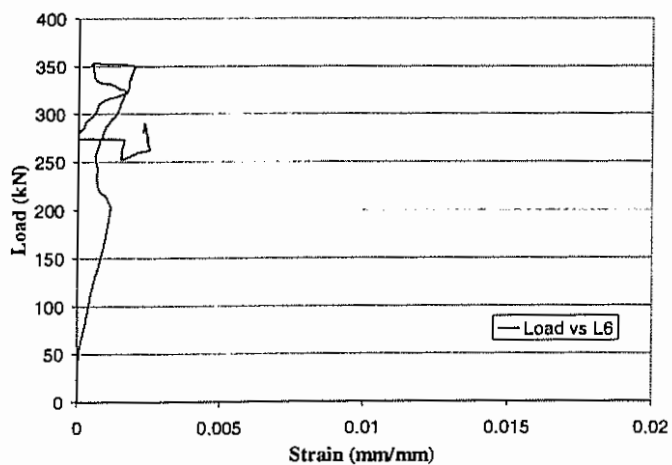
(b.) Load vs L3 Strain Gauge



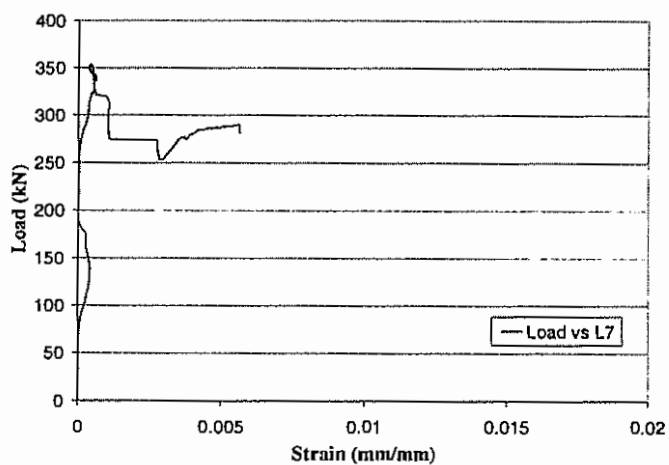
(c.) Load vs L4 Strain Gauge



(d.) Load vs L5 Strain Gauge



(e.) Load vs L6 Strain Gauge



(f.) Load vs L7 Strain Gauge

Figure B-18: Continued

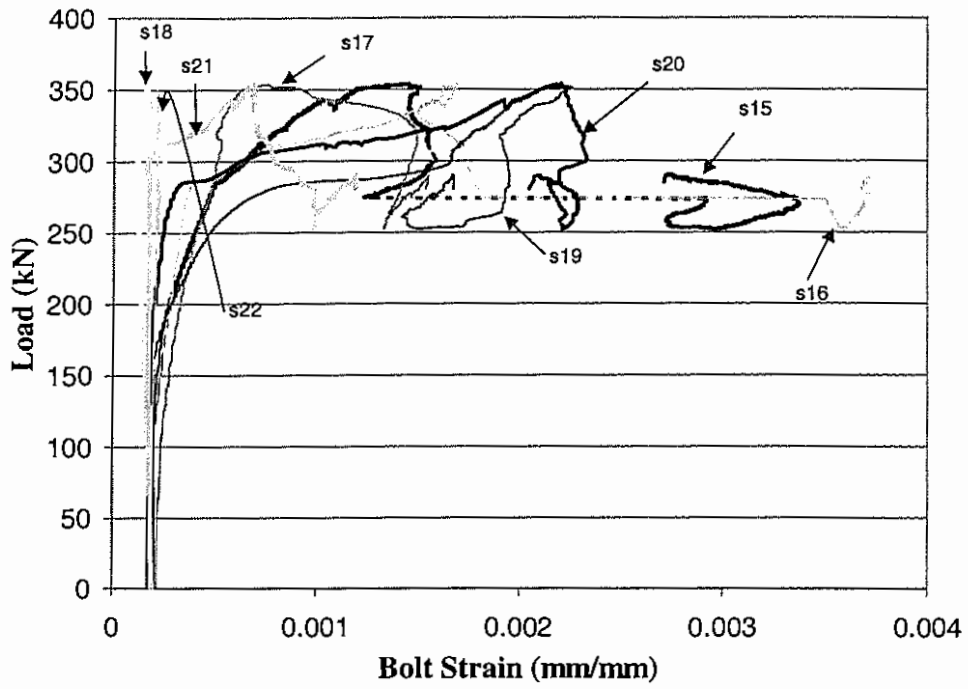
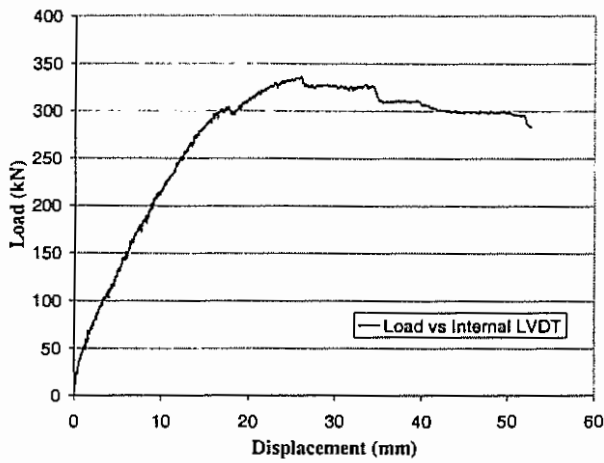
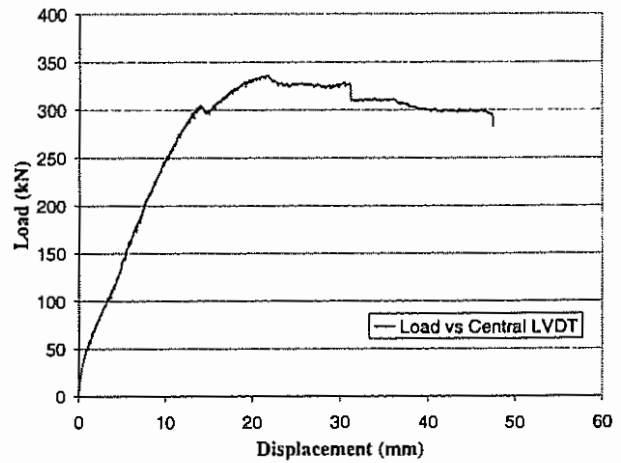


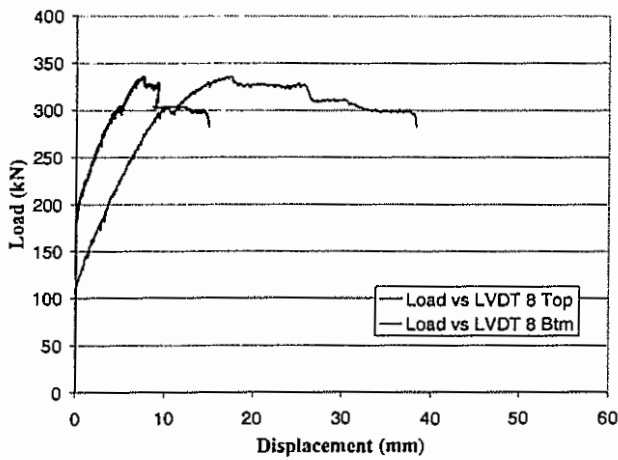
Figure B-19: Load-Bolt Strain Graphs of Specimen SB5



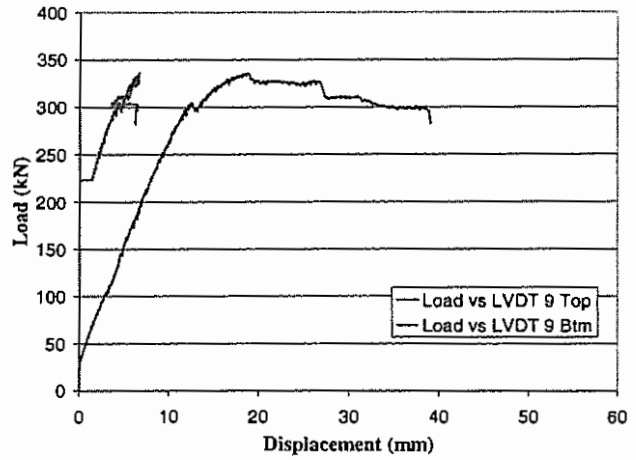
(a.) Load vs Internal LVDT



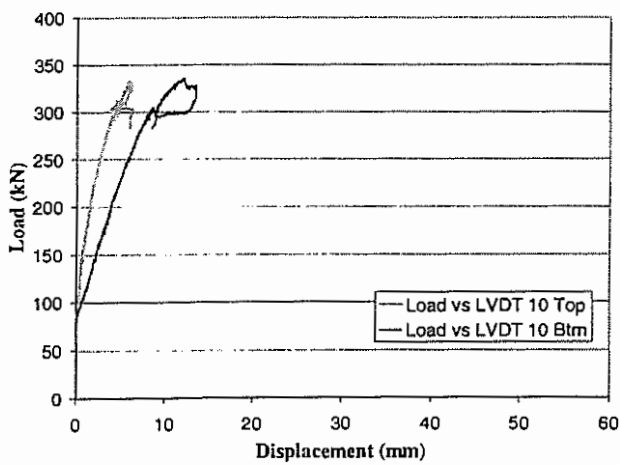
(b.) Load vs Central LVDT



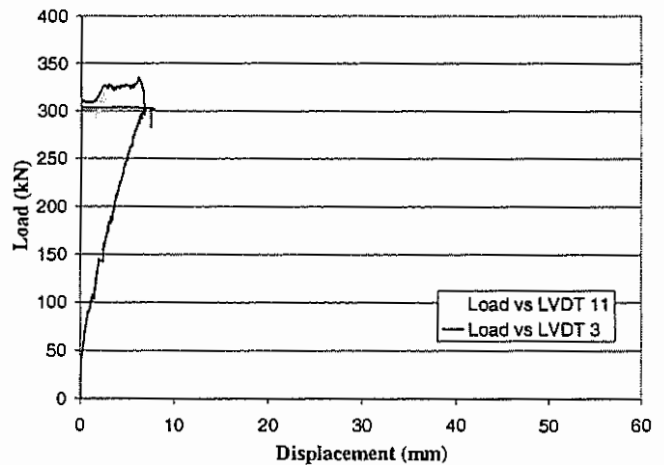
(c.) Load vs LVDT 8 Top, 8 Btm



(d.) Load vs LVDT 9 Top, 9 Btm

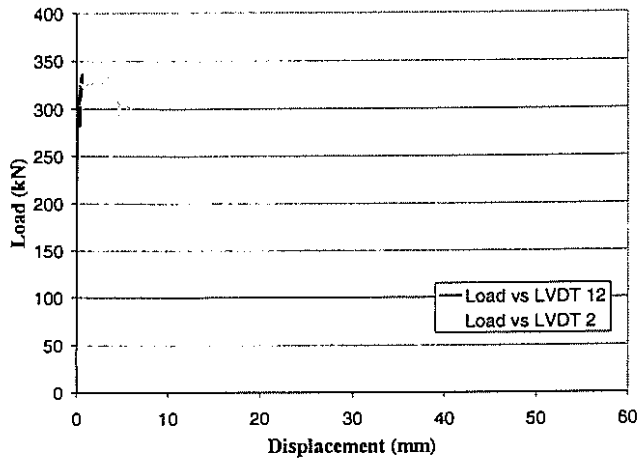


(e.) Load vs LVDT 10 Top, 10 Btm

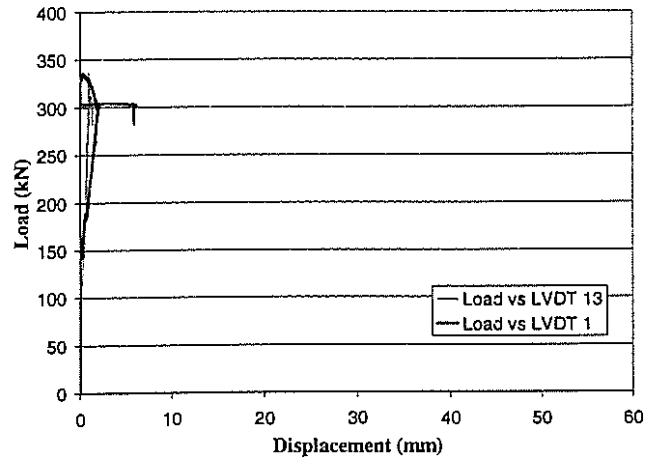


(f.) Load vs LVDT 11, 3

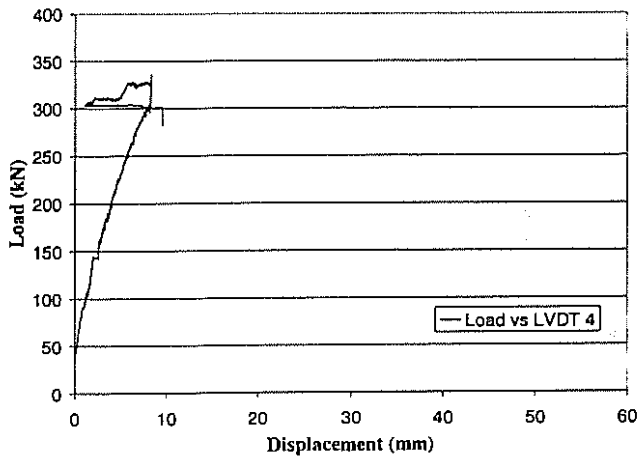
Figure B-20: Load-Displacement Graphs of Specimen SB6



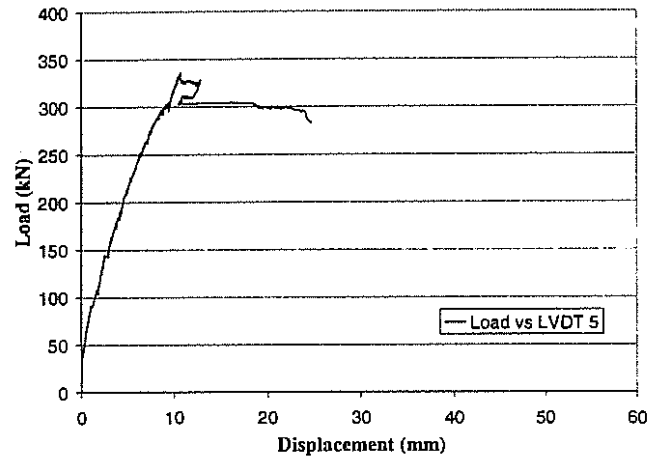
(g.) Load vs LVDT 12, 2



(h.) Load vs LVDT 13, 1

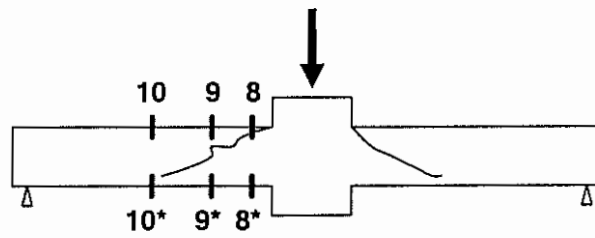
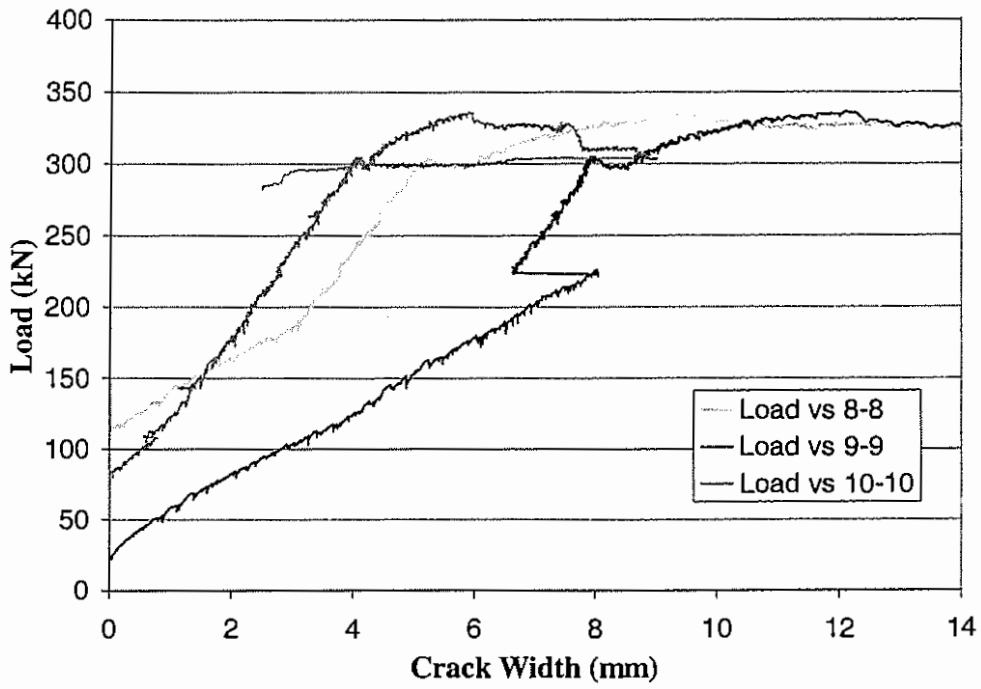


(i.) Load vs LVDT 4



(j.) Load vs LVDT 5

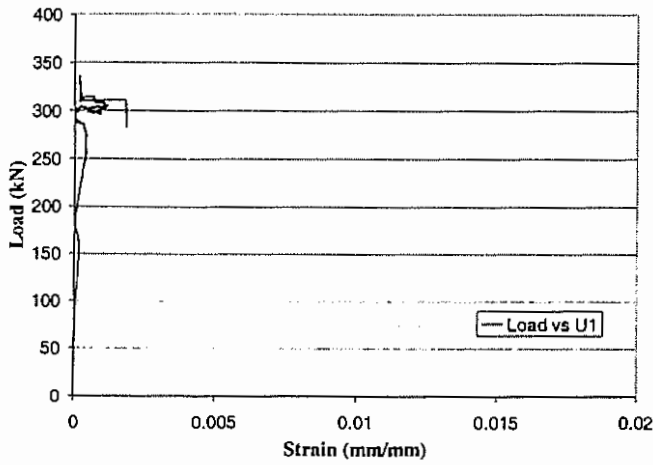
Figure B-20: Continued



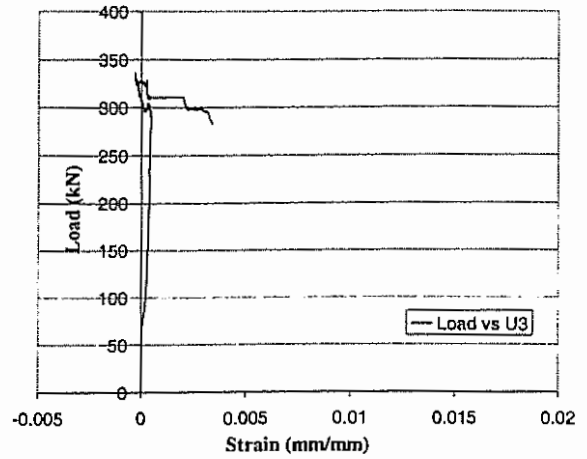
Positions of LVDT pairs around the column

Figure B-21: Load vs Vertical Crack Width of Specimen SB6

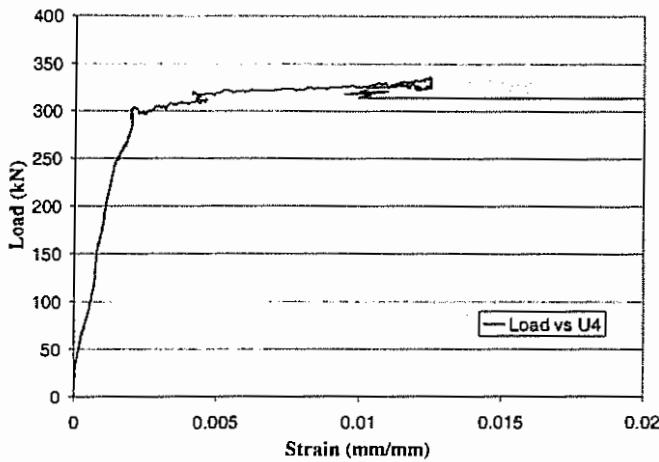
Note: *See Figure 3-18



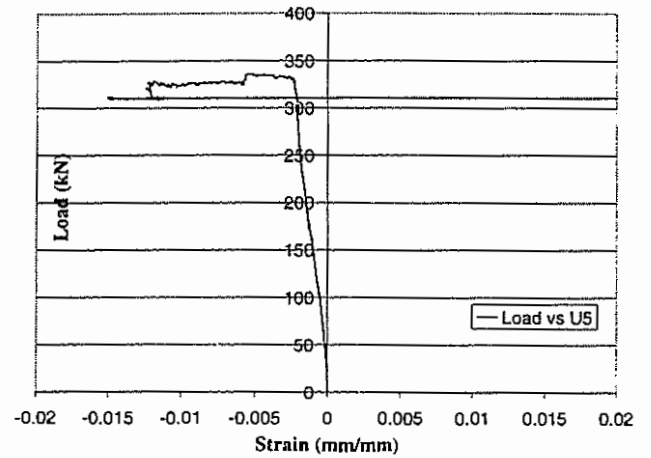
(a.) Load vs U1 Strain Gauge



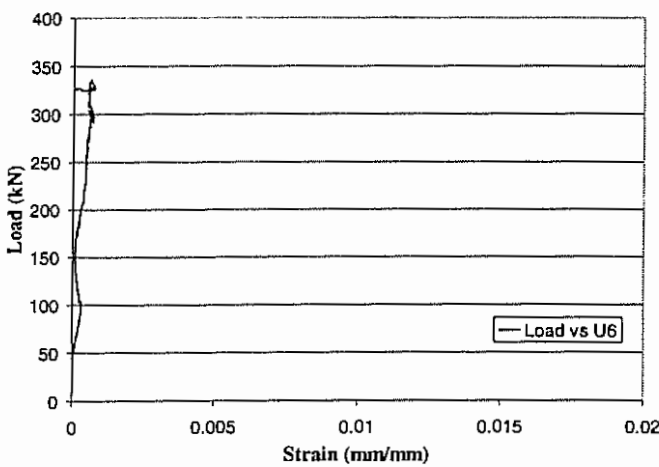
(b.) Load vs U3 Strain Gauge



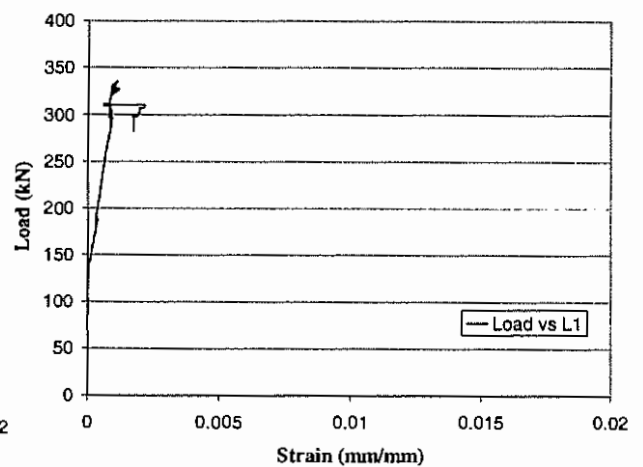
(c.) Load vs U4 Strain Gauge



(d.) Load vs U5 Strain Gauge

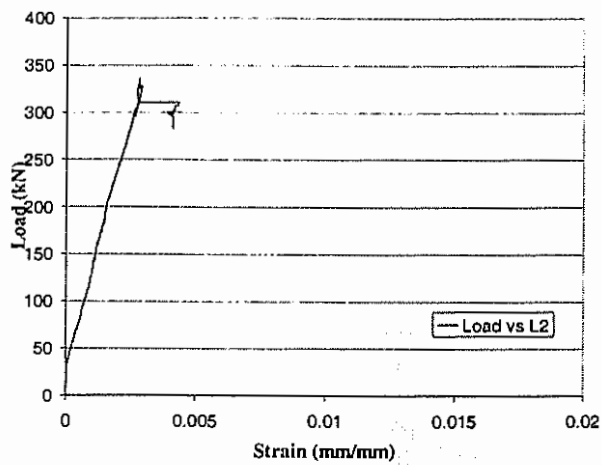


(e.) Load vs U6 Strain Gauge

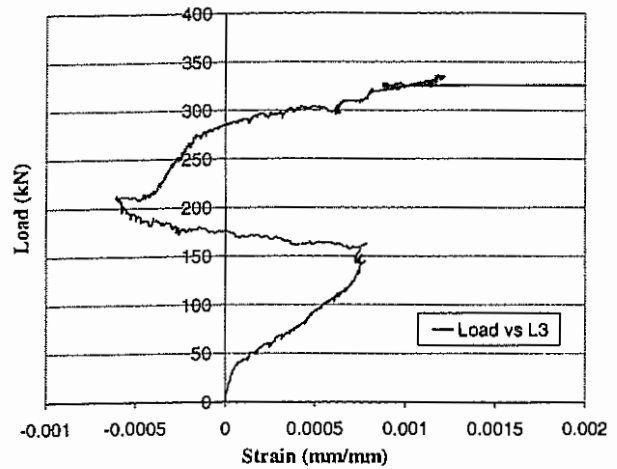


(f.) Load vs L1 Strain Gauge

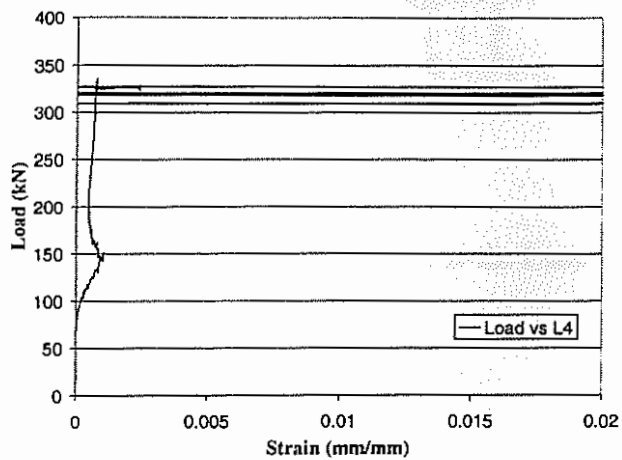
Figure B-22: Load-Longitudinal Reinforcement Strain Graphs of Specimen SB6



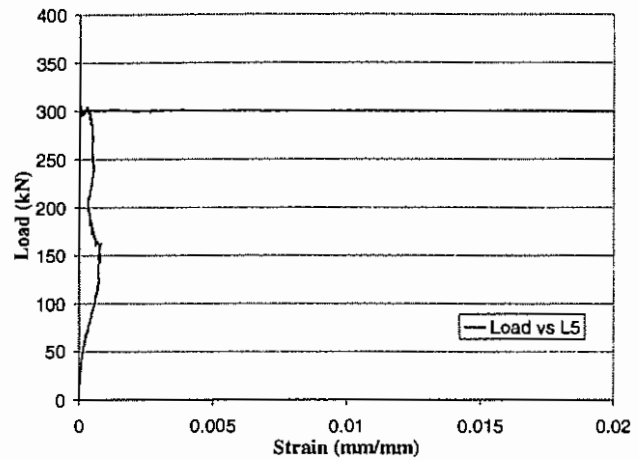
(g.) Load vs L2 Strain Gauge



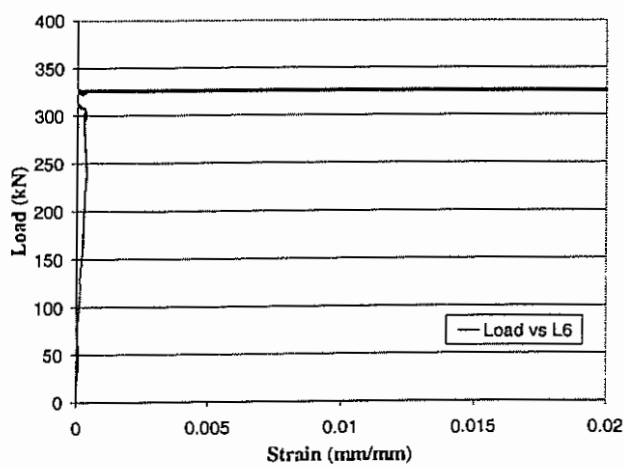
(h.) Load vs L3 Strain Gauge



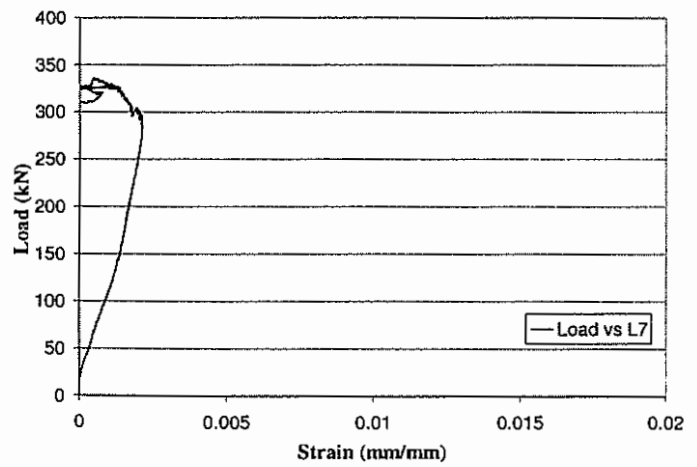
(i.) Load vs L4 Strain Gauge



(j.) Load vs L5 Strain Gauge



(k.) Load vs L6 Strain Gauge



(l.) Load vs L7 Strain Gauge

Figure B-22: Continued

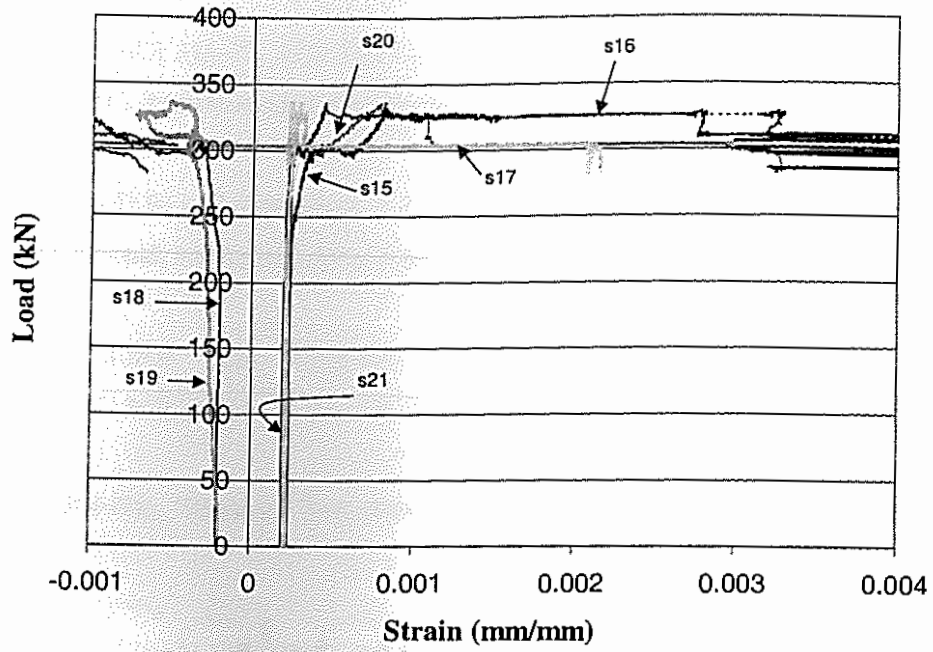


Figure B-23: Load-Bolt Strain Graphs of Specimen SB6

References

ACI 318-99, ACI 318-77, ACI 318-63 “Building Code Requirements for Reinforced Concrete (ACI 318-89)”, American Concrete Institute, Detroit, 1999, 1977, 1963

Alexander, S.D.B, and Simmonds, S.H., “Bond Model for Concentric Punching Shear”, ACI Structural Journal, v.89, no. 3, May-June 1992, pp. 325-334

Alexander, S.D.B, and Simmonds, S.H., 1987 “Ultimate Strength of Slab-Column Connections”, ACI Structural Journal, v.84, No.3, May-June 1987, pp. 255-261

ASTM E 8M-00b, “Standard Test Method for Tension Testing of Metallic Materials [Metric]”, 2000

Bazant, Z.P., and Cao, Z., “Size Effect in Punching Shear Failure of Slabs”, ACI Structural Journal, v.84, no.1, Jan-Feb. 1987, pp. 44-53

Bortolotti, L., “Punching Shear Strength in Concrete Slabs”, ACI Structural Journal, v.87, no.2, Mar-Apr. 1990, pp 208-219

Braestrup, M.W., Nielsen, M.P., Jensen, B.C. and Bach, F., “Axisymmetric Punching of Plain and Reinforced Concrete”, Report No. 75, Structural Research Laboratory, Technical University of Denmark, 1976, 33 pp.

Broms, C.E., “Punching of Flat Plates-A Question of Concrete Properties in Biaxial Compression and Size Effect”, ACI Structural Journal, v.87, no.3, May-June 1990, pp.292-304

Canadian Standards Association, “Design of Concrete Structures for Buildings”, CAN3 A23.3-M94, A23.3-M77, Rexdale, Ontario, 1994, 1977

Canadian Standards Association, “Limit States Design of Steel Structures”, CSA S16-M94, Rexdale, Ontario, December 1994

Canadian Standards Association, "Splitting Tensile Strength of Cylindrical Concrete Specimens", A23.3.2-13C, Rexdale, Ontario, September 2000

Canadian Standards Association, "Compressive Strength of Cylindrical Specimens", A23.3.2-9C, Rexdale, Ontario, September 2000

CEB Comite Euro-International Du Beton, "CEB-FIP Model Code 1990 – Final Draft", Bulletin d'Information, No.203 -205, Lausanne, Switzerland, 1990

Cope, R.J., and Clark, L.A, "Concrete Slabs Analysis and Design", Elsevier Applied Science Publishers, London and New York, 1984

Dilger, W.H., and Ghali A., "Shear Reinforcement for Concrete Slabs", Proceedings, ASCE, Journal of Structural Division, v.107, no. ST12, December 1981, pp.2403-2420

Elgabry, A.A. and Ghali, A., "Design of Stud-Shear Reinforcement for Slabs" ACI Structural Journal, v.87, no.3, 1990 pp.350-361

El-Salakawy, E.F, "Shear Behaviour of Reinforced Concrete Flat Slab-Column Edge Connections with Openings", Thesis, Menoufia University, Egypt, 1998

El-Salakawy, Ehab F., Polak, Maria A., Soudki, K.A., "New Shear Strengthening Technique for Concrete Slab-Column Connections" ACI Structural Journal, v 100, n 3, May-June, 2003, pp. 297-304

Eurocode2, "Design of Concrete Structures-Part1: General Rules and Rules for Buildings", ENV 1992-1-1:1991, Comité Européen de Normalisation, Brussels

FIB Bulletin XX., "Punching of Structural Concrete Slabs-A State-of-the-art report", FIB Task Group 4.3, Lausanne, Switzerland, 2001

Ghali, A, Sargious, M.A, and Huizer, A, "Vertical Prestressing of Flat Plates Around Columns", Shear in Reinforced Concrete, ACI Special Publication SP-42, Vol.2, 1974, pp. 905-920

Kinnunen, S., and Nylander, H., "Punching of Concrete Slabs without Shear Reinforcement", Transactions of the Royal Institute of Technology (Sweden), no.158, Stockholm, 1960, 112 pp.

Long A.E., "A Two-Phase Approach to the Prediction of the Punching Strength of Slabs", ACI Journal, v.73, No.2, February 1975, pp. 37-45

Macgregor J.G., Bartlett F.M., (2000), "Reinforced Concrete, Mechanics and Design", 1st Canadian Edition, Prentice Hall Canada Inc, Scarborough, Ontario

Marzouk , H., and Hussein, A, "Experimental Investigation on the Behaviour of High-Strength Concrete Slabs", ACI Structural Journal, v.88, No.6, November-December 1991, pp. 701-713

Moe, J., "Shearing Strength of Reinforced Concrete Slabs and Footings under Concentrated Loads", Development Department Bulletin D47, Portland Cement Association, Skokie, Illinois, April 1961, 130 pp.

Rankin, G.I.B, and Long, A.E, "Predicting the Punching Strength of Conventional Slab-Column Specimens, Proceedings Institution of Civil Engineers, Part 1, 82, April 1987, pp.327-346

Reagan, P.E., "Design for Punching Shear", The Structural Engineer, No.6, Volume 52, June 1974, pp.197-207

Shehata, I.A.E.M, and Regan, P.E. (1989). "Punching in R.C. Slabs" Journal of Structural Engineering, Vol.115, No. 7, July, 1989, pp. 1726-1739

Structural Use of Concrete, Part 1: Code of Practice for Design and Construction (BS 8110), British Standards Institution, London, 1985, 126 pp.